SHOX2, A THALAMUS-SPECIFIC TRANSCRIPTIONAL REGULATOR OF THALAMOCORTICAL NEURON FIRING AND SPINDLE OSCILLATIONS IN MICE

An abstract
submitted on the 24th day of March 2023
to the Program of Neuroscience
in partial fulfillment of the requirements
of the School of Science and Engineering
of Tulane University
for the degree
of
Doctor of Philosophy

by

Isabella G Febbo

APPROVED:

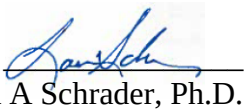

Laura A Schrader, Ph.D.
Advisor

Jeffrey Tasker, Ph.D.

Carmen Canavier, Ph.D.

Maria Galazo, Ph.D.

Abstract

Precise network connectivity and membrane properties of cells within the brain underlie neuro-typical activity. These membrane properties contribute to cell identity and dysregulation of such properties can propagate to behavioral dysfunction. Thalamocortical neurons (TCNs) exhibit characteristic burst and tonic activity and create thalamus-cortex network connectivity that enables proper function of the thalamus and thalamocortical network. Together, these neural elements generate sensory perception, and are involved in cognition, motor response, and memory consolidation.

Transcription factors are critical to proper development of such cellular identity and function. Previously, we determined that a subset of TCNs express the transcription factor, Shox2, which has been associated with development and maintenance of ion channel expression in cells of the heart and spinal cord and found that it is also critical for ion channel regulation and proper current dynamics in TCNs. In this study, we further investigated the contribution of Shox2 to TCN burst and tonic firing and the network activity and rodent behavior that this firing generates.

Loss of TCN expression of *Shox2* at P6 and P21 does not alter gross development of VB cortical targets, but loss of *Shox2* expression at P21 does affect TCN firing and current densities. This effect on current densities and firing translates to an effect on thalamocortical oscillations—spindle density was significantly reduced. Further, key behaviors associated with spindles and proper thalamic function are significantly

affected: memory consolidation and somatosensory perception. Thus, Shox2 is a key transcription factor in the regulation of proper thalamic function in mice.

SHOX2, A THALAMUS-SPECIFIC TRANSCRIPTIONAL REGULATOR OF THALAMOCORTICAL NEURON FIRING AND SPINDLE OSCILLATIONS IN MICE

A dissertation
submitted on the 24th day of March 2023
to the Program of Neuroscience
in partial fulfillment of the requirements
of the School of Science and Engineering
of Tulane University
for the degree
of
Doctor of Philosophy

by

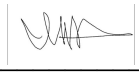

Isabella G Febbo

APPROVED: _____
Laura A Schrader, Ph.D.
Advisor

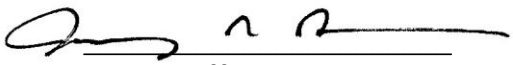

Jeffery Tasker, Ph.D.

Carmen Canavier, Ph.D.

Maria Galazo, Ph.D.

Acknowledgements

I would most like to thank my advisor, Dr. Laura Schrader. Words fall short in trying to explain how grateful I am for the time and effort you put in to mentoring me. Your compassion and intellectual and emotional support gave me the confidence to get here, and to take the next steps in my career. Your curiosity and aptitude for scientific investigation are endlessly inspiring. The world would benefit greatly from many more scientists and mentors like you. Thank you so very much, Laura, for making me laugh and think as much as you did. I would not have made it to dissertation submission with any other advisor.

I would like to extend my sincere gratitude to my committee. Each of you has played a unique and critically supportive role. Dr. Carmen Canavier has endlessly supported my interest in computational neuroscience, through facilitating the successful completion of a published computational project, writing numerous letters of reference, and continuously explaining 'the math' to me. I thank you. Dr. Maria Galazo has influenced, strengthened, and performed multiple experiments outlined in this dissertation, and has continuously demystified the thalamus for me, thank you so very much. Dr Tasker has provided critical questions and helpful critiques at every presentation and milestone along the way. Thank you for your unyielding interest in neuroscience and your enthusiastic support of my presentations and project. All of you have provided much appreciated support and encouragement along the way and have helped shape me as a scientist.

I would like to thank our collaborators at Baylor College, Dr. Anne E Anderson, and Dr. Luis Martinez, without whom this project would not be as impactful.

I would like to thank many members of the Tulane Brain Institute, current and past. This is truly a wonderful, supportive, and inclusive community, and I know I have made lifelong friends here. Specifically in the Stern basement, I would like to thank Dr. Matthieu Maroteaux, who I initially met because he was teaching me patch-clamp electrophysiology, and now has become a dear friend. I would also like to thank Lee Vaasjo for his friendship and boundless enthusiasm for neuroscience, as well as Dr. Sabrina Kragness for her sharp humor and wit, Youad Darwish for her friendship and emotional and scientific support, and Xiao Han. I extend my gratitude to all of my mentees/labmates in no particular order: Valerie Warkins, Trevor Roy, Abigail Sullivan, Habby Wang, Nadia Vargas, Emily Meyer, Pranshu Khana, Gelena Jones, and Jaide Liang. Thank you all for your help. Very importantly, I am so grateful for two members of my cohort, Nina Baumgartner and Jill King. Their friendship and support have been critical. Rachel Wise has also been a critical friend and mentor. I am also so grateful for the stimulating conversation and irreplaceable friendships that came out of ComBaT B-sides journal club with Alexis Ducote and Dr. Dan Burnston.

My friends outside of the Tulane scientific community were foundational support as well: Katharina Tomisato, Lestat, Mikaela Pitcan, Irie, Zack Morris, Lala, Rachel Barnett, Anna Donnel, Kumquat, Eli Lewis, Chad Stefancin, Kiviana Diaz, Rachel Moss, Mel Evans, Holly and Sandivel, Santiago Pandolfi, and many, many more. My family: My Pop (Doc Febbo), my mother (Christine Febbo), Sophronia Zora Febbo, Huckleberry Febbo, Roxann Angela Febbo, Rocco Dartanian Febbo, Otto Sinclair Febbo, and as of last week, Ziggy Febbo. Of course, I must extend the final and biggest thank you to the love of my life, the best partner in crime I could ever ask for, my dog, Ruby. I cannot properly express the abundance of gratitude I have for everyone involved in helping me through this process. Thank you, all.

Table of Contents

List of Figures

Chapter 1 Introduction

Perception of sensory information is our first line of interaction with life. From there, decisions are made, emotions are had, and memories are formed. Most sensory information is received by an area in the center of your brain called the thalamus. The thalamus relays this sensory information to the cortex where reciprocal connections send it back to the thalamus. This generates loops of cyclic electrical activity between the thalamus and the cortex, known as thalamocortical oscillations. These thalamocortical oscillations generate our perception of and response to sensory information. Thus, dysregulation of these oscillations can have a myriad of effects such as: faulty sensory perception, motor impairment, and memory deficits, all of which are individually or combinatorially present in a range of neuropsychiatric disorders that have been associated with thalamic dysfunction.

1.1 Psychiatric disorders and the thalamus

One such disorder is schizophrenia. Thalamocortical dysfunction has long been implicated as a possible mechanism that could give rise to the wide range of schizophrenia symptoms, which include abnormal emotion, motor activity, and sensory perception (Andreasen, 1997; Andreasen et al., 1998). This theory has received support from structural and functional imaging studies in humans (Minzenberg et al., 2009; Shenton et al., 2001), and, notably, using resting state fMRI, Woodward et al. determined that when comparing neuro-typical patients to schizophrenic patients, those with schizophrenia had reduced prefrontal-thalamic connectivity and increased

motor/somatosensory-thalamic connectivity (Woodward et al., 2012). Further, when observing schizophrenic patients after their first episode, Braus et al. found that when presented with basic auditory and visual stimuli, schizophrenic patients had reduced neural activity in the right thalamus and right prefrontal cortex (Braus et al., 2002). A systematic review of neural correlates of multisensory integration in schizophrenia seeks to understand neural dynamics that generate multisensory integration, and cites a review of neural oscillations that states, although "the neural foundations of multisensory processes, constituting oscillations, networks and functional connectivity, are still not well-understood", they do conclude that areas of the cortex tightly connected to the thalamus are key locations of oscillatory dysregulation (Gröhn et al., 2021).

Autism spectrum disorders (ASD) is another sensory perception disorder where thalamic dysfunction has been implicated. ASD patients do not present with a *deficit* in sensory perception, rather a *difference*. ASD patients can outperform typically developing peers in some sensory discrimination tasks, but present with deficits in others (David et al., 2010; Groen et al., 2009; Milne et al., 2002; O'Riordan et al., 2001; Shah & Frith, 1983). Researchers found that there is no singular sensory disruption profile for children with ASD, but that a vast majority of them have either hyper or hypo-reactivity to a range of sensory modalities (Kadlaskar et al., 2022). As previously reviewed, one theory to explain this discrepancy that has considerable experimental support is that patients with ASD excel at sensory perception tasks that do not require integration into ongoing neural processing (oscillations), such as detecting figures embedded in more complex line drawings or 'copying impossible figures', but when stimuli include aspects of motion, such as determining the direction (left versus right) of a moving dot, which requires

integration into oscillatory processing, ASD patients have a deficit in performance (Dakin & Frith, 2005; Simon & Wallace, 2016). This alludes to a disruption in thalamocortical processing which is further supported by evidence that there is both functional and anatomical underconnectivity from thalamus to cortex in patients with ASD (Nair et al., 2013).

In summary, neurodevelopmental disorders, including schizophrenia and ASD, present with aberrant thalamocortical connectivity and activity, and studies in both fields support a hypothesis that dysregulated sensory perception and resultant motor and limbic effects could generate from an inability to properly integrate sensory perception into ongoing thalamocortical oscillations. Interestingly, recent studies have determined that a biomarker for both schizophrenia and ASD is a reduced density of spindle oscillations (Farmer et al., 2018; Manoach et al., 2016). It has been determined that there is one brain structure that generates this spindle oscillation frequency: the thalamus.

1.2 The thalamus and thalamocortical circuitry

1.2.1 The thalamus

The thalamus is much more than a sensory relay for the cortex; it is a, “unifying entity that operates as the ultimate gatemaster” (Steriade & Llinas, 1988). At the center of the brain, it is a structure composed of 50-60 nuclei and subnuclei that are highly interconnected to other brain structures (Mashour & Alkire, 2013). These nuclei are associated with sensory, motor, and limbic functions and are interconnected with the cortex, amygdala, striatum, hippocampus, and hypothalamus (Jones, 2007; Oh et al., 2014). As such, patients with focal thalamic lesions present with cognitive and emotional

disorders, including amnesia, attentional neglect, aphasia, depression and dementia (Carrera & Bogousslavsky, 2006; De Witte et al., 2011; Kopelman, 1995).

1.2.2 Organization of the thalamus

Structurally, the thalamus is composed of two symmetric halves about the midline. Each side is split by a Y-shaped internal medullary lamina, which divides the thalamus on each side into 3 anatomically distinct nuclei: a lateral nuclear group, a medial and midline nuclear group, and an anterior nuclear group. An inhibitory shell that surrounds the lateral thalamus is called the reticular nucleus, which also provides connectivity between the nuclei. (Bordes et al., 2020; Sheridan & Tadi, 2022; S. M. Sherman, 2017).

In **figure 1.1**, you can see the location of the thalamus in the center of the brain (darker round mass in center of brain on left) and the midline, anterior, and lateral nuclei in orange, green, and pink respectively.

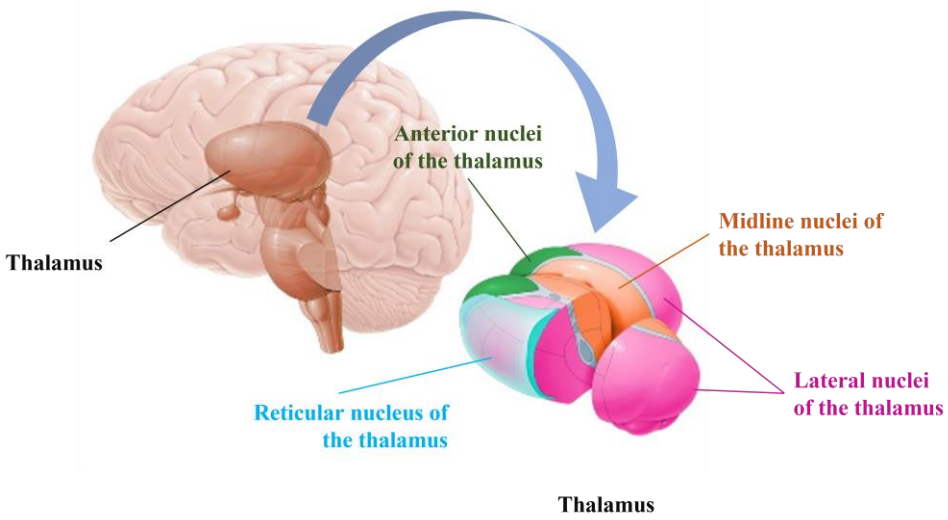

Figure 1.1 *Thalamus schematic*

The thalamus is located in the center of the brain (darker round mass in center of brain on left of image). On the right, a schematic of the thalamus is extruded. Structurally, it is composed of two symmetric halves about the midline of the brain. Each symmetric half can be further subdivided into the midline nuclei (orange), located along the midline of the brain, the anterior nuclei (green), located at the anterior of the thalamus, the lateral nuclei (pink), located laterally, and the reticular nucleus (blue), which wraps around and provides connectivity between the other nuclei.

1.2.3 Functional classification of thalamic nuclei

Functional classification of thalamic nuclei is a topic of debate. This is mainly because many inferences of nuclei function come from their synaptic connectivity within the brain, our knowledge of which is continuously evolving (S. Murray. Sherman & Guillery, 2013). One classification style groups the nuclei into 3 categories: relay nuclei, association nuclei, and midline and intralaminar nuclei (Paxinos, 2004). Another classification suggests grouping the nuclei into 3 groups, on a continuum of function, from sensorimotor to limbic: sensorimotor (relay), sensorimotor-limbic, and limbic. (Vertes et al., 2015). The first group in both classification systems, relay and sensorimotor, consists of the relay nuclei.

1.2.4 First order and higher order nuclei—a difference in circuitry and information

Most relay nuclei are located anatomically in the lateral nuclear group, and they can be subdivided into first order and higher order. First order relay nuclei receive peripheral or ascending sensory or motor information and relay it to various layers of the cortex. They include: the lateral geniculate complex (LGN), medial geniculate nucleus (MGN), ventral posteromedial (VPM) ventral lateral nucleus (VL), ventral anterior nucleus (VA) and ventral medial nucleus (VM). Higher order relay nuclei receive inputs from sensorimotor cortex and project to higher order areas of the cortex, such as the PFC. Higher order relay nuclei located in the lateral nuclear group are the lateral posterior (LP) nuclei and posteromedial nucleus (PO). Two other higher order relay nuclei are the laterodorsal nucleus (LD)—located in the anterior thalamus—and the mediodorsal nucleus (MD)—located in the midline thalamus.

First order relay nuclei receive inputs from brainstem afferents carrying sensorimotor information from the peripheral nervous system. These nuclei are sensorimotor information specific, for example, auditory information is received by the MGN, and somatosensory information is received by the VB. Thalamocortical neurons (TCNs) within these nuclei then relay this information to the sensorimotor associated cortical areas. Relay neurons within these nuclei also synapse on cells within the reticular nucleus.

A classical cortical processing view, that is coming under scrutiny (Burns & Rajan, 2021), is that once the sensorimotor signal is received by the layer IV of the cortex, it is sent to sub-granular layers (layers II and III) for higher order processing and lateral cortical spread, and infragranular layers (layers V and VI) for neocortical modulation. Despite the likelihood of increased complexity for this cortical process, layer VI corticothalamic neurons do indeed send reciprocal connections back to the thalamus (Jones, 2007). These corticothalamic projections synapse on thalamocortical neurons and inhibitory GABAergic neurons of the reticular nucleus of the thalamus. Projections from Rt and layer VI of the cortex synapse on TCNs of the original nucleus, serving to modulate their signal output to the cortex and Rt. This modulated signal—meaning a signal that does not come solely from the periphery—is considered higher order.

Higher order thalamic nuclei receive corticothalamic inputs from layer V of the cortex (Ojima & Murakami, 2011). This is the main distinction between a higher order nucleus or relay cell and a first order one. The driving input for higher order nuclei comes from the cortex, whereas the driving input for first order nuclei comes from ascending pathways (S. Murray. Sherman & Guillery, 2013). While all thalamic nuclei do receive

cortical input from layer VI, only higher order nuclei receive projections from layer V (Abramson & Chalupa, 1985; Llano & Sherman, 2008). First and higher order TC relay neurons are known to be critically important to the generation and maintenance of brain rhythms.

1.2.5 The reticular nucleus

The reticular nucleus is an inhibitory shell of the dorsal thalamus. It is comprised of mainly GABAergic neurons. It receives input from layer VI of the cortex and projects densely to the dorsal thalamus, situating it as a key component of an oscillating thalamocortical network. Early studies of the thalamus identified the reticular nucleus as the pacemaker of some thalamus-derived oscillation frequencies, such as sleep spindles. It was noted that sleep spindles are abolished in TCNs that are disconnected from the reticular nucleus (Steriade et al., 1985) and that the reticular nucleus in isolation from the dorsal thalamus, could still generate spindle rhythms (Steriade et al., 1987). These experiments did not rule out that the cortex may be regulating spindles within the reticular, however, in 1996, Timofeev and Steriade recorded from the thalamus of heavily anesthetized, decorticated cats and found that the sleep spindle was still generated (Timofeev & Steriade, 1996).

These GABAergic reticular interneurons synapses on first and higher order TCNs. They express parvalbumin, or are parvalbumin positive (PV^+), which has been used extensively to label and isolate these cells and determine their functional role in oscillations. In one such experiment, *in vivo* optical activation of these PV^+ interneurons of the reticular nucleus influenced the firing mode of TCNs, and generated state-dependent neocortical spindles (Halassa et al., 2011). This study highlights one example

of how the inhibitory drive from the reticular nucleus to the dorsal thalamus regulates TCN firing activity and thalamocortical oscillatory state. I will discuss TCN firing activity in more detail later in this text. The inhibition from the reticular nucleus is also a critical element in the transition from sleep to wakefulness (Brown et al., 2012; Fernandez et al., 2018). While it is well established that the inhibitory reticular nucleus is likely regulating the pace of many thalamocortical oscillations, the PV^+ interneurons only synapse within the thalamus, so relay of thalamic oscillations to the cortex is only achieved through TCN cortical connectivity.

1.2.6 A simplified example of the flow of information through the thalamus

To describe this circuitry and the flow of sensory information, I present a simplified example of somatosensory information processing: Brainstem afferents carrying somatosensory information from the peripheral nervous system synapse on TCNs within the primary somatosensory—the ventrobasal (VB)—nucleus. Depolarization of VB TCNs results in tonic firing of TCNs, which is received by cortical neurons and interneurons. Anatomically, the largest VB TCN input to the cortex is layer IV somatosensory—barrel—cortex. Layer VI corticothalamic neurons send reciprocal connections back to the thalamus. Here, they synapse on PV^+ interneurons of the reticular nucleus as well as TCNs of the VB and the higher order somatosensory nucleus, the posteromedial (PoM). Interneurons of the reticular nucleus synapse on TCNs of the VB and PoM, which connect reciprocally back to the cortex, and altogether, this generates thalamocortical oscillations. These thalamocortical oscillations are associated with the generation of higher order cognition, such as memory consolidation and motor response to stimuli.

This original sensory stimulus is not restricted to processing within the VB and PoM nuclei (somatosensory associated nuclei). Although not distinctly shown, lateral spread of thalamic information through the apical dendrites of pyramidal neurons to other cortical columns likely sends this input information back to other higher order thalamic nuclei, such as the anterior nuclei group (Rubio-Garrido et al., 2009). Through this highly interconnected thalamocortical network, an original sensory input possibly becomes the basis for and/or gets integrated into ongoing brain-wide activity, thalamocortical oscillations, that is continuously processing how to think, feel, and act.

1.2.7 A crucial component of thalamic information processing: synchronicity

The synchronized firing of neuronal populations is considered to underlie many higher order processes in the brain (Buzsáki, 2006). Synchronously firing cells within the thalamocortical circuit is the neural activity that underlies thalamocortical oscillations. Hypersynchronicity or desynchronization of this circuit is hypothesized to underlie some epilepsies, and aspects of ASD and schizophrenia (Beenhakker & Huguenard, 2009; Ludwig et al., 2003; Simon & Wallace, 2016). Synchronicity and timing of this circuitry is regulated by many mechanisms including feedforward inhibition (Bruno, 2011), and the expression of key ion channels within the membrane of thalamocortical neurons that generate tonic firing in response to depolarization and burst firing in response to hyperpolarization from the parvalbumin positive interneurons of the reticular nucleus (Fogerson & Huguenard, 2016). Without the relay of synchronous firing activity of thalamocortical neurons to the cortex, sensory perception and higher order motor and limbic functions would not exist as we know them.

1.3 Thalamocortical neuron membrane characteristics are foundational to thalamocortical oscillations

Thalamocortical neurons (TCNs) are glutamatergic relay neurons located within the relay nuclei of the thalamus. Their projections and connectivity are previously described. This section details the presence and necessity of key ion channels within their membranes that result in their specific firing activity within the thalamocortical circuit that is foundational to sensory perception and thalamocortical oscillations/brain rhythmicity.

Brainstem afferents depolarize TCNs during wake and arousal states, as they relay peripheral sensory information to the thalamus. At depolarized membrane potentials, TCNs that reach firing threshold produce a tonic firing response that is received by the cortex (M et al., 1984). Tonic firing of TCNs is critical for sensory perception. Of note, however, the alternate firing mode of TCNs, burst firing, also happens during wake states and appears to be critical for attention orienting to a stimuli, but it is never rhythmic, like during sleep (Guido & Weyand, 1995).

TCNs also receive GABAergic inputs from the reticular nucleus. During wake states, these synapses perform their typical inhibitory role, however, during sleep, the loss of the glutamatergic depolarizing tone from the brainstem transitions the membrane to a voltage at which the hyperpolarization received from the GABAergic synapses from the reticular nucleus results in rhythmic burst firing of TCNs, which is received by the cortex. In the first stage of sleep, Non-REM (NREM), the cortex begins to oscillate at a slow delta (1 Hz) oscillation frequency. Within the down states of this delta wave, a higher frequency and shorter latency oscillation, the sleep spindle (7-14 Hz) occurs. This

spindle oscillation, although recorded in the cortex, has been shown to be generated by the thalamus (Timofeev & Steriade, 1996).

1.3.1 TCNs are critical for spindle generation and spindle relay to cortex

Studies of thalamic circuitry indicate that it is the inhibitory neurons of the reticular nucleus, that are the generator and pacemaker of these spindles. In vivo, spindles have been shown to be generated in deafferented TRN neurons (Steriade et al., 1987), but are abolished in TCNs after they are disconnected from TRN neurons (Steriade et al., 1985). It has also been shown that specific deletion of ion channels in TRNs that underlie TRN burst firing reduces the power of sleep spindles (Astori et al., 2011). However, in vitro studies suggest that the TCN to TRN connectivity is still critical to spindle generation since disruption of these connections abolishes spindles (von Krosigk et al., 1993). Further, TRN neurons are inter-thalamic so relay of the spindle, or any signal, to the cortex is only achieved by the firing of TCNs. Even though TCNs do not generate sleep spindles, they maintain an important role in their maintenance and relay to cortex.

1.3.2 Tonic firing of TCNs is important for spindle generation while burst firing affects synchronicity of the thalamocortical network

While it has been proposed that the rhythmic burst firing of TCNs is critical to spindle maintenance—bolstered by in vivo studies which have shown that it is synchronous with up states of cortical spindles (Andersen & Eccles, 1962)—abolishment of TCN burst firing through deletion of a critical ion channel for the burst, the T-type Ca^{2+} channel, does not affect the density, length, or amplitude of cortical spindles (J. Lee et al., 2013). In this study, TCNs in mice with the deletion only fired tonic spikes during

spindles, and in the control mice, tonic spikes were more abundant than bursts specifically during spindle episodes, but not more abundant during non-spindle periods. In animal models where transmission of TCN burst firing to the cortex is disrupted, hypersynchronicity—which manifests behaviorally as the disorder: absence epilepsy—of the thalamocortical circuit is prevented (Kim et al., 2001). Thus, burst and tonic firing of TCNs are both critical TC oscillation maintenance.

1.3.3 HCN and T-type channels generate rhythmic burst firing

When TCNs burst fire during sleep, they do so rhythmically. They are pacemaker cells, meaning they fire rhythmically/oscillate. Another example of pacemaking cells are the electrically active cells of the sinoatrial node of the heart, which generate the rhythmic firing of a heartbeat. This property of TCNs is generated by key ion channels within their membranes: hyperpolarization-activated cyclic-nucleotide-gated (HCN) channels and low threshold T-type calcium channels. Together, the kinetic interplay of these channels gives rise to rhythmic bursting when the neuron is hyperpolarized. The frequency of this rhythmic bursting can drive or synchronize with the frequency of local and/or network oscillations, depending upon the neural circuit. In the case of TCN pacemakers, TCNs are hyperpolarized by GABAergic reticular neurons, which activates HCN channels and deinactivates T-type channels. The deinactivation of the low threshold T-type channels primes them for activation near resting membrane potential. Simultaneously, the opening of the HCN channels allows a depolarizing current into the neuron such that the membrane is depolarized to the potential that activates the T-type calcium channels, around -65mV. Activation of T-type calcium channels permits a large, depolarizing, calcium current to enter the neuron. This current results in a wave of

membrane depolarization that facilitates the occurrence of several rapid action potentials—a burst. Hyperpolarization starts this process over again, and the result is a train of evenly spaced bursts. The number of bursts that happen per second defines the frequency.

1.3.4 Cav3.1: T-type calcium channels expressed in thalamocortical neurons

Due to their de-inactivation, activation and inactivation kinetics, T-type calcium currents are important pace-making currents in pace-making systems throughout the body, such as the nodal like cells in the heart (Cribbs, 2010; Zhou & January, 1998). T-type calcium channels are inactivate at depolarized voltages, hyperpolarization removes this inactivation, and the activation voltage threshold of T-type calcium channels is typically around -55 mV (Zhou & January, 1998), which is a low-voltage activation compared to other Ca^{2+} channels, such as L-type. Thus, T-type calcium channels are usually activated when the membrane voltage recovers from hyperpolarization. T-type calcium currents can induce long rebound calcium spikes, or low threshold spikes (LTSs), which typically cause depolarization sufficient to reach threshold and cause multiple Na+ spikes (Perez-Reyes, 2006). Further, these calcium channels are transient-opening (T-type), with rapid inactivation time and small single-channel current, making the T-type calcium current a transient current at the whole cell level (Cheong & Shin, 2013). This transient activity facilitates the termination of an LTS.

The low-threshold, hyperpolarization de-inactivated, depolarizing wave that facilitates sodium mediated spiking in thalamocortical neurons was first described by Jahnsen and Llinas (Jahnsen & Llinas, 1984; Jahnsen & Llinás, 1984). They observed that in an in vitro, guinea pig slice preparation, release from hyperpolarized states (below

-60mV) produced an LTS that was inactivated when stimulated at membrane potentials positive to -55mV (**figure 1.2**). This current was determined to be T-type Ca^{2+} channel mediated, and has since been shown to be critical for thalamic functions, such as sleep stabilization, sensory information relay, and prevention of certain epilepsies (Anderson et al., 2005; Cheong & Shin, 2013; Knox et al., 2018b).

There are three types of calcium channels that can mediate T-type current: Cav3.1, Cav3.2 and Cav3.3, each of which is associated with a specific α1 subunit α1G, α1H, and α1I, coded respectively by the genes: CACNA1G, CACNA1H, and CACNA1H 30 (Iftinca, 2011). Cav3.1 is selectively expressed in thalamocortical neurons, whereas Cav3.3 and to a lesser extent, Cav3.2 are expressed in reticular neurons (Astori et al., 2011; Talley et al., 1999). This can be visualized in **figure 1.3**, where alpha-1G, 1H, and 1I show expression of 3.1, 3.2, and 3.3, respectively. The schematic to the right can be used to localize the dorsal thalamus versus the reticular. This is important because this difference in expression between the reticular and dorsal thalamus has been a critical component of dissecting the different functional roles of burst firing in thalamocortical neurons, versus reticular neurons (Astori et al., 2011; Matsumoto-Makidono et al., 2016; O'malley et al., 2020).

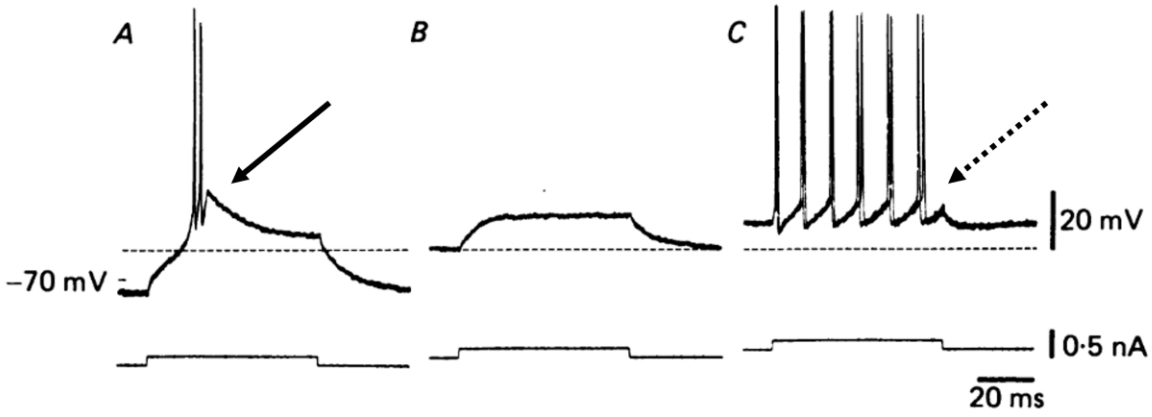

Figure 1.1.2 *Example burst and tonic responses of thalamocortical neurons, adapted from Jahnsen and Llinas 1984*

Patch clamp recordings of A) A direct stimulation response while a thalamocortical neuron was being constantly hyperpolarized, results in a post anodal LTS crested by a TTX sensitive cluster of action potentials, indicated by solid arrow. B) The same, subthreshold stimulation with no hyperpolarization produces not LTS or sodium dependent spikes. C) With further depolarization by a direct current, the current pulse produces a train of tonic action potentials, indicated with dotted arrow.

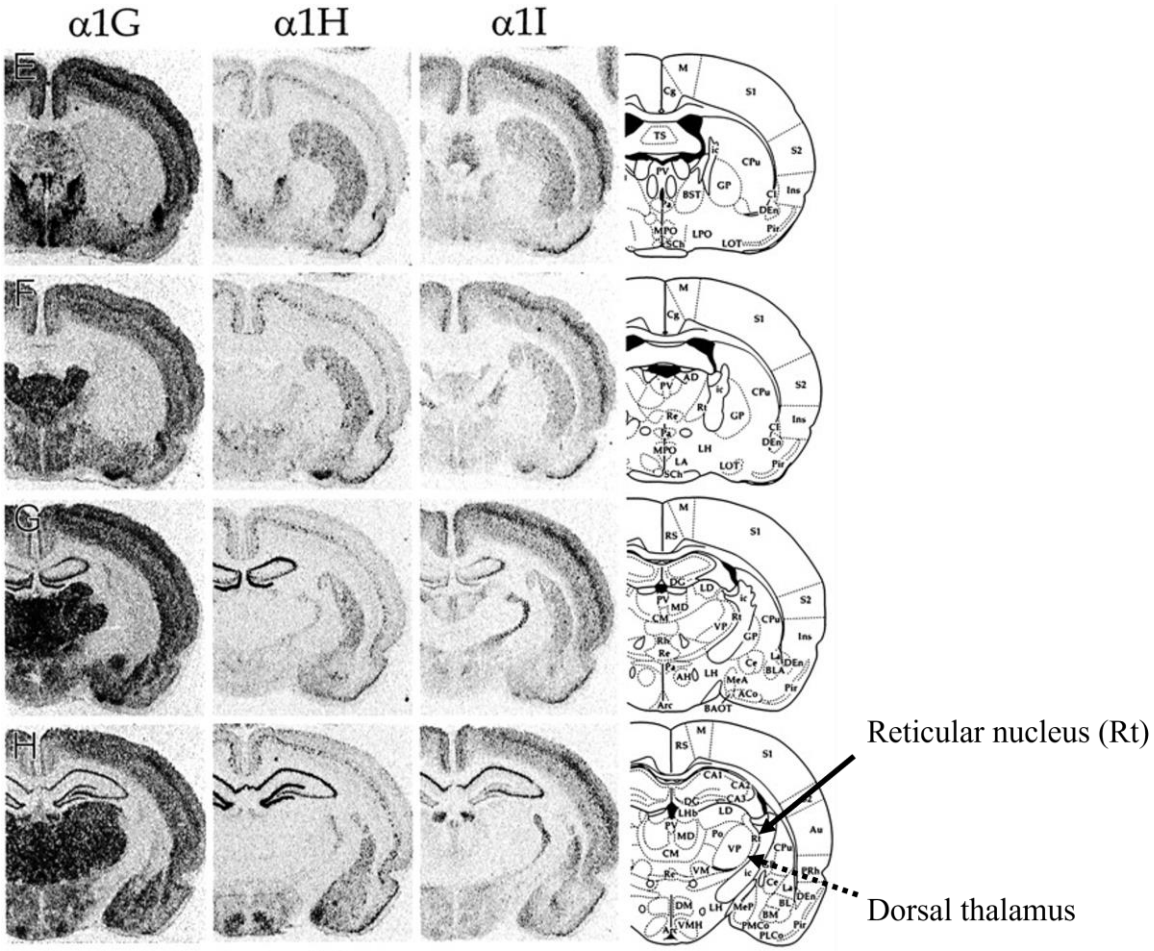

Figure 1.1.3 *Expression CaV 3.1 (α1G), 3.2 (α1H), 3.3 (α1H) in the thalamus of adult mice, adapted from Talley et al 1999.*

Sections were hybridized with oligonucleotides specific for α1G (left panels), α1H (middle panels), and α1I (right panels) and exposed to autoradiographic film. Far left panel: Expression of CaV 3.1 can be seen throughout the dorsal thalamus and selectively not in the reticular nucleus. Second and third panels: Expression of CaV3.2 and 3.3 can be seen selectively in the reticular thalamus, and not in the dorsal thalamus. Far right panel: coronal diagram of brain regions in the slices in each row. Rt=reticular, VP and PO=nuclei of the dorsal thalamus Solid arrow indicates reticular nucleus location on the border of the dorsal thalamus, indicated with a dotted arrow. (Talley et al., 1999)

1.3.5 HCN4 channels are expressed in thalamocortical neurons

Hyperpolarization-activated cyclic nucleotide-gated (HCN) channels are non-selective cyclic adenosine monophosphate (cAMP)-gated cation channels. They are expressed in the heart and brains of vertebrate animals, are activated at hyperpolarized potentials (less than -50mV), allow a non-specific cation current to depolarize cells, and are critical to pacemaking firing properties (Lüthi & McCormick, 1998). There are four subtypes of HCN channels, HCN1, HCN2, HCN3, and HCN4, whose voltage-dependent activation properties have quantitative differences. HCN2 and HCN4 channels are activated at the most hyperpolarized voltage and have the slowest activation/inactivation kinetics (Altomare et al., 2003), which makes HCN2/4 channels critical for low-frequency pacemaking for several reasons. The low hyperpolarized activation threshold prevents activation from subtle membrane fluctuations, only large hyperpolarization of the cell membrane activates it, making I_H more stable and selectively responsive. Secondly, the slower activation/inactivation kinetics of HCN2/4 make I_H last longer and thus control the rhythmic oscillations at a lower frequency. Unlike HCN1, which is predominately expressed in the cortex and hippocampus, and HCN2 which is expressed in the cortex, thalamus, midbrain and hindbrain, HCN4 is selectively expressed in the thalamus (Abbas et al., 2006; Notomi & Shigemoto, 2004). The integral role that the activity of I_H, or the funny current (I_F –my initials), plays in thalamocortical bursting and pacemaking activity, was first described in 1990 by McCormick and Pape, and was observed in guinea pig and cat recordings (McCormick & Pape, 1990). Since this description, knockout models of HCN4 have defined the critical role that I_H plays in the rhythmicity of the thalamocortical network (Zobeiri et al., 2019).

1.3.6 Potassium channels expressed in thalamocortical neurons

These channels are not the only ones critical for TCN contributions to TC oscillations. Potassium channels contribute to subthreshold membrane characteristics that promote oscillations (Amarillo et al., 2014, 2018), and they also play a critical role in their rapid generation of action potentials during burst and tonic firing. Kv3.X channels are involved in the rapid repolarization of an action potential, and their presence in neurons correlates with narrow APs, fast afterhyperpolarization, and high-frequency firing beyond 200 Hz (Rudy et al., 1999). These channels are activated when the membrane is depolarized to potentials more positive than −20 mV, which is 10–20 mV more depolarized than any other known mammalian voltage-gated K+ channel (Coetzee et al., 1999). Kv3.1 and Kv3.3 subunits are expressed in the thalamus, but their expression is highest in the reticular nucleus (Weiser et al., 1994, 1995), where deletion diminishes TRN rebound burst firing and disrupts TC oscillations in vitro and in vivo (Espinosa et al., 2008a).

The voltage gated potassium channel 3.2 (Kv3.2) is a subtype of Kv3.X potassium channels that rapidly repolarizes the membrane and has delayed deactivation (current kinetics in figure below). By using *in situ* hybridization and immunohistochemistry, roughly 90% of Kv3.2 mRNA in the entire CNS, was localized to TCNs in the thalamus (Rudy et al., 1999). Kv3.2 is required to sustain high frequency firing rates by rapid repolarization of the membrane in TCNs, and genetic KO of Kv3.2 reduces peak firing rate (Kasten et al., 2007). Together, these data indicated that expression of Kv3.2 channels in TCNs is critical to overall TC oscillatory function. Below is a figure excerpt from Rudy et al. showing the select expression of Kv3.2 in the

thalamus, and it's rapid activation and delayed rectification current kinetics (**figure 1.4**) (Rudy et al., 1999).

The transcriptional control of these channels in general is poorly understood. Work from our lab has demonstrated that the transcription factor, Shox2, is important for regulation of T-type and HCN channels in the thalamus (Yu et al., 2021) and our gene ontology analysis implicates that it plays a role in the regulation of potassium channels as well.

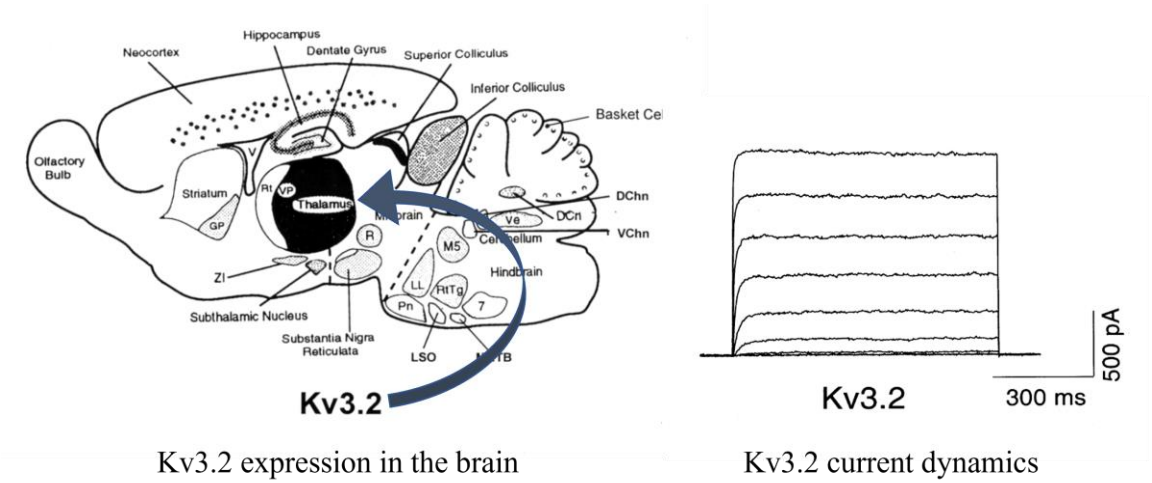

Kv3.2 expression in the brain Kv3.2 current dynamics

Figure 1.4 *The delayed rectifier, Kv3.2 is selectively expressed in the thalamus, and has rapid activation and delayed rectifier current kinetics, adapted from Rudy et al 1999.*

Left) Distribution of Kv3.2 mRNA in the rat brain (similar patterns have been observed for some Kv3 transcripts in mice). The levels of expression of the Kv3.2 gene based on in situ hybridization studies by Weiser et al.21 are represented in these diagrams by different grades of shading. Note the high expression in dorsal thalamus and absence in reticular nucleus. Abbreviations: 7, facial nucleus; DChn, dorsal cochlear nucleus; DCn, deep cerebellar nuclei; GP, globus pallidus; LL, lateral lemniscus nuclei; LSO, superior olive; M5, trigeminal motor nucleus; MNTB, medial nucleus of the trapezoid body; Pn, pontine nuclei; R, red nucleus; Rt, reticular thalamic nucleus; RtTg, reticulo tegmental nucleus of the pons; VChn, ventral cochlear nucleus; Ve, vestibular nucleus; VP, ventral-posterior complex of the dorsal thalamus; ZI, zona incerta. **Right)** Kv3.2 current in transfected HEK293 cells. Families of K+ currents recorded from a holding potential of −80 mV during depolarizing pulses from -40mV to +40mV in 10 mV increments.

1.4 Shox2 as a key regulator of TCN characteristics in mice

Neuropsychiatric disorders that arise from oscillation disruption are largely considered to be developmental disorders. During development, cell types differentiate through the expression of different genetic factors, such as transcription factors. The expression of certain transcription factors determines cell migration, morphology, membrane characteristics, and ultimately function of a cell within the neural circuit. With the thalamocortical neuron as a key cell type in the generation and maintenance of thalamocortical oscillations, a transcription factor that gives rise to their connectivity and membrane properties is of principal interest to the study of neuropsychiatric disorders.

1.4.1 SHOX

The short stature homeobox gene (SHOX) encodes a transcription factor that has been associated with Leri-Weill dyschrondrosteosis and Turner Syndrome (Belin et al., 1998; Rao et al., 1997). Patients with these syndromes are at increased risk for various neurodevelopmental pathologies, including learning disabilities and developmental delay, epilepsy, and abnormal visuospatial, social, and executive function. While these neurodevelopmental deficits are consistent with disrupted thalamic function, the mechanisms of these impairments are unknown.

1.4.2 Shox2

Rodents do not express the SHOX gene but do express a closely related paralog with identical DNA-binding homeodomains, called Shox2. It is believed that mouse Shox2 (mShox2) has assumed the function of hSHOX and hSHOX2. Shox2 is a member of the homeobox family of genes containing a 60-amino acid residue motif that

represents a DNA binding domain. Significantly, investigation of noncoding elements functioning as enhancers that are conserved between hSHOX and mShox2 revealed that the deeply conserved sequences are neural enhancers, suggesting ancestral function of SHOX and mShox2 in the central nervous system, justifying investigation of the role of mShox2 in the CNS. The role of Shox2 in nervous system development is unknown, but the Nestin-Cre; Shox2fl/- mouse that causes deletion of *Shox2* in neurons dies at approximately postnatal day (PND) 1, suggesting that CNS-expressed Shox2 is necessary for survival, however the specific mechanisms of this lethality are not known. In addition, *Shox2* expression is necessary for pacemaker activity in the sinoatrial node and other areas involved in pacemaker activity. Previous studies found that Shox2 plays a decisive role in the differentiation of pacemaker cells in the sinoatrial node of the heart and pulmonary vein. These areas of the cardiovascular system possess pace-making automaticity mediated by the prominent expression of pacemaker-related HCN channels and T-type calcium channels. Another study found that Shox2 is expressed in a subpopulation of excitatory interneurons rhythmically active during locomotor-like activity in the ventral spinal cord.

Our recent publication shows that *Shox2* is expressed in thalamocortical neurons during development and into adulthood, and that Shox2 regulates expression of several ion channels important for TCN firing properties. This control of ion channel expression leads to increased seizure susceptibility in *Shox2* knockdown mice. Considering the information presented, in this dissertation I propose that Shox2 is a transcription factor that is important for stabilization of TCN firing properties and thalamocortical oscillations, and proper thalamus function in mice.

Specifically, I hypothesized that the activity of the transcription factor, *Shox*2, within the thalamus is (aim 1) *critical to thalamocortical neuron expression of ion channels that drive their unique firing characteristics*. Without these firing characteristics, (aim 2) *relay of sensory information to the cortex is likely to be impaired*, and the (aim 3) *thalamocortical oscillations* that are critical to a myriad of higher order brain functions, *will be disrupted*. **Figure 5** is a graphical abstract of this hypothesis.

These aims are designed to determine whether Shox2 is a critical component of thalamic function in mice and present it as a possible component of thalamus-related neuropsychiatric disorders.

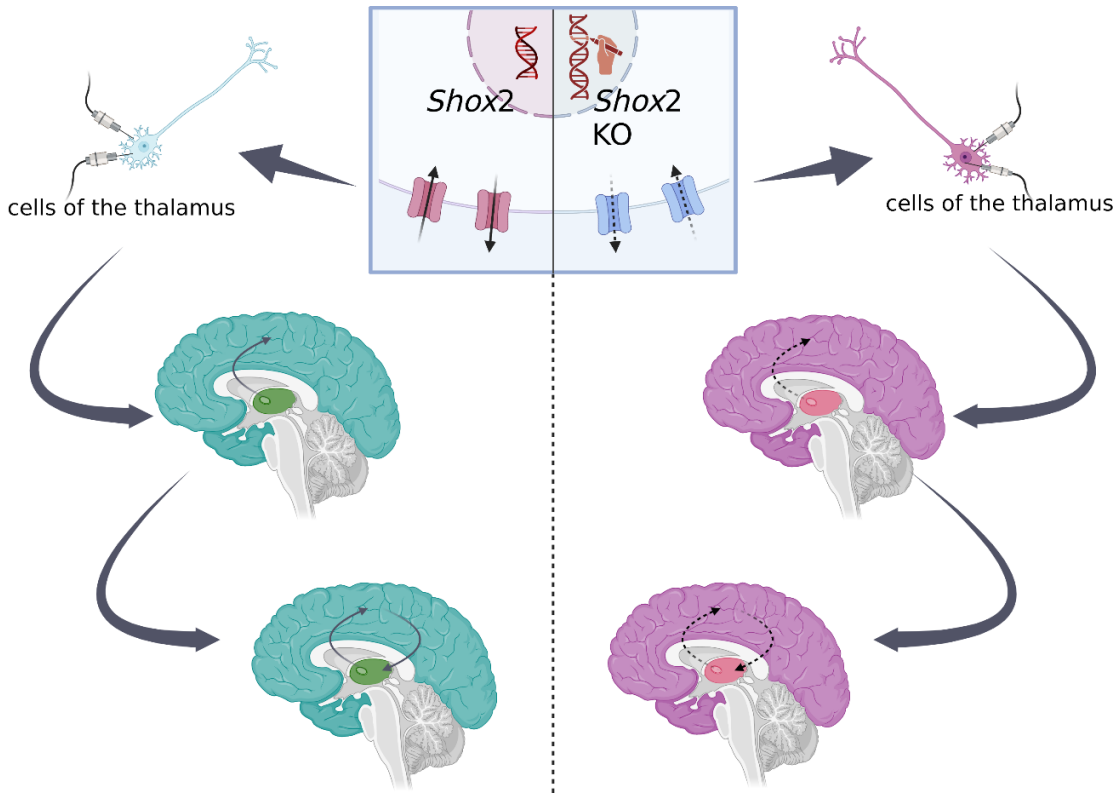

Figure 1.5 *Graphical abstract of dissertation.*

Left (starting from top): I hypothesize that activity of the transcription factor, Shox2, within the thalamus of mice, is critical for ion current dynamics that underlie firing characteristics of thalamocortical neurons, relay of sensory information, and proper thalamic oscillatory activity. **Right (starting from top):** I test this hypothesis by generating a within thalamus, Shox2 KO, determining that key ion currents are reduced, burst and tonic firing of TCNs is disrupted, sensory perception is impaired, and thalamus-derived spindle oscillation occurrences are significantly reduced.

Chapter 2 Aim 1: *Shox2* expression in ventrobasal thalamocortical neurons regulates membrane characteristics and firing properties

2.1 Introduction Aim 1: Firing characteristics in a first order nucleus (VB) and the hypothesized involvement of Shox2

TCNs are intrinsic oscillators that burst fire in response to hyperpolarization and tonic fire in response to depolarizations. These properties are generated by TCN membrane expression of specific ion channels, notably, T-type Ca^{2+} and HCN channels, and subtypes of potassium channels (Amarillo et al., 2014, 2018; Espinosa et al., 2008b). T-type Ca^{2+} and HCN channels mediate TCNs synchronous burst firing in response to hyperpolarization (Jahnsen & Llinas, 1984; Jahnsen & Llinás, 1984; Lüthi & McCormick, 1998), while potassium channels are critical to timing of tonic firing in response to depolarization (Kasten et al., 2007; Rudy & Mcbain, 2001).

Work from our lab has demonstrated that the transcription factor, Shox2, is important for regulation of T-type and HCN channels in the thalamus (Yu et al., 2021). Previously, we found that Shox2 is expressed in TCNs in adult mice. TCNs express HCN2, HCN4, and Cav3.1 channel protein subunits that are important for firing properties of TCNs, and we hypothesized that Shox2 coordinates the expression of genes for these ion channels to affect action potential firing activity of TCNs. Using global conditional KO animals, we further demonstrated that Shox2 is important for firing properties likely by affecting expression of mRNA of multiple ion channels, including Cav3.1, HCN2, and HCN4.

From these studies, I **hypothesized** that expression of Shox2 in thalamocortical neurons is crucial for their burst firing properties. To test this hypothesis, I utilized 2 mouse models: Shox2Cre;Ai14 (an RFP reporter mouse where RFP expression indicates Shox2 expression), and a *Shox*2$^{fl/fl}$ mouse, where the *Shox*2 gene is surrounded by lox-p sites and in the presence of Cre, the gene encoding for *Shox*2 is excised. To generate a thalamus specific KO, I stereotactically injected a GFP-cre virus into the VB of P21 Shox2$^{fl/fl}$ mice. With these two models, I was able to obtain patch-clamp recordings from *Shox2*-expressing, *Shox2*-negative, and Shox2-KO TCNs. I then compared membrane and firing properties of these three groups of thalamocortical neurons.

To first determine if there were intrinsic differences in the properties TCNs that express Shox2 and TCNs that do not, in **aim 1a**, I compared *Shox2*-expressing versus *Shox2*-negative TCNs. I **hypothesized** that *Shox*2-expressing TCNs in the VB will have significantly more T-type Ca^{2+} and HCN current, generating a larger burst with more action potentials per burst than *Shox*2-negative TCNs. Then, to determine if loss of Shox2 disrupts membrane and firing characteristics in TCNs, in **aim 1b** I compared these characteristics in *Shox2*-expressing versus *Shox2* KO TCNs. My hypothesis was similar to that of aim 1a. I **hypothesized** that *Shox*2-expressing TCNs have significantly more T-type Ca^{2+} and HCN current, generating a larger burst with more action potentials per burst than *Shox*2-KO TCNs. Together, these two subs-aims address the overall aim of determining whether *Shox2* expression is critical for membrane and firing characteristics of TCNs in the VB nucleus of the thalamus. **Figure 2.1** is a graphical representation of aim 1.

2.2 Methods Aim 1

2.2.1 Methods Aim 1a: Shox2-expressing versus *Shox2* negative TCNs.

Shox2cre mice (obtained from the Chen lab) were crossed with Ai14 reporter mice (obtained from JAX laboratories), generating a *Shox2*-RFP reporter mouse. Since cell visibility in the thalamus is low in older mice due to myelination, Cre positive, P21 mice were used for electrophysiology experiments.

Electrophysiology slice preparation: Mice were anaesthetized with isoflurane and decapitated. Brains were quickly removed and immersed in oxygenated (95% O_2 and 5% CO_2), frozen to a slurry, sucrose cutting solution (in mM: 252 sucrose, 2.5 KCl, 26 $NaHCO_3$, 1.25 $NaH_2PO_4 \cdot H_2O$, 10 Glucose, 1 $CaCl_2$, 5 $MgCl_2$). 400µm coronal slices that contained the largest cross-sections of the VB nucleus (depicted in **figure 2.2, left**) were obtained with a Vibratome Series 3000 Plus Tissue Sectioning System. The collected slices were transferred to 37˚C, oxygenated artificial cerebral spinal fluid (aCSF: in mM, 125 NaCl, 2.5 KCl, 26 $NaHCO_3$, 1.24 NaH_2PO_3, 25 Glucose, 2 $MgSO_4$, 2 $CaCl_2$) for 20 minutes. Slices were then placed in oxygenated, room temperature, aCSF for at least 45 minutes before recordings started. On the electrophysiology rig, slices were continuously perfused with oxygenated, 32˚C aCSF. *Shox2*-expressing TCNs were identified by their location within the VB and their expression of RFP, whereas *Shox2*-negative TCNs were identified by location and absence of RFP expression. Glass pipettes were pulled to a resistance of 3-5 MΩ, filled with internal solution (in mM, 120 Kglu, 20 KCl, 0.2 EGTA, 10 Hepes, 4 NaCl, 4 Mg2+ATP, 14 phosphocreatine, 0.3 Tris GTP—pH adjusted to 7.2-7.25 by KOH , osmolarity 305-315mOsm) and placed on a silver chloride electrode

attached to a headstage. The headstage output to a MultiClamp 700B amplifier, Digidata 1322A digitizer, and a PC running Clampex 10.3 software (Molecular Device).

To determine the effect of *Shox2* expression on T-type Ca^{2+} current in Shox2 TCNs, the following properties were investigated in the presence of 1 μM TTX to block voltage-gated sodium channels:

T-type Ca^{2+} current: *Shox2*-expressing and *Shox2*-negative TCNs were patched and in voltage clamp and a series of three steps were performed. First, the cell was held at -50 mV as a resting condition, second the cell was hyperpolarized to -100mV for one second to effectively de-inactivate T-type channels, and third the cell was depolarized to one of a series of membrane voltages starting at -90 mV and increasing to 0 mV in increments of 5 mV. To isolate the T-type current, the de-inactivation step was replaced with a step in which the cell was held at -50 mV. To confirm the elicited current was T-type, these experiments were redone in the presence of a T-type channel blocker, 2μM TTAP2.

To analyze activation and amplitude of the T-type current, the current during each voltage step without activation of T-type channels was subtracted from the current with activation. The timing and amplitude for the peak current of each membrane voltage step was recorded for analysis.

To determine the effect of *Shox2* expression on the HCN activity in *Shox2*-expressing versus *Shox2*-negative TCNs, the following experiments were performed:

Sag: In current clamp, cells were hyperpolarized by -350 pA current with consecutive steps, increasing by +10 pA increments for one second. To calculate sag, which is a gradual depolarization of the membrane while TCNs are

hyperpolarized and is generally attributed to the HCN current, the difference between the membrane voltage at the end of the one second hyperpolarization and the beginning of the hyperpolarization was calculated.

HCN current: In voltage clamp, the HCN current was elicited by hyperpolarizing the cell membrane to -150mV for 1 second with incremental steps increasing by 20pA from -50 mV. The amplitude of HCN current will be measured as the difference between the end current of one second hyperpolarization and the beginning instantaneous current at -150mV hyperpolarization.

To determine the effect of *Shox2* expression on the post-anodal burst in *Shox2*-expressing versus *Shox2*-negative TCNs, the following experiments were performed:

Area under the curve: In current clamp, a series of one second hyperpolarizing steps, beginning at -350pA and increasing by 40 pA for 9 traces, were run. The burst following each hyperpolarization was analyzed for the area under the curve. This was done by selecting the section of the trace immediately following the release of hyperpolarization from the moment the membrane potential crosses resting of the neuron until 0.295s after that moment. The entire trace was zeroed to the resting membrane potential of the neuron, and then integrated. The area was then plotted against the stimulus and a two-way ANOVA to determine effects of expression, *Shox2*-expressing versus *Shox2*-negative TCNs, was used to investigate differences.

Number of action potentials per post-anodal wave: On the same traces, event analysis was performed with a threshold set to 20mV above the burst wave. Action potentials were considered as events that passed this threshold.

To determine the effect of *Shox2* expression on *membrane properties* in Shox2 TCNs, the following properties were investigated as described:

Input resistance: In current clamp, an IV protocol (a series of currents were injected for one second, beginning at -350pA and increasing by 40pA each sweep until it reaches 500pA) was performed. An IV curve (plot of membrane voltage versus current applied) was generated, and input resistance was defined as the slope of the linear portion of the line (approximately the section from -80mV to 40mV membrane potential).

Membrane potential: Membrane potential was determined to be the average of a 30 second trace during a time of no membrane activity and while the cell is not being injected with current. Based on recordings thus far, TCN resting membrane potential averages around -70mV, thus, TCNs with a RMP less than -55mV were not considered for analysis.

2.2.2 *Methods Aim 1b: Shox2*-expressing versus *Shox2* KO TCNs.

Prenatal KO of *Shox2* is lethal, thus, a postnatal induction of *Shox2* KO must be utilized. To generate a targeted VB KO mouse model, I made bilateral VB injections to P21 $Shox2^{fl/fl}$ littermates with either a GFPcre virus to generate and label *Shox2* KO cells, or a nonspecific RFP virus to generate and label control cells. After surgery, I allowed a one-week incubation period for the virus to take effect and then euthanized the mice at P28 for electrophysiology. This model is diagramed in **figure 2.2, right.**

Surgeries: Stereotaxic surgeries were performed on P21, Shox2$^{fl/fl}$ mice. Mice were anesthetized with isoflurane, with an oxygen flow rate of 1 L/min and an isoflurane concentration of 2-3% for induction, and 0.5-1.5% for maintenance. Once fully anesthetized, as determined by the lack of response to toe pinch, tail pinch, and eye poke as well as a slowed respiratory rate, ophthalmic ointment was applied to both eyes and subcutaneous buprenorphine was injected into the scruff. Next, mice were ear-barred and secured within a stereotaxic surgery rig. To remove hair from the surgery region, I briefly applied Nair, rinsing within 60 seconds. Sterile ethanol wipes and iodine were used to prep the surgery site before a small, lateral incision to the center of the head was made with sterilized scissors and forceps. Forceps and a sterilized razor were used to clear the skull of additional tissue layers. Bregma and lambda were located and aligned to within .02 horizontal mm of each other. Then, preloaded pipettes of virus in the nanoject injector were used to find the location of holes to be drilled on left and right sides of the skull. Equal volumes (300nL of approximately $7x10^{-12}$ titer virus in saline, diluted at a 1:1 ratio) of CTL and KO virus were injected into P21 VB location (AP: 1.1, ML: 1.5, DV: 3.4; as determined previously by ink injections). Surgery sites were closed using vetbond, and mice are allowed to recover on a heating pad. 1-2 weeks later, mice were used in electrophysiology experiments.

Electrophysiology methods are the same as reported in aim 1a. Coronal slices that contain the largest cross-sections of the VB nucleus were continuously perfused with 32˚C aCSF. *Shox2* KO TCNs were identified by their location within the VB and their expression of GFP, whereas control TCNs were identified by location and expression of RFP. Of important note, GFP-expression does not indicate that this cell previously

expressed *Shox2* or was a *Shox2*-expressing TCN, thus some GFP cells that were recorded from and are included in the KO results, are not KO cells, rather they are *Shox2*-negative TCNs.

RT-qPCR tissue processing and analysis for mRNA expression: To confirm knockdown of Shox2 in the $Shox2^{fl/fl}$+ viral AAV2cre model, we performed unilateral injections of a GFPcre virus into the left VB of $Shox2^{fl/fl}$ mice, and control, non-specific RFP virus into right VB, creating a within mouse control with *Shox2* KO on the left and control conditions on the right. At P35, we analyzed the VB for *Shox2* mRNA expression. Unilateral KO male and female mice were anesthetized by isoflurane inhalation followed by decapitation. The brains were removed and a 1-mm thick slice through the thalamus was removed via razor blade, the location of cut was determined by Paxinos and Franklin Mouse Brain Atlas. VB thalamus tissue was collected with 1-mm stainless steel punching tool. The collected tissues were stored in 50 μL RNA later solution and stored in −80 freezer. To homogenize collected tissues, 350 μL of RLT lysis buffer from Qiagen RNeasy Mini Kit was added to the tissue and homogenized with a pestle mortar. The homogenized tissues went through sonication with a Q55 sonicator (Qsonica) and then 350 μL cold, 70% EtoH was added to the sample. After this, I, followed the instructions book from Qiagen RNeasy Mini Kit. Once RNAs were isolated from tissues, I performed qRT-PCR with the *Shox2* primer (Forward primer (5'→3') CCGAGTACAGGTTTGGTTTC, Reverse primer (5'→3') GGCATCCTTAAAGCACCTAC) and normalized with GAPDH (F: GTCGGTGTGAACGGATTTG, R: TAGACTCCACGACATACTCAGCA) to determine expression of *Shox2* mRNA.

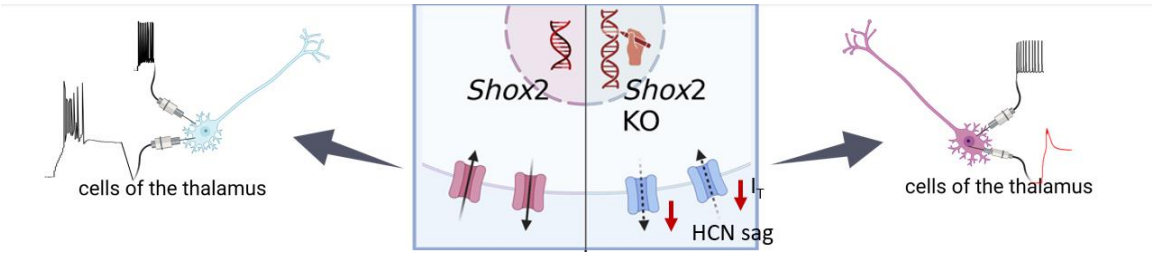

Figure 2.1 *Aim 1 Graphical abstract*

(Left) Schematic depicting the hypothesis that Shox2 expression in the thalamus underlies proper ion channel regulation that is critical for characteristic burst and tonic firing of TCNs, and that loss of Shox2 **(right)** will reduce membrane current activity and reduce firing in burst and tonic mode.

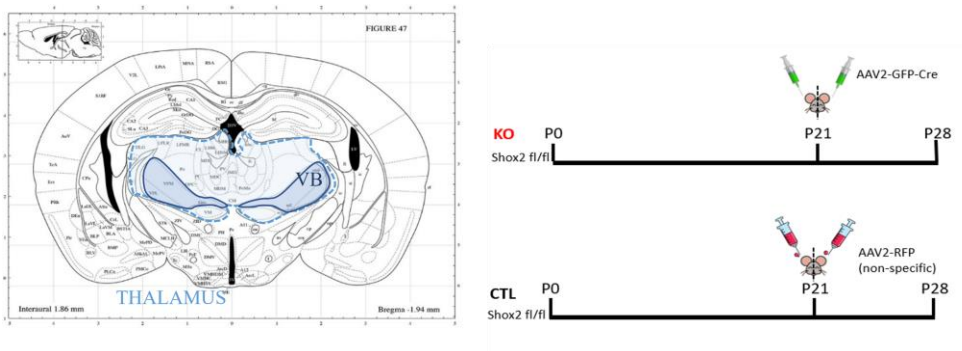

Figure 2.2 *Electrophysiology methods-coronal section used and experimental timeline.*

(Left) Image from brain atlas of coronal section used in slice electrophysiology experiments. The entire thalamus is outlined in light blue and the ventrobasal (VB) nucleus is outlined in dark blue. This section provides the largest cross-sectional area of the VB for maximum ability to locate VB TCNs. **(Right)** Schematic depicting experimental mice and timeline used for generating Shox2 KO cells and fluorescent control cells to patch and record from. Littermate, P21, $Shox2^{fl/fl}$ mice received either AAV2-GFPcre stereotactic VB injections, creating Shox2-KO TCNs, or AAV2-RFP stereotactic VB injections, creating fluorescent control TCNs. Patch clamp recordings were performed at least a week after surgeries.

2.3 Results Aim 1

2.3.1 *Results Aim 1a: Shox2*-expressing versus *Shox2*-negative TCNs

I investigated *Shox2*-expressing TCNs in the VB nucleus, which is a nucleus that consists largely of first order relay TCNs. I sought to determine if *Shox2*-expressing TCNs were a distinct subtype of TCN in the VB by recording from *Shox2*-expressing TCNs and *Shox2*-negative TCNs. However, there were relatively few *Shox2*-negative TCNs (n=5) as compared to *Shox2* expressing TCNs (n=12) within the VB. We observed fewer action potentials per burst in *Shox2*-negative TCNs, but there were not enough negative recordings to make a conclusive statement. It may be that *Shox2*-negative TCNs are the sparse, higher order TCNs within the VB, but this would mean that *Shox2*-expressing TCNs are a subset of first order TCNs. I do not think *Shox2*-expressing TCNs make up only a subset of first order TCNs, because, according to the expression in the reporter mouse, they project to layer I cortex (**figure 3.3**), which is higher order TCN specific. TCNs with multiple spikes are considered to be first order, existing in the VB, although few TCNs with single spikes do exist in VB (Desai & Varela, 2021). TCNs with single spikes have been reported to be interneurons, however, very few interneurons exist in VB (Campbell et al., 2020).

Recordings from *Shox2*-expressing versus *Shox2*-negative TCNs yielded no obvious differences in that both responded with tonic firing in response to depolarization and burst firing after release from hyperpolarization. This can be seen in example voltage responses to a range of current injections in *Shox2*-expressing (top, black traces) versus *Shox2*-negative (bottom, blue traces) (***figure 2.3***). Since differences in burst firing have been reported within this nucleus, we analyzed burst firing timing and action potential

frequency between the two cell types. Both cell types yielded post-anodal response with a low-threshold Ca^{2+} spike that facilitated either a burst or a single action potential. Multiple action potential bursts were more likely to be *Shox2*-expressing (n=8/12) whereas single action potentials were more likely to be *Shox2*-negative (n=3/5) (***figure 2.4.a***).

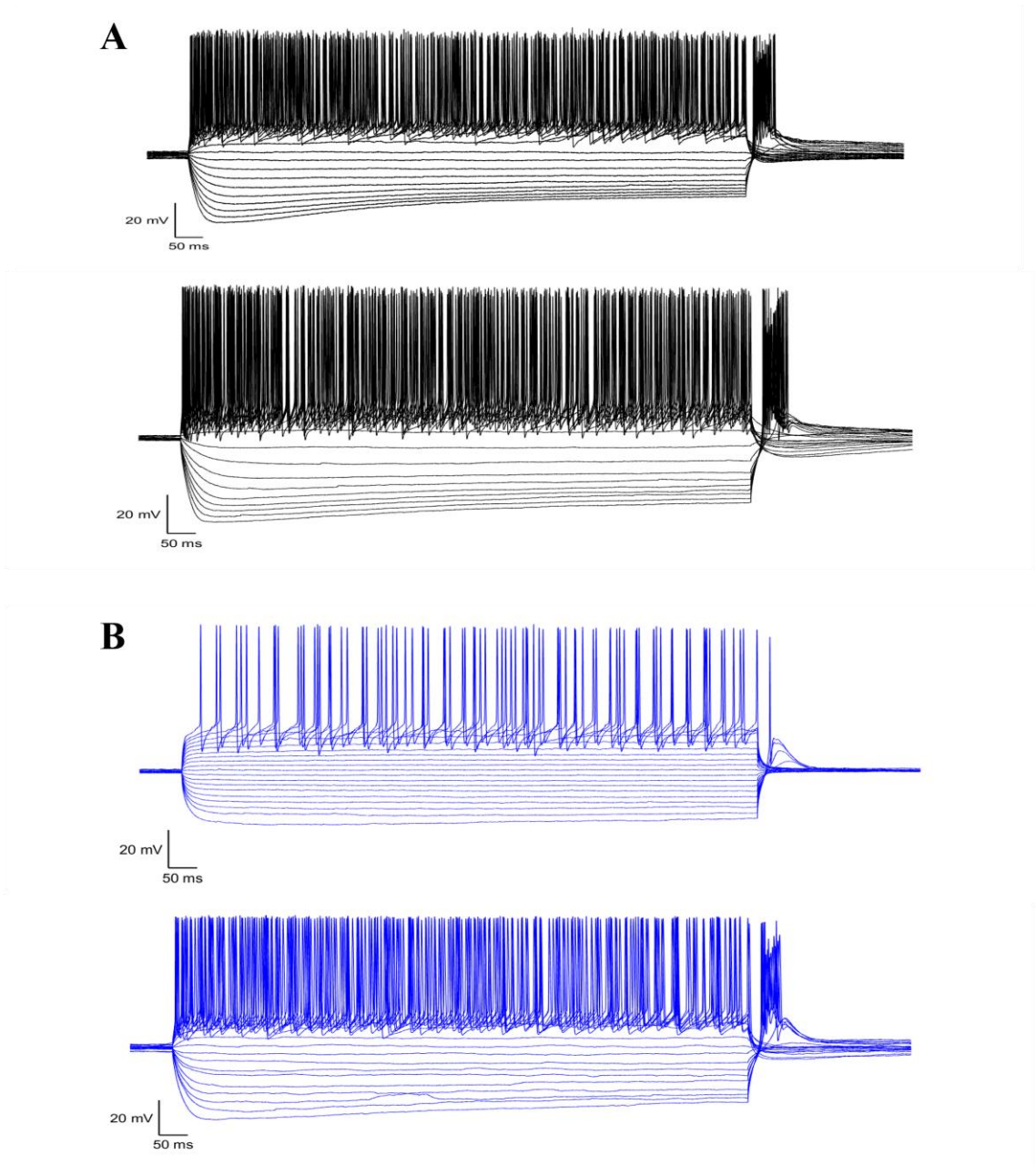

Figure 2.3 Example voltage responses of *Shox2*-expressing versus *Shox2*-negative TCNs

Figure 2.3 Example voltage responses of *Shox2*-expressing versus *Shox2*-negative TCNs

A: Example voltage responses of 2 Shox2-expressing TCNs (black) to a range of current injections, starting at -350pA and in increasing increments of 40pA until the final step of 410pA. Note the rapid tonic firing responses to depolarization, HCN sag, and rebound burst facilitating multiple action potentials. **B**: Example voltage responses of 2 Shox2-negative TCNs (blue) to the same range of current injections. Both display rapid tonic firing responses to depolarization, but in the top blue example, the post-anodal response only facilitates a single action potential, and there is negligible HCN sag.

Post anodal spike timing of Shox2-expressing *v Shox2*-negative *TCNs*

Literature supports the theory that post-anodal responses of single action potentials and multiple action potential burst firing TCNs play two different roles. Fort this reason, when comparing *Shox2*-expressing to *Shox2*-negative TCNs, I subdivide them into two different post-anodal response groups: single AP response and multiple AP burst **(figure 2.4.a)**.

Post anodal spike timing of Shox2-expressing *v Shox2*-negative *TCNs that respond with multiple APs per burst*

To determine if there was a difference in timing of action potentials between the *Shox2*-expressing to *Shox2*-negative TCNs that have post-anodal responses of multiple action potential bursts, I analyzed the frequency of firing during bursts **(figure 2.4.b, left).** The n for *Shox2*-negative TCNS bursting is low (n=2), however, the spread of *Shox2*-expressing burst frequency encapsulates the *Shox2*-negative TCNs, indicating that there is a range of frequencies for Shox2-expressing burst firing. There was no significance test run due to the low n. To further analyze the timing, I measured the time between each consecutive spike (intraburst interval) during a burst. *Shox2* expressing and negative TCNs followed a similar time spacing between burst APs **(figure 2.4.b, right).**

To determine if there was a difference in the onset of the burst between *Shox2*-expressing and *Shox2*-negative TCNs, I analyzed the timing of the first action potential of each burst and subsequent APs. Once again, there is a range of when the bursts start, however, the average of *Shox2*-expressing bursts start before *Shox2*-negative bursts with multiple APs (**figure 2.4.c**).

Post-anodal spike timing of Shox2-expressing *v Shox2*-negative *TCNs that respond with single APs*

Of the cells that had only one AP in response to release from anodal stimulation, (*Shox2*-expressing n=4, *Shox2*-negative n=3), there is a significant delay in the *Shox2*-expressing TCNs APs (**figure 2.4.d**). These data indicate that there may be a difference between *Shox2*-expressing and *Shox2*-negative burst timing, however, a greater number of *Shox2*-negative cells need to be recorded from to make any conclusions about burst phenotypes. A possible solution to the low number of *Shox2*-negatvie TCNs to be recorded from would be to investigate bursting properties another nucleus with a higher percentage of *Shox2*-expressing TCNs, such as in a higher order nucleus.

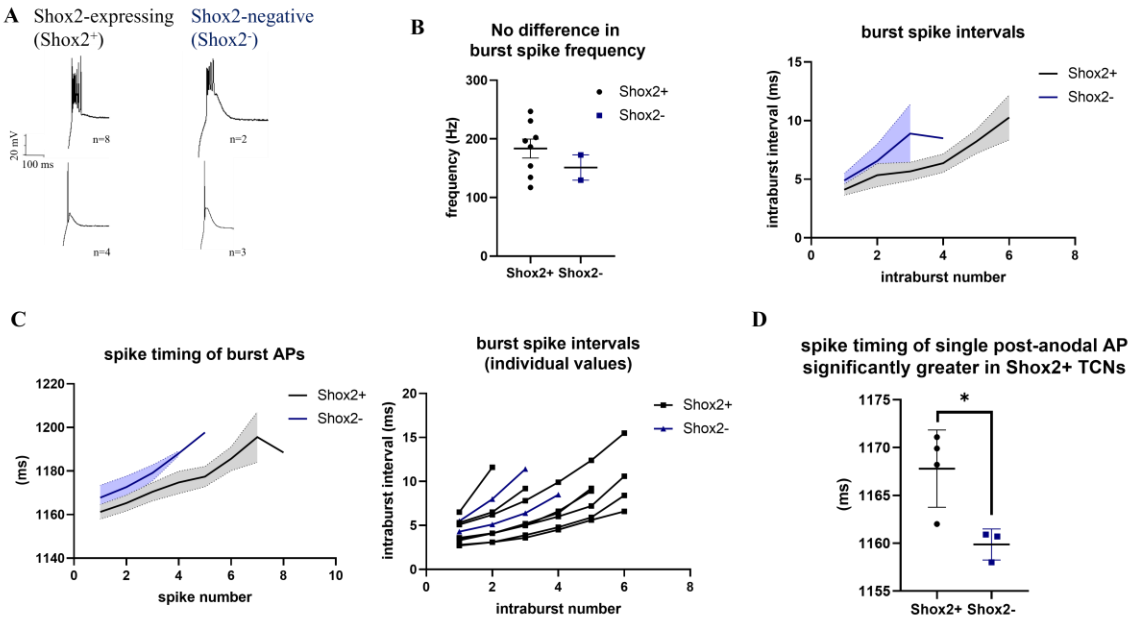

Figure 2.4 *Comparing post-anodal spike timing in Shox2-expressing versus Shox2-negative TCNs*

A) Example post-anodal responses from (left, top and bottom) Shox2-expressing TCNs and (right, top and bottom) Shox2-negative TCNs. Both cell types exhibit multiple or single AP responses to anodal stimulation, however, Shox2-expressing TCNs are more likely to have multiple action potentials (n=8/12), and Shox2-negative TCNs are more likely to have single action potential responses (n=3/5). **B)** When comparing the frequency of action potentials during burst clusters in *Shox2*-expressing versus *Shox2*-negative (left) and inter-spike intervals (right) no significant differences were found, due to low n. **C)** When comparing the timing of the first spike of a burst clusters in *Shox2*-expressing versus *Shox2*-negative TCNs, no significance was found again due to low n. **D)** When comparing the timing of post-anodal single action potential responses in *Shox2*-expressing versus *Shox2*-negative TCNs, there was significant delay in *Shox2*-expressing TCNs of roughly 10ms (student's t test, p=0.0254).

Characteristics of Shox2-expressing *v Shox2*-negative *TCNs*

When analyzing metrics other than post-anodal spike timing and considering all *Shox2*-expressing TCNs versus all *Shox2*-negative TCNs, I did find some significant differences. *Shox2*-expressing TCNs had significantly more post-anodal action potentials than *Shox2*-negative TCNs **(figure 2.5.c)**. However, I found that *Shox2* expression did not significantly affect the area under the burst curve (***figure 2.5.b***).

After comparing burst properties of *Shox2*-expressing versus *Shox2*-negative VB TCNs, I went on to isolate the T-type calcium current in *Shox2*-expressing and *Shox2*-negative TCNs. I calculated the current density at -90mV to 0mV (in increments of 10mV) membrane potentials directly after hyperpolarization (a detailed description of current isolation can be found in the methods of this section). I found no significant difference in the T-type current density between the two cell types (**figure 2.5.d**).

I also analyzed the difference in voltage sag in response to hyperpolarization (attributed to the HCN current), input resistance, membrane potential, and I_T. The HCN sag had a range for both cell types, indicating a range in HCN current activity for both. The HCN attributed sag is the slow membrane depolarization that occurs while a cell is being hyperpolarized. HCN attributed sag is calculated as the difference, in mV, between the beginning of the trace and the end. I found no significant differences in any of these metrics (***figure 2.5.e***).

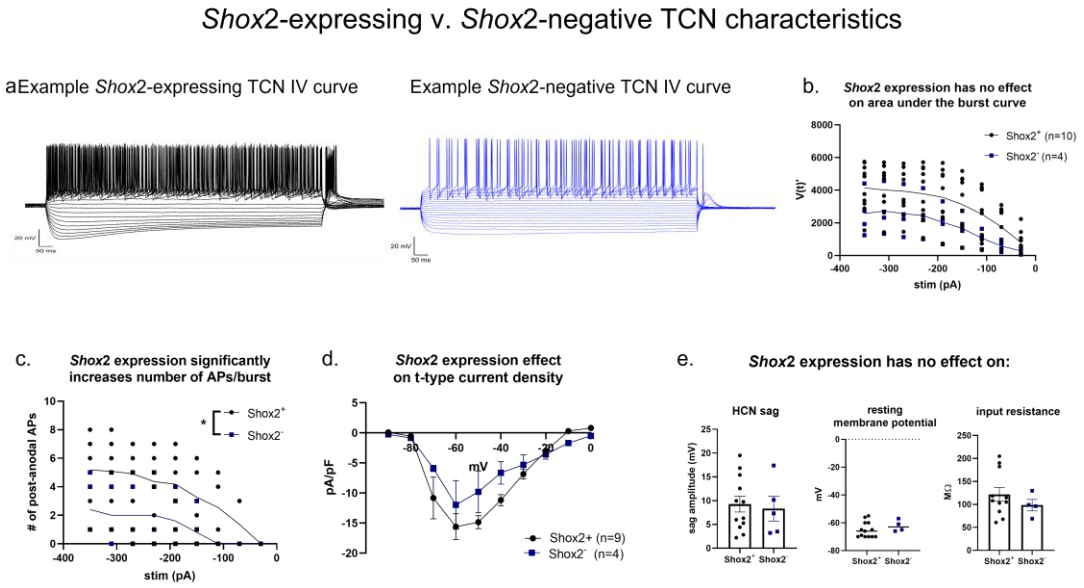

Figure 2.5 *Shox2-expressing versus Shox2-negative TCN characteristics*

a) Patch clamp recordings, showing example voltage response of a Shox2+ TCN (black, left) and a Shox2- TCN (blue, right) to current stimulation described in figure 9. **b)** The area under burst curve was determined by taking the integral of the voltage response over time to release from varying hyperpolarizing current injections (-350pA:40:0pA). Black trace is the average of Shox2+ TCNs, blue trace is the average of Shox2- TCNs. There is no significant difference between the two cell types. **c)** Number of actions potentials per post-anodal burst was quantified and compared in Shox2+ versus Shox2- TCNs. Shox2+ TCNs have significantly more action potentials per burst than Shox2- TCNs, as determined by a 2-way ANOVA, p=0.0325. **d)** Shox2 expression has no significant effect on T-type current in TCNs. **e)** Shox2 expression has no significant effect on sag generated from I_H, input resistance, or resting membrane potential.

In conclusion for aim 1a, the only significant difference found between *Shox2*-expressing and *Shox2*-negative TCNs I found, was the number of action potentials per post-anodal burst. I observed a significant increase in the number of action potentials per post-anodal burst in *Shox2*-expressing TCNs. There was no significant difference in HCN attributed sag, or in T-type Ca^{2+} current, thus our hypothesis is null. The sparsity of *Shox2*-negative TCNs, inhibiting the clear determination of VB TCN characteristics that are Shox2 attributable, necessitates the generation of a KO model to further determine Shox2 function.

2.3.2 *Results Aim 1b: Shox2*-expressing versus *Shox2*-KO TCNs

Before analyzing effects of *Shox2* KO on VB TCN activity, we confirmed that our viral injections generated a *Shox2* KO in the VB of the thalamus. To do this, we created a within mouse control, injecting our cre virus into the VB of one hemisphere, and a non-specific RFP control virus into the VB of the opposite hemisphere of P21, $Shox2^{fl/fl}$ mice. Imaging confirms location of injection is VB, and mRNA processing of left versus right VB thalamus tissue punches confirms a *Shox2* knockdown of 77% (**figure 2.6**).

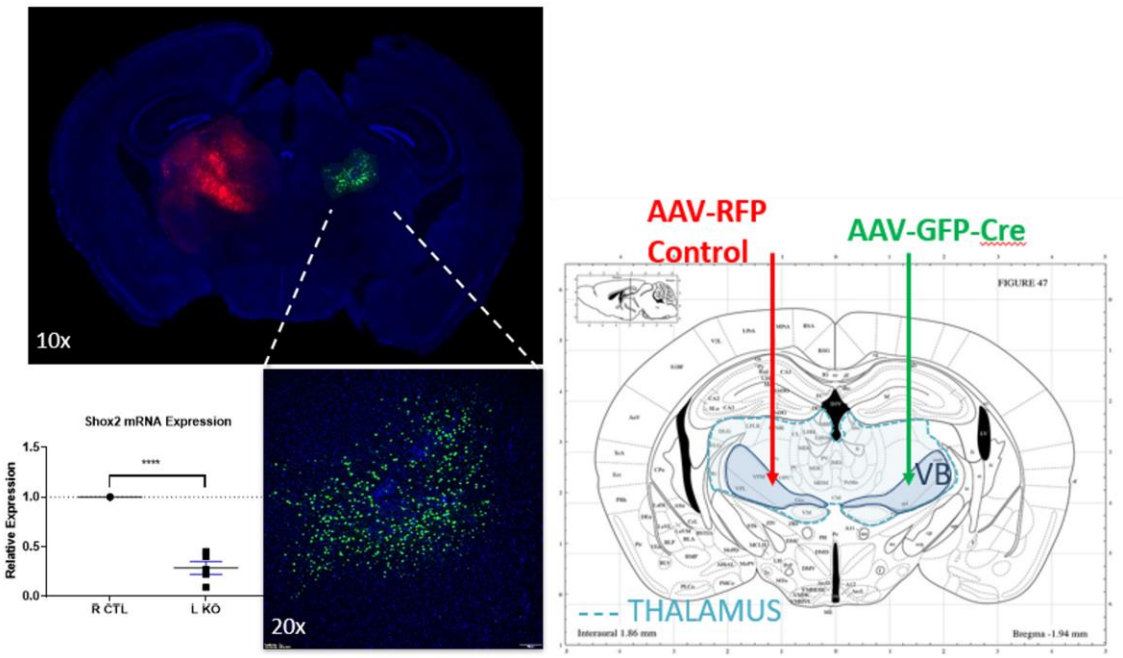

Figure 2.6 *Unilateral Shox2 KO in VB nucleus of thalamus*

Left top: Stereotaxic injections of CTL & KO virus into VB of Shox2$^{fl/fl}$ mice were performed at P21 to create within animal control. Red expression shows localization of virus, but no affect to cell health or function. The green expression of virus indicates cre-recombination has occurred. Left bottom: Shox2 mRNA expression from VB punches confirms a 77% reduction of Shox2 mRNA in the KO versus CTL side.

After confirming an effective knockdown of *Shox2* in our model, we performed patch clamp electrophysiology on fluorescent control and Shox2 KO cells. **Figure 2.7, a and b** show voltage responses of 2 example VB TCNs from $Shox2^{fl/fl}$ mice that have received VB injections with a non-specific RFP-AAV2 virus. In **figure 2.7.a,** the cell is resting around -60mV and hyperpolarizing sweeps evoke a depolarizing current that results in a slow increase of membrane potential during hyperpolarization (sag), which is attributed to I_H. Release from hyperpolarization results in post-anodal bursts with multiple action potentials per burst. Depolarization of the cell from -60mV results in some burst firing, which is a common observation in healthy VB TCNs (M. S. Sherman, 2001), that transitions to tonic firing with increased current injection. In the second example of a fCTL VB TCN response to current injections, sag is once again visible, less robust burst and tonic firing is observed, but both are still intact.

Figure 2.7, c and d are two example responses of *Shox2* KO VB TCNs, from a $Shox2^{fl/fl}$ mouse that has received VB stereotactic injections with a GFPCre-AAV2 virus. In **figure 2.7.c**, the cell is resting around -60mV and hyperpolarizing sweeps fail to evoke I_H. Post-anodal burst responses are still observed, but with at most, one action potential per burst. Tonic firing is extremely limited. The second example of a KO VB TCN response to current injections (**figure 2.7.d**) also has a resting membrane potential around -60mV, however, it exhibits a less robust burst with truncated action potentials, no tonic firing, and an absence of sag. Both cells also have an increase in volage response to the same amplitude of current injection, indicating an increase in input resistance compared to control TCNs.

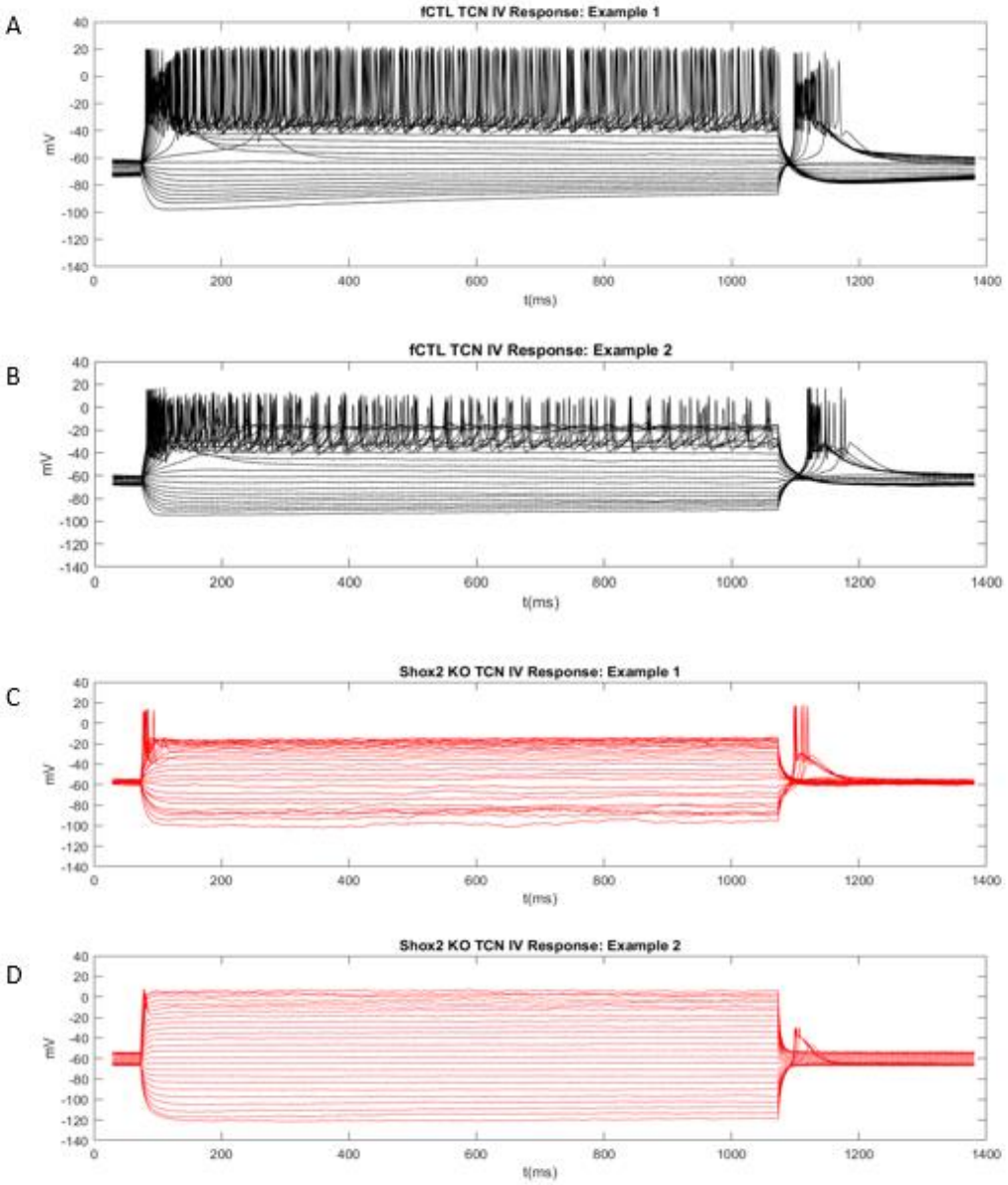

Figure 2.7 *Example voltage responses of fluorescent control (fCTL) cells and Shox2 KO cells to steps of current injection*

Figure 2.7 *Example voltage responses of fluorescent control (fCTL) cells and Shox2 KO cells to steps of current injection*

a) Voltage response of an example VB TCN from a $Shox2^{fl/fl}$ mouse that has been infected with a non-specific RFP-AAV2 virus. The cell is resting around -60mV and hyperpolarizing sweeps evoke a depolarizing current that results in a slow increase of membrane potential during hyperpolarization (sag), which is attributed to I_H. Release from hyperpolarization results in post-anodal bursts with multiple action potentials per burst. Depolarization of the cell from -60mV results in some burst that transitions to tonic firing**. b)** second example of a fCTL VB TCN response to current injections exhibits less robust burst and tonic firing, but still intact. **c)** Voltage response of an example VB TCN from a $Shox2^{fl/fl}$ mouse that has been infected with a GFPCre-AAV2 virus. The cell is resting around -60mV and hyperpolarizing sweeps fail to evoke I_H. Post-anodal burst responses are still observed, but with at most, one action potential per burst. Tonic firing is extremely limited. **d)** second example of a KO VB TCN response to current injections exhibits less robust burst, with truncated action potentials and no tonic firing.

Shox2-expressing versus Shox2 KO TCNs: bursting and membrane effects

Figure 2.8.a shows examples of *Shox2*-expressing (top) and *Shox2*-KO (bottom) TCN responses to release from various levels of hyperpolarization. of *Shox2*-expressing cells display robust burst responses with a cluster of multiple action potentials per burst. *Shox2*-KO cell responses have a diminished low-threshold spike (LTS) and either no action potentials, such as in this example, or at most a single action potential per burst. Analysis of these responses revealed that P21 KO of *Shox2* significantly reduces the number of action potentials per burst (**figure 2.8.b, left**) and area under the post-anodal burst curve (**figure 2.8.b, right**) is significantly reduced in the *Shox2* KO cells

With this effect to the burst firing, and the knowledge that I_H and I_T are critical currents for burst generation, I then analyzed *Shox2*-expressing and *Shox2* KO VB TCNs for differences in HCN attributed sag, and I_T. I found the difference in voltage sag in response to hyperpolarization (attributed to the HCN current) to be significantly reduced in *Shox2*-KO cells, indicating a reduction in I_H (**figure 2.8.c**) Isolation of T-type Ca^{2+} current revealed that Shox2 KO at P21 significantly reduces I_T in KO cells compared to Shox2-expressing TCNs (**figure 2.8.d**). I isolated the T-type calcium current as described in the methods of this section and example traces from a Shox2-expressing cell (**figure 2.8.d, top left**) and a Shox2 KO cell (**figure 2.8.d, bottom left**) can be visualized. The amount of inward current at various voltage clamp holdings (-90mV:10:0mV) was measured. This can be visualized as the inward responses after the release from hyperpolarization in *Shox2*-expressing and *Shox2*-KO traces in figure 18. The current was rapidly activating and transiently inactivated. It was not present without hyperpolarization, and was effectively blocked with 2μM TTAP2, confirming the current

to be T-type calcium. Quantifying the density of this current in 7 *Shox2*-expressing versus 5 *Shox2*-KO cells confirmed that I_T was significantly reduced in Shox2-KO cells.

I also analyzed these cells for differences in input resistance and resting membrane potential. There was a significant increase in input resistance in the KO cells, but there is no effect to resting membrane potential (**figure 2.8.e).**

.

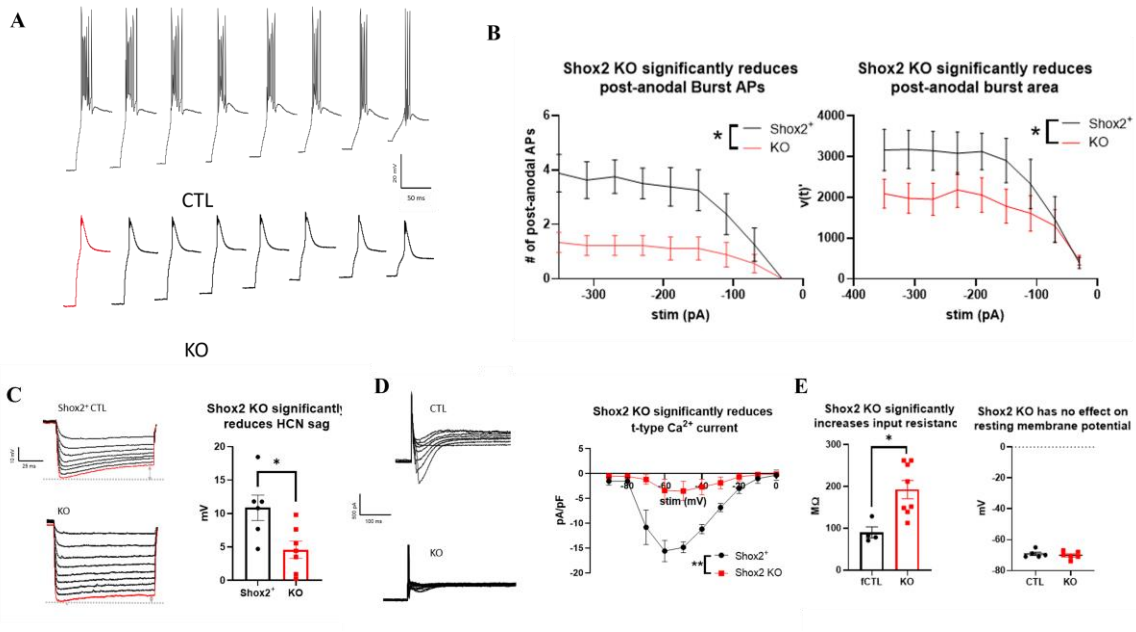

Figure 2.8 *Shox2 KO v. Shox2 expressing TCN burst and membrane characteristics*

Figure 2.8 *Shox2 KO v. Shox2 expressing TCN burst and membrane characteristics*

A) Example post-anodal burst response of Shox2+ cell (top) and KO cell (bottom) to various hyperpolarizing current injections. Shox2+ cells display robust burst responses with a cluster of multiple action potentials per burst. KO cells responses display a diminished LTS and either no action potentials, such as in this example, or only a single action potential per burst. **B)** *Shox2 KO significantly reduces the area under post-anodal burst curve and number of action potentials per burst.* **Left:** Black trace is the average of Shox2+ TCNs, red trace is the average of Shox2 KO TCNs. KO cells have significantly less action potentials per post-anodal burst (2-way ANOVA, p=0.0115). **Right:** Area under burst curve was determined by taking the integral of the voltage response over time, upon release from varying hyperpolarizing current injections (-350pA:40:0pA). Shox2 KO cells were determined to have a significantly smaller area under the burst curve as determined by 2-way ANOVA, p=0.024. **C) Left:** Example responses of CTL (top) and KO (bottom) cells to different amplitudes of hyperpolarizing current injections. Note the reduced change from the start of the hyperpolarization to the end in the KO cell, indicated by the grey arrow distance from the dotted grey line. **Right:** Quantification of these traces reveals that Shox2 KO significantly reduces HCN sag in response to hyperpolarization (student's t-test, p=0.017). **D)** *Isolation of T-type Ca2+ current revealed that Shox2 KO significantly reduces* I_T. **Left:** Subtraction of inactivation and activation T-type protocols to isolate T-type Ca^{2+} current in CTL (top) and KO (bottom) cells. **Right:** Shox2 KO cells have a significantly reduced T-type Ca^{2+} current, determined by 2-way ANOVA, p<0.0001. **E)** Shox2 KO cells have significantly increased input resistance (student's t-test, p=0.017). There is no effect to resting membrane potential.

Shox2-expressing versus Shox2 KO TCNs: significant effects to tonic firing.

Tonic firing of TCNs has also been shown to be critical to thalamocortical oscillations (Amarillo et al., 2014; J. Lee et al., 2013) and has been shown to be tightly regulated by channels other than HCN and T-type (Kasten et al., 2007). I investigated the effect to tonic firing of VB TCNs in the absence of Shox2 and found it to be dysregulated. **Figure 2.9.a** shows representative traces of CTL (*Shox2*-expressing) (left) and KO (right) TCNs in response to a 160pA injection of current while being held at -50mV. Analysis of all tonic firing reveals that depolarization of *Shox2*-expressing TCNs resulted in tonic firing that began at current injections of 50 pA and saturated at an average of 50 action potentials (APs) per second with an injection of 400 pA of current. However, KO TCNs did not begin firing until over 100 pA of injected current, and at 400 pA of current injection they averaged 17 Aps/s (**figure 2.9.b**). Further analysis shows that the peak amplitude of actions potentials during tonic firing is significantly reduced in KO cells (**figure 2.9.c**), action potential halfwidth is significantly increased (**figure 2.9.d**) but there is no effect to time to action potential peak (**figure 2.9.e**).

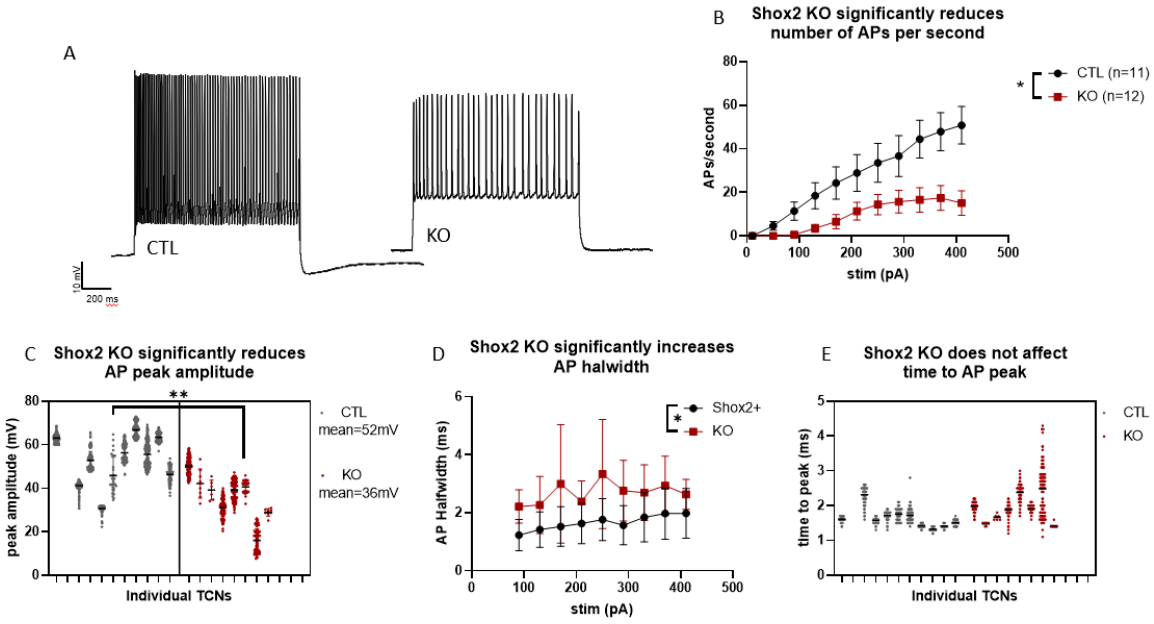

Figure 2.9 *Shox2 KO effects on action potential characteristics*

A) representative traces of CTL Shox2^{+} (left) and KO (right) TCNs in response to a 160pA injection of current when being held at -50mV**. B)** Saturation curves of action potentials (APs) per second in CTL (black) and KO cells (red) in response to increasing current injections. KO cells have significantly fewer APs/s (2-way ANOVA, p=0.0129**). C)** APs in KO cells are significantly smaller in amplitude (nested t-test, p=0.062). **D)** KO significantly increases AP halfwidth. **E)** KO has no effect on time to AP peak.

2.4 Discussion Aim 1

In summary, P21, VB *Shox2* KO dysregulates burst and tonic firing in VB TCNs and alters membrane properties. We found that in *Shox2* KO VB TCNs, there were significantly fewer action potentials per burst. We also found a significant reduction in HCN attributed sag, as well as I_T. During tonic firing, *Shox2* KO VB TCNs had significantly reduced firing frequency, significantly reduced action potential peak, and a significantly increased action potential halfwidth. These effects to tonic firing as well as burst suggest that Shox2 KO affects channels other than HCN and T-type, such as Kv3.2 and other TCN specific potassium channels.

This effect to burst and tonic firing/reduction of thalamocortical action potentials from a first order relay nucleus, implies that relay of somatosensory information is impaired in Shox2 KO. Since we have only recently discovered *Shox2* expression in TCNs, their cortical connectivity has not been established. Thus, in the next chapter, we confirm *Shox2*-expressing TCNs have typical cortical and reticular connectivity, then investigate the effect of VB *Shox2* KO on somatosensory perception and gross development of their cortical targets.

Chapter 3 Aim 2: Determine whether *Shox2* expression in the VB of the thalamus is critical for function and development of the somatosensory processing circuit

3.1 Introduction Aim 2: *VB to barrel cortex TC projections relay somatosensory information and are important for cortical barrel formation during development*

As mentioned previously, the thalamus is composed of first order and higher order nuclei, which send primary sensory information or higher order information, respectively, to the cortex via thalamocortical projections. To focus the scope of our investigation, we chose to examine the initial relay of sensory perception and investigate first-order circuitry. Since we are interested in the role of Shox2 and we see high expression of Shox2 in the circuitry that processes somatosensory information, we have chosen to investigate the first-order somatosensory circuit.

Sensory specific thalamic nuclei relay information to sensory specific areas of the cortex—i.e., the somatosensory nucleus of the thalamus relays primary somatosensory information to the somatosensory cortex, also called the barrel cortex. In the mouse, somatosensory information processing can be subdivided into head and body. Somatosensory information received by the head is initially received by the whiskers. The whiskers are topographically organized on the mystacial pad. Each whisker terminates in a single barrelette of the mystacial pad. This somatosensory signal is relayed from the barrelette to a corresponding barreloid in the ventral posterior medial (VPM) nucleus of the thalamus. From here, thalamocortical neurons within the VPM relay this signal from the barreloid to the corresponding barrel in layer IV of the

somatosensory (barrel) cortex. The barrels of the barrel cortex are discrete anatomical units, with each one representing a single whisker, as diagramed in **figure 3.1** (Woolsey & Van der Loos, 1970).

While it has been reported that VPM (the first order somatosensory nucleus of the thalamus) projections synapse in all layers of the barrel cortex (Wimmer et al., 2010), they have been shown to innervate layer IV most densely. Optogenetic stimulation of VPM projections evokes responses from layer IV that are significantly larger than any other layer (Sermet et al., 2019), and the strongest excitatory influence upon the cortical column is provided by presynaptic layer 4 neurons (Lefort et al., 2009). Also, VPM projections selectively target excitatory and inhibitory neurons inside of the barrels of layer IV, not the septa (Wimmer et al., 2010). Due to our relatively recent identification of *Shox2*-expressing TCNs, whether this subset of TCN follows the typical reticular and cortical connectivity schema of other VB TCNs remains unknown. If this connectivity is present, whether *Shox2* expression in these VB TCNS is necessary for the relay of somatosensory information from the whiskers to the cortex is also not known.

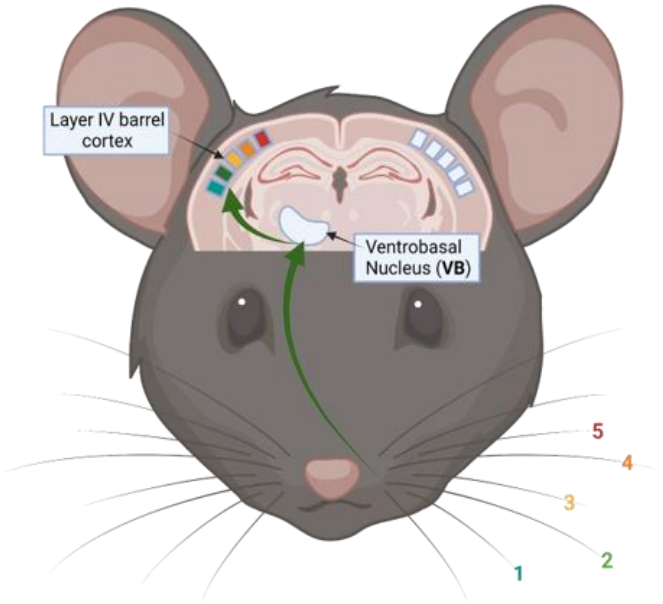

Figure 3.1 *Diagram of single whisker sensory information being relayed to a single barrel.*

Somatosensory information from a whisker, labeled with a green number 2, is relayed to the ventrobasal (VB) nucleus of the thalamus (indicated by green arrow). From here, it is then relayed to a single barrel (indicated by green arrow up to the layer IV barrel cortex, and single green square) in the layer IV, somatosensory barrel cortex. These barrels create a topographic map in the cortex, with each whisker represented by a different barrel in the cortex, as indicated by the color coding of the whisker numbers corresponding to the colors of the barrels in the cortex. This well-defined organization of somatosensory information processing in the mouse has made the barrel cortex an invaluable model for researchers seeking to dissect the processing of sensory information.

Proper development of the barrel microcircuitry is integral to proper integration of first-order somatosensory signals received from the thalamus and ultimately overall sensory perception. Thalamocortical projections are integral to proper development of the barrel cortex and distinction of layers within the cortex. We have previously shown that Shox2 is important for maintenance of TCN firing characteristics in adults, and it has also been reported that loss of TCN neurotransmission at P7 completely disrupts cortical barrel formation (H. Li et al., 2013). However, although Shox2 has been shown to be important for development in other organs, such as the heart (Puskaric et al., 2010; Sun et al., 2015), whether *Shox2* expression plays a role in the development of cortical barrels remains unknown.

In this chapter, I detail experiments and results that determine whether Shox2 expression in the VB of the thalamus is critical for function and development of the somatosensory processing circuit. To do this, I first answer whether Shox2-expressing TCNs possess typical VB TCN connectivity within the thalamocortical circuit, and whether their expression of *Shox2* in the VB is necessary for proper whisker somatosensory perception. I **hypothesize** that *Shox*2-expressing TCNs have typical cortical (inhibitory and excitatory neurons in layer IV barrels) and reticular connectivity (PV^+ interneurons) of TCNs, and that loss of Shox2 will disrupt whisker somatosensory perception. Then, I investigate whether loss of Shox2 in the VB disrupts gross organization of barrels in the barrel cortex, and I **hypothesize** that loss of VB Shox2 at P6, but not P21, will disrupt barrel formation. This aim and hypothesis are depicted in **figure 3.2**.

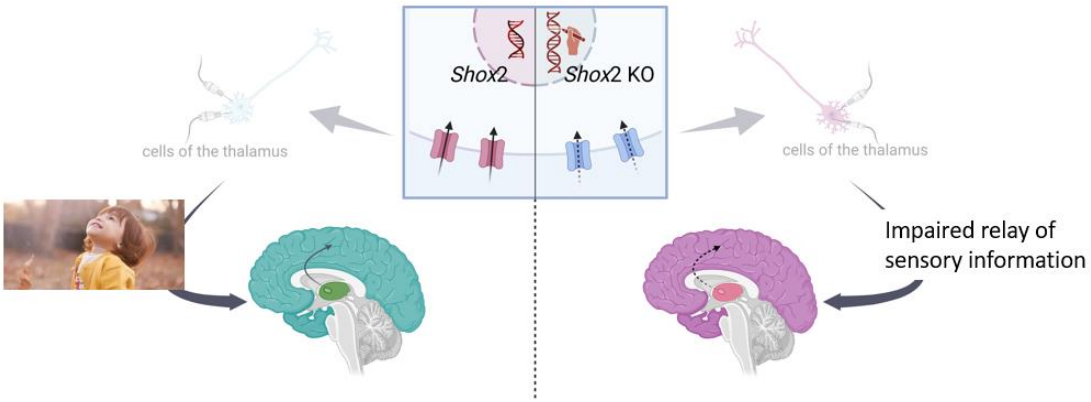

Figure 3.2 *Graphical abstract of aim 2*

Aim 2: to determine whether expression of Shox2 in VB TCNs is necessary for function and development of the somatosensory circuit. I hypothesize that knockdown of Shox2 in the VB nucleus of the thalamus will impair somatosensory perception.

3.2 Methods Aim 2

3.2.1 Methods Aim 2a: Defining Shox2-expressing TCN connectivity and determining whether expression of VB Shox2 is necessary for somatosensory perception.

Immunohistochemistry:

Mice were deeply anesthetized by injection with isoflurane, perfused transcardially with ice-cold PBS followed by 4% paraformaldehyde in PBS and decapitated for brain collection. Mouse brains were placed in 4% paraformaldehyde in PBS at 4◦C overnight for post-fixation. To cryosection the brains, they were sequentially placed in 15 and 30% sucrose in PBS solutions at 4◦C until saturation. The brain samples were embedded in optimal cutting temperature compound and stored at −20◦C and cryo-sectioned in 20–50 μm coronal or sagittal slices with Leica CM3050S cryostat.

For IF staining, slices were washed with 50 mM Tris-Buffered Saline with 0.025% Triton X-100 (TTBS) and blocked in 2% bovine serum albumin (BSA) in TTBS for 2 h at room temperature. Primary antibodies were diluted in blocking solutions and applied on slides overnight at 4◦C. Fluorescence-conjugated secondary antibodies were diluted 1:1000 in blocking solutions and applied on slides for 1 h at room temperature. 1:1000 DAPI was applied for 5 min at room temperature for nuclei staining and then washed off. The slices were mounted on slides with mounting media (Vector Laboratories, H-1000) and imaged under a confocal microscope.

Field recordings:

Thalamocortical orientation slices were obtained (Agmon & Connors, 1991) from 3-4 week old Shox2Cre;TdtChrd2 mice and maintained in the previously described solutions/recording apparatus. A recording electrode of 1-2 MΩ was filled with aCSF and

placed in the layer IV barrel cortex of the slice. A blue LED light was placed as close as possible to the recording electrode, while a 5ms light stimulus was trigged by an external stimulation box.

Sticky tape whisker task:

Mice were habituated to the recording chamber for 3 hours, 3 consecutive days in a row. On the third day, after 2 hours, videos were recorded as stickers were placed on either left- or right-side whiskers. Latency to removal was scored by a blinded observer. Each value is an average of three trials.

3.2.2 Methods Aim 2b: Determining whether Shox2 expression is necessary for gross barrel formation during development

Determining whether loss of VB Shox2 at a critical postnatal developmental window (P6) disrupts gross formation of cortical barrels.

Cytochrome Oxidase Staining for coronal barrels:

Tissue Preparation: Animals were perfused with saline followed by cold 4% PFA, then brains were rinsed in PBS before slicing and sliced in 50µm slices with the vibratome.

Staining solution: Staining solution (for 100ml): 4g sucrose, 50 mg Cytochrome C, 50 mg DAB, PBS to complete 100 ml.

Procedure: Tissue was rinsed in PBS 3 times for 5 minutes. Staining solution was added to wells and incubated on a rocker gently for 3-4 hours at 37°C. The reaction was stopped with 3X5 min washes in deionized water.

CO Staining for flattened cortices view of barrels:

Tissue preparation: The mice were perfused with PB (0.1M, pH 7.4) followed by 2% PFA 2% PFA, which resulted in softer tissue for flattening, which absorbed the CO staining better. Brains were removed and cut down the middle sagittal plane with a razor. Using a razor and spatula, subcortical structures were separated from the cortex. Excess cortical regions were removed (i.e., nucleus accumbens, striatum and orbitofrontal cortex) resulting in an even thickness slice of cortex containing the barrels. To ensure smooth flattening, a cut was made across the long side of the frontal cortex. The shelled cortex was placed cortex-down on glass, two rolls of clay (10-20% thinner than brain) were placed on either side to act as spacers, and another glass slide was placed on top. Glass was taped together, and the entire apparatus was placed in a dish of 1% PFA for 24 hours.

Slicing and Staining: Cortex was rinsed in PB (0.1M, pH 7.4) for 15 minutes. Afterwards, 80-150 µM slices were obtained on the vibratome. Slices were rinsed 3 times for 12 minutes in PBS. Staining solution (as described previously) was added, and slices were incubated on a gentle rocker for 3-4 hours at 37℃. The reaction was stopped with one 15-minute rock in 4% PFA. Slices were then washed with PBS 3 times for 10 minutes.

Barrel Analysis: Coronal barrel formation was analyzed using FIJI image analysis software. Briefly, lines scanning for pixel intensity were traced across 3 barrels. Pixel intensity values were plotted and analyzed for variance between barrels and septa in CTL vs KO sides. Flattened barrel formation was analyzed using the program Reconstruct. After sectioning, any slice containing a section of barrels was imaged. Images of flattened barrels from the same hemisphere were combined into a project and realigned

using the vasculature (visible as white dots/no CO staining within the barrels). Markers for the same vasculature holes were placed on each image, and these were used to align and overlay the images, creating a complete map of flat barrels for each hemisphere.

3.3 Results Aim 2

3.3.1 Results Aim 2a: Shox2-expressing TCNs synapse on cortical layers IV and VI, and the reticular nucleus, and expression is necessary for whisker somatosensation

I investigated *Shox2*-expressing TCNs in the VB nucleus, which is a nucleus that consists largely of first order relay TCNs. First order relay TCNs of the VB project to the somatosensory barrel cortex and to the reticular nucleus of the thalamus. In the barrel cortex, they project to all layers, but anatomically most densely to layer IV and layer VI (Oberlaender et al., 2012). In layers IV, VB TCNs project to excitatory and parvalbumin positive (PV^+) inhibitory cells within the barrels (Agmon & Connors, 1991; Constantinople & Bruno, 2013). VB TCNs also synapse on PV+ neurons of the reticular nucleus (Jones, 2007).

Since Shox2+ TCN connectivity has not yet been classified, we confirmed that typical connections and firing of TCNs were present. I **hypothesized** that *Shox*2-expressing TCNs have typical cortical (inhibitory and excitatory neurons in layer IV barrels and layer VI) and reticular connectivity (PV^+ interneurons) of TCNs, and that loss of Shox2 will impair whisker somatosensory perception. To test this hypothesis, I utilized immunohistochemistry staining in a Shox2-RFP reporter mouse to visualize synapses to the cortex and the reticular nucleus. To confirm our immunohistochemistry-based identification of synapses, I designed an experiment to confirm functional connectivity by optogenetically activating *Shox2*-expressing TCNs while recording field activity in the

cortex of slices. To investigate whether Shox2 expression in the VB is necessary for somatosensory perception from the whiskers, I used the unilateral, P21, VB KO model and performed a sticky tape test by placing a piece of sticky tape on either left (KO) or right (CTL) whiskers and recording latency to removal.

Shox2-expressing TCNs synapse on cortical layers IV and VI, and the reticular nucleus.

To visualize *Shox2*-expressing cell somas and projections, we crossed a Shox2cre mouse with an Ai14Tdt reporter mouse—with red fluorescent protein (RFP) as the reporter. A sagittal image from this reporter mouse (**figure 3.3a**) reveals localization of *Shox2* expression in the thalamus with projections to various layers of the cortex, including cortical layers IV (**box IV**) and VI (**box VI**), as well as projections to the reticular nucleus (**box Rt**). Below this expression image is a reference Allen Brain Atlas image of the same sagittal section. To visualize synaptic connectivity in layer IV and VI and the reticular nucleus (**figure 3.3b**, left column from top to bottom, respectively), we utilized the reporter mouse to visualize *Shox2*-expressing projections in red (**figure 3.3b**, second column), stained for glutamatergic synapses (Shank2 antibody) in far red (**figure 3.3b**, second column), and PV^+ interneurons in these areas (**figure 3.3b**, third column). We merged these three wavelengths (**figure 3.3b**, far right and first column) and visually identified synapses. Two white arrows in row2 2-5 point to the same location where the three wavelengths can be seen, and a synapse is identifiable either somatically (top arrow in each image) or dendritically (bottom arrow in each image) for each area.

Sagittal imaging showing Shox2 expression and 100X image locations

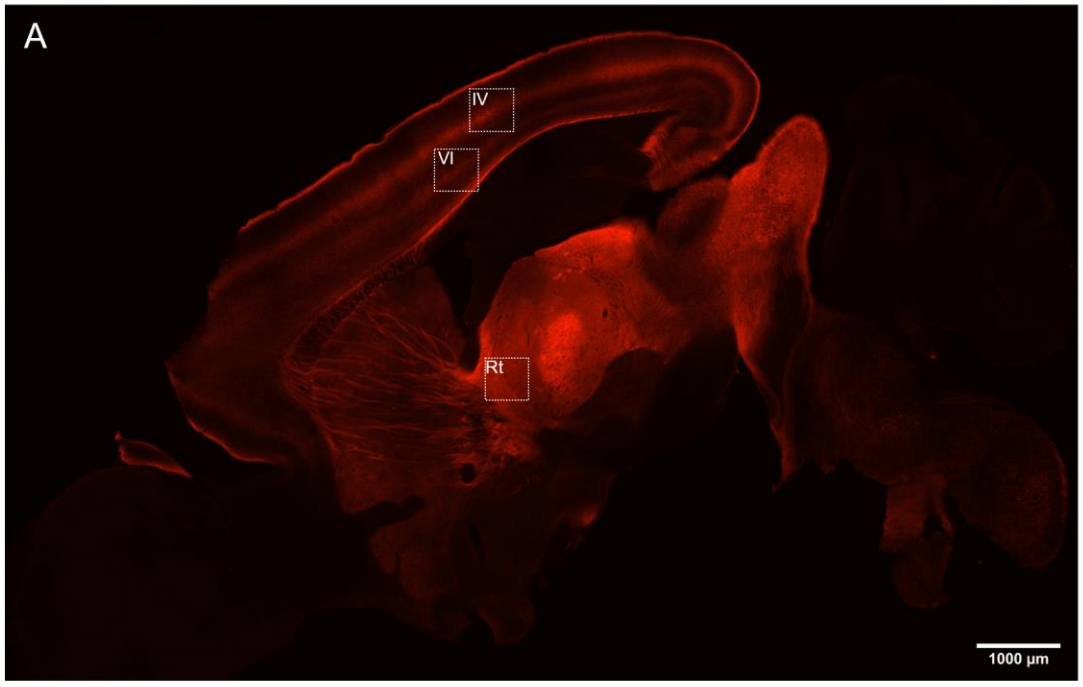

Sagittal map from Allen Brain Atlas

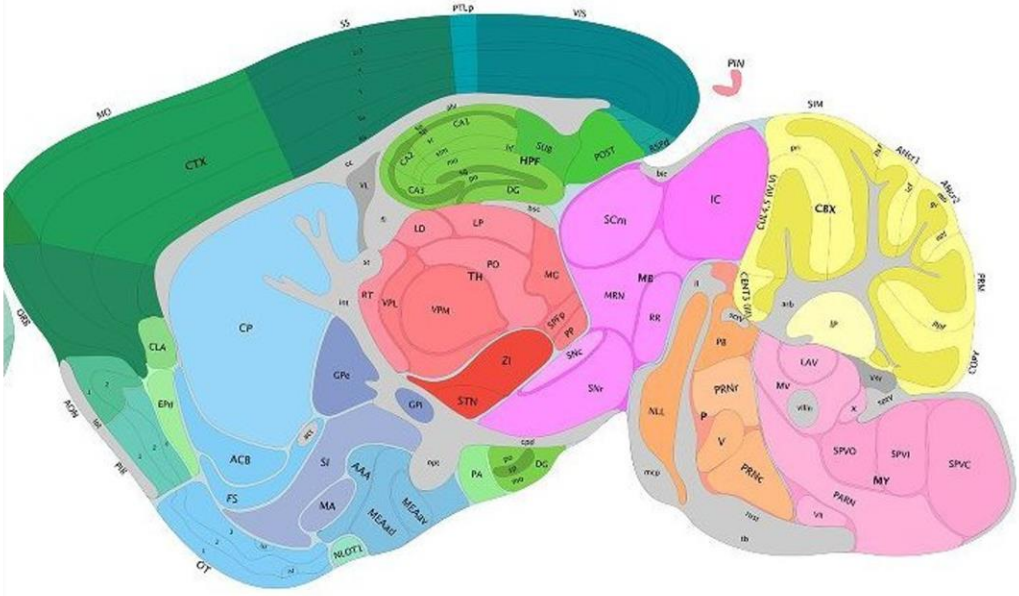

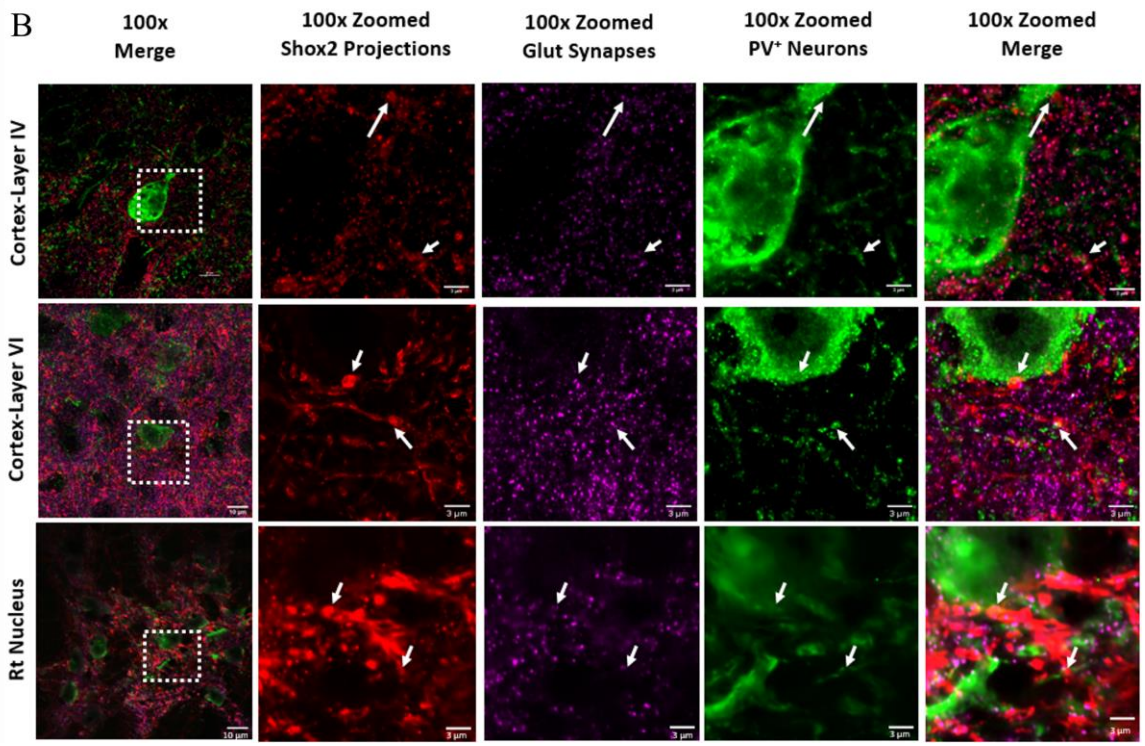

Figure 3.3 *Shox2 expression and cortical and reticular synapses*

A) Top: Sagittal image from a Shox2cre;Ai14Tdt reporter mouse—with red fluorescent protein (RFP) as the reporter reveals localization of *Shox2* expression in the thalamus with projections to various layers of the cortex, including cortical layers IV (**box IV**) and VI (**box VI**), as well as projections to the reticular nucleus (**box Rt**). Bottom: Allen Brain Atlas image of the same sagittal section Abbreviations and link to sagittal image can be found here. **B)** Column 1: 100x images from boxed areas on sagittal image, from top to bottom: layer IV cortex, layer VI cortex, reticular nucleus (Rt). White boxes show zoomed areas of columns 2-4 for each row. Column 2: Zoomed area from column 1 showing *Shox2*-expressing projections. Round 'feet' were determined to be presynaptic terminals. Column 3: Zoomed area from column 1 showing Shank2 staining, puncta were determined to be glutamatergic synapse sites. Column 4: Zoomed area from column 1 showing PV^+ interneuron staining, areas with somas and dendrites were chosen. Column 4: Zoomed area merged. Areas of colocalization somatically (top white arrow for each row) and dendritically (bottom white arrow for each row) were identified as synapses. Arrows point to same location in rows 2-5 to show expression at wavelength.

Field recordings confirm synaptic connectivity

To confirm proper identification of synapse with immunohistochemistry, I established that there was a glutamatergic and GABAergic cortical response when Shox2-expressing projections were selectively activated. To achieve this, crossed a Shox2Cre mouse with a ChrdTDtomato mouse, creating a mouse model in which Shox2-expressing projections can be selectively activated with a blue light. Using a thalamocortical slice orientation that keeps thalamocortical projections to the cortex intact (Agmon & Connors, 1991), I recorded field activity from an electrode placed within the barrels of the layer IV barrel cortex, and selectively activated Shox2-projections with a blue LED light pulse. This elicited a consistent upward response within the barrels (**figure 3.4**). I then bath applied gabazine to block inhibitory synapses and observed a response of increased amplitude and reversed polarity, and followed this by application of AP5 and DNQX, blocking glutamatergic synapses, and preventing a cortical response to light pulses. This confirmed the residual response was glutamatergic. This revealed that there is an inhibitory and excitatory component of the cortical postsynaptic response to Shox2-expressing TCN activation.

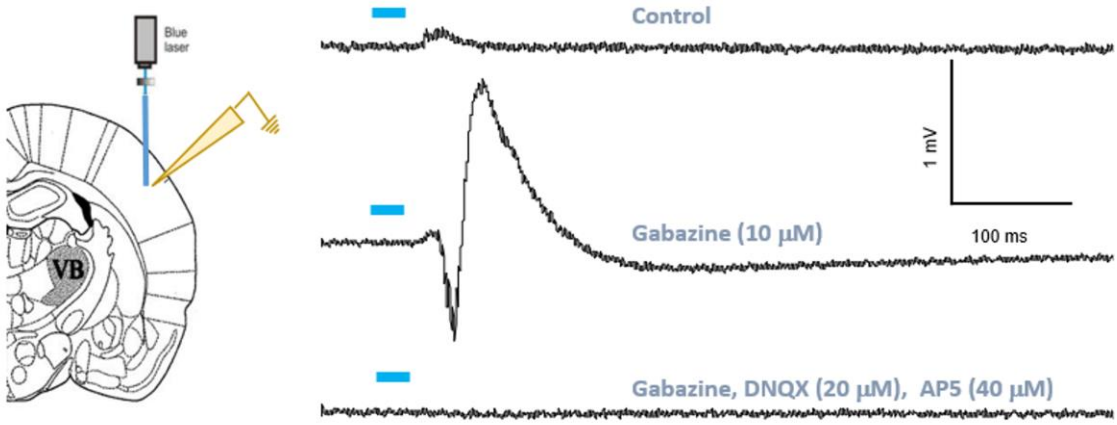

Figure 3.4 *Optogenetic activation of Shox2-expressing projections evokes GABAergic and glutamatergic field responses in layer IV barrel cortex.*

Thalamocortical slices were obtained from Shox2cre;ChrdTDtomato mice. Field recording electrodes were placed within barrels of the layer IV barrel cortex (schematic on left). Selective activation of *Shox2*-expressing projections using 5ms blue light elicited an upward response (top trace/control). Application of 10µM gabazine to block GABAergic synapses reversed the polarity of the response and increased the amplitude (middle trace). Application of 20µM DNQX and 40µM AP5 to block glutamatergic synapses confirmed that the response was synaptic (bottom trace). Example traces, n=5.

Shox2 expression is necessary for somatosensation

Previously in our lab, the activity and somatosensation acuity of global *Shox2* KO mice was investigated. In an open field test, total activity was not altered, and anxiety levels were decreased in KO mice. Interestingly, when a small piece of sticky tape was placed on the foot of a KO mouse, there was a significantly increased latency to removal, indicating that the *Shox2* KO mice had a deficit in somatosensation. I investigated whether *Shox2* expression selectively in the VB was necessary for proper somatosensation in mice.

The VB nucleus processes sensory information from the whiskers (Jones, 2007). Thus, I adapted the previously used sticky tape sensory test by applying the sticker to the whiskers instead of the paw. Further, I tested the unilateral VB KO model previously described, to create a within mouse control for this experiment. Stickers were placed on either left (KO) or right (CTL)-side whiskers and latency to removal was recorded. In addition to the within mouse control, we used non-injected $Shox2^{fl/fl}$ mice to test for handedness. In the control, non-injected mice, there was no significant difference between left and right-side latency to removal, which indicates that there is no pre-existing handedness (**figure 3.5, left**). *Shox2* was knocked down in the right VB, corresponding with contralateral left whiskers (L KO), and the left control VB was injected with a control virus and corresponds with the right whiskers (R CTL). Time to removal of the sticker from the left whiskers was significantly increased compared to the right, indicating that KO of Shox2 in the VB nucleus of the thalamus significantly impairs somatosensation through the whiskers (**figure 3.5, right**).

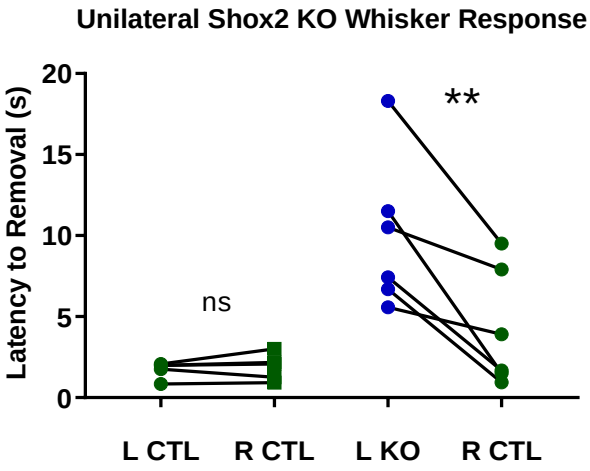

Figure 3.5 *VB Shox2 KO impairs whisker somatosensory perception*

In a targeted VB, unilateral Shox2 KO mouse ($Shox2^{fl/fl}$ and stereotactically injected cre virus), stickers were placed on either left- or right-side whiskers and latency to removal was recorded. Each value is an average of three trials. **First group:** The 3 control (CTL) subjects are non-injected $Shox2^{fl/fl}$ mice to test for handedness. There is no significant difference between left- and right-side latency to removal, which indicates that there is no pre-existing handedness. **Second group:** A within mouse study in which *Shox2* was knocked down in the right VB, corresponding with contralateral left whiskers (L KO), and the left control VB was injected with a control virus (R CTL). KO of Shox2 in the VB nucleus of the thalamus significantly increases latency to tape removal.

Aim 2a summary and discussion

Aim 2a supports the hypothesis that Shox2-expressing TCNs have layer IV and VI cortical connectivity, and reticular connectivity. It also supports the hypothesis that relay of somatosensory information from the thalamus to the cortex is impaired in the absence of VB *Shox2*-expression. This disruption in somatosensation could be explained by a significant decrease in action potentials from *Shox2*-expressing TCNs to the cortex and reticular (observed in aim 1), but it could be that loss of VB *Shox2*-expression disrupts thalamocortical circuitry architecture as well. In 2013, Li et al. showed that loss of TCN neurotransmission (action potentials from TCNs to cortex were absent) at P7 completely disrupts cortical barrel formation (H. Li et al., 2013).

3.3.2 Results Aim 2b: VB Shox2-expression is not important for the gross development of TCN cortical targets: layer IV barrels.

Aim 2a revealed that VB *Shox2*-expression is necessary for whisker somatosensation. In aim 1, I observed a significant decrease in *Shox2*-KO TCN action potentials and aim 2a confirmed that this decrease of action potentials is realized by the cortex and reticular nucleus of the thalamus, two critical TCN targets in the somatosensory circuit. This loss of action potentials within this circuit may explain the impairment of somatosensation, but it may also be that loss of Shox2 disrupts the biological circuitry as well. Glutamatergic relay from TCNs, which is significantly reduced in *Shox2* KO mice, is critical to cortical organization. Specifically, it was shown that in the absence of Vglut2 –preventing TCN firing—cortical barrel formation is abolished (H. Li et al., 2013). The cortical barrel field is a major component of the

thalamocortical circuitry architecture involved in whisker somatosensation. Since we saw a significant reduction of action potentials in aim 1, an impairment of sensory information relay in aim 2a, and Shox2 has been shown to be important developmentally (Ha & Dougherty, 2018; Puskaric et al., 2010; Sun et al., 2015), we asked whether *Shox2*-expression is important for the gross development of cortical barrels.

I **hypothesized** that loss of VB Shox2 at P6, but not P21, would disrupt barrel formation. To test this hypothesis, I created two models: one P6 and one P21 unilateral, VB, *Sho*x2 knockout model. This generated within mouse controls, such that I was able to compare left versus right hemisphere barrels of the same mouse. The P6 timepoint model was created in collaboration with Dr. Maria Galazo. Dr. Galazo performed unilateral ultrasound injections of a GFPcre virus into the VB of $Shox2^{fl/fl}$ mice, creating a within mouse control with a *Shox2*-KO on the left and control conditions on the right. I aged these mice to adulthood, P35, then analyzed for disruptions in barrel formation in the KO versus CTL sides. The P21 timepoint model was created via stereotaxic injection surgeries. I performed unilateral injections of a GFPcre virus into the left VB of $Shox2^{fl/fl}$ mice, and control, non-specific RFP virus into right VB, again creating a within mouse control with a *Shox2*-KO on the left and control conditions on the right. When these mice reached adulthood, P35, I analyzed them for disruptions in barrel formation in the KO versus CTL sides. **Figure 3.6.a** is a schematic of both models. I validated the unilateral P6, VB, *Shox*2-KO model using the previously described thalamic punch and RT-qPCR methods and confirmed a unilateral knockdown of *Shox2* in this model (**figure 3.6.b**). The P21, unilateral KO model was previously confirmed (**figure 2.6 and 3.6.b**).

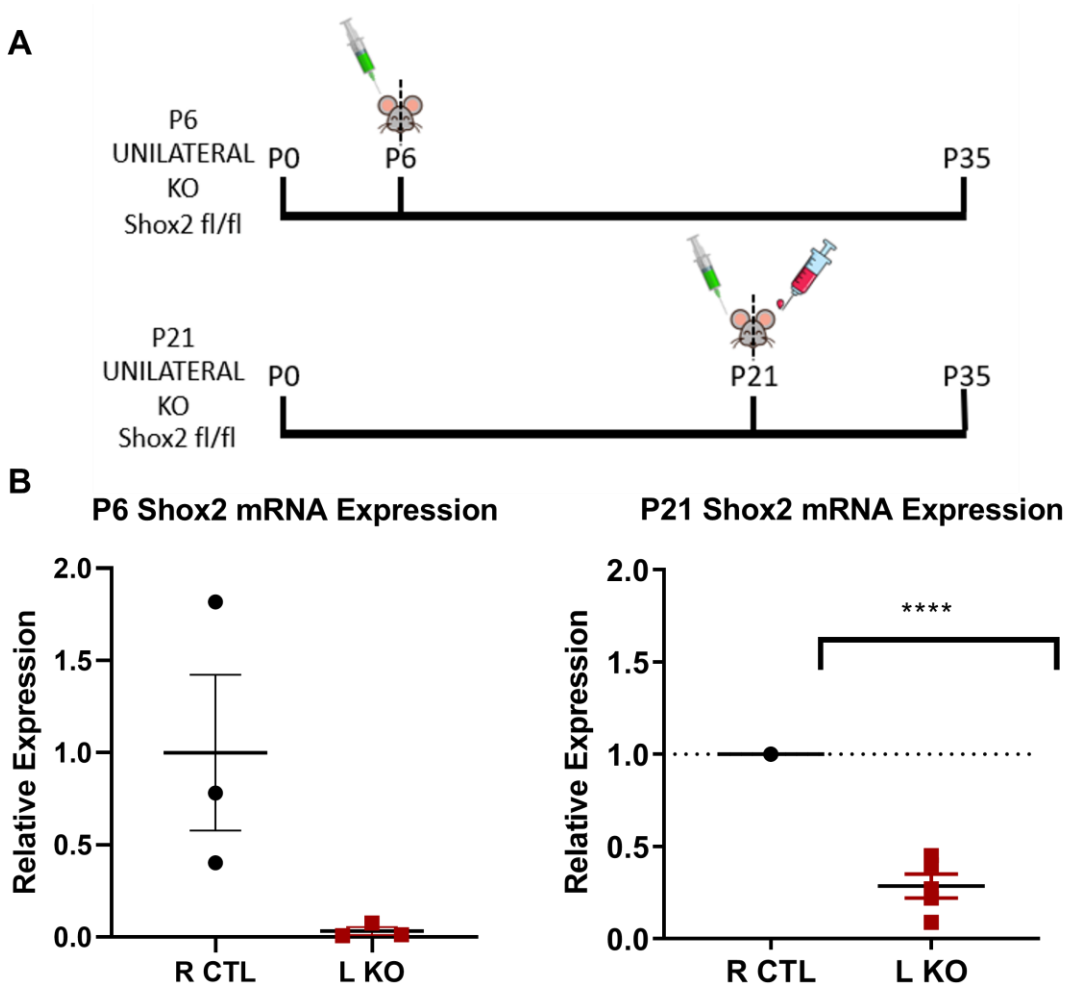

Figure 3.6 *P6 and P21 unilateral KO schematic and confirmation*

A) Schematic diagram of unilateral P6 and P21 KO mouse experimental timeline. Top: P6 Shox2$^{fl/fl}$ mice received unilateral, P6, VB injections of an AAV2-GFPcre virus ultrasonically. Bottom: P21 Shox2$^{fl/fl}$ mice received unilateral, VB injections of an AAV2-GFPcre virus and an RFP control virus (does not cause cre recombination) stereotactically. At P35, both sets of mice were analyzed for their VB, *Shox2* mRNA expression. **B)** *Shox2* mRNA expression from VB punches confirms a reduction of *Shox2* mRNA in the KO versus CTL side in both P6 and P21 models.

Coronal barrel imaging suggests that P6 KO of Shox2 disrupts barrel formation

To investigate the proper formation of barrels, I used cytochrome oxidase (CO) staining visualize barrels, which has been shown to be an indicator of neuronal activity and is a well-established marker for cortical barrels. I then compared the results in CTL versus KO sides of the cortex. Coronal results suggest that there is a significant effect to the definition of cortical barrels in the P6 (**figure 3.7.a**) but not P21 (**figure 3.7.b**) unilateral KO. I quantified this effect by measuring the variance of pixels between barrel septa (**figure 3.7.c**) and I found that the P6 KO side had a significantly reduced change in pixel intensity between barrels, but the P21 KO did not (**figure 3.7.d**). This suggests that loss of VB Shox2 at P6 results in a significant loss of distinction between barrels.

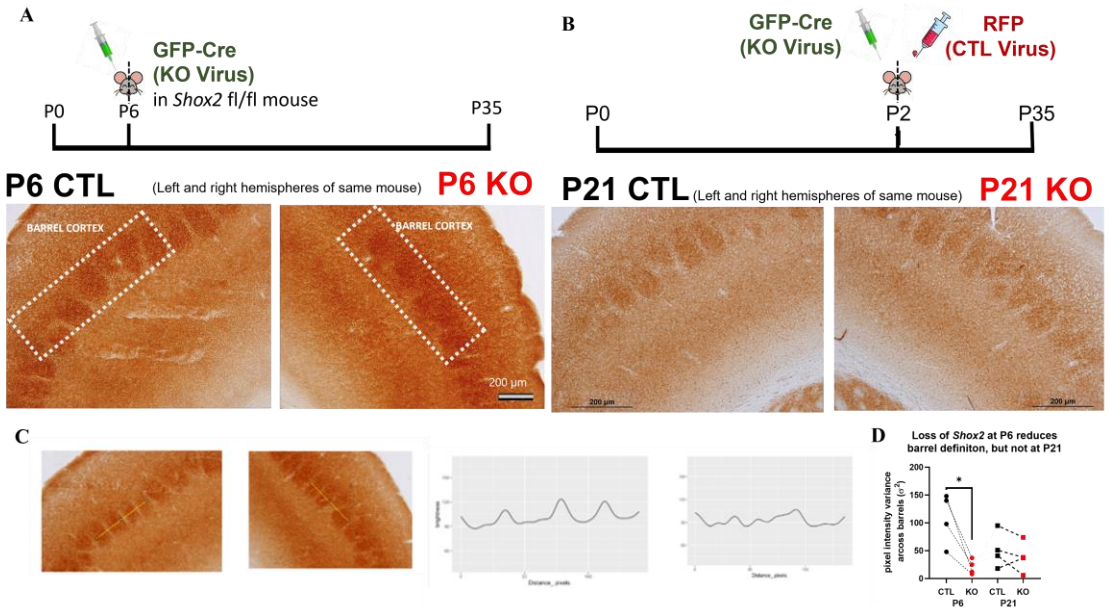

Figure 3.7 *Coronal cytochrome oxidase (CO) staining of unilateral KO cortex suggests that KO of Shox2 at P6 but not P21 disrupts barrel formation.*

A) Top: schematic of P6 KO model, Bottom: cytochrome oxidase staining visualizing barrel formation in a single coronal slice of a (**left)** P6 CTL and **(right**) P6 KO mouse. KO side appears to be less defined and have darker septa (inter-barrel definition). White dotted rectangle highlights barrels. **B)** Top: schematic of P21 KO model, Bottom: cytochrome oxidase staining visualizing barrel formation in a single coronal slice of a (**left)** P21 CTL and **(right**) P21 KO mouse. No obvious differences between CTL and KO were observed. **C)** Left: Example image where a line is traced across three barrels and the variance of pixels between barrels (septa) is measured. Right: Plot of pixel variance across barrels as measured by the traced line. **D)** Quantification of pixel variances. We found that the P6 KO had a significantly reduced change in pixel intensity between barrels, whereas the P21did not, suggesting that there was a significant loss of distinction between barrels at P6.

Flattened barrel imaging shows that P3, P6, and P21 KO of Shox2 does not disrupt gross barrel formation

Viewing cortical barrels coronally does not provide the full image of barrel formation. A more complete view of the formation and presence or absence of barrels is provided by a flattened view (**figure 3.8.a, and b**). Thus, to confirm or deny our effect, I repeated the experiment with the unilateral P6 and P21 KOs. However, this time I flattened the cortex, sliced the cortical barrel field parallel to the layers of the cortex, and reconstructed the sliced layers to obtain the full image of the barrels. I then compared the results to a map of the barrel cortex (**figure 3.8.b**) and found that all barrels were present in the P21 CTL and KO (**figure 3.8.c, top row**), as well as the P6 CTL and KO (**figure 3.8.c, middle row**).

Since I observed no differences in the P6 KO, I then hypothesized that since the critical developmental widow for barrel formation is around P6, by injecting directly at P6, I did not allow time for the virus to knockdown Shox2 in these cells *before* the critical window. To test this hypothesis, I performed the same experiment, but at the P3 timepoint. Once again, there was no gross effect to cortical barrel formation (**figure 3.8.c, bottom row**).

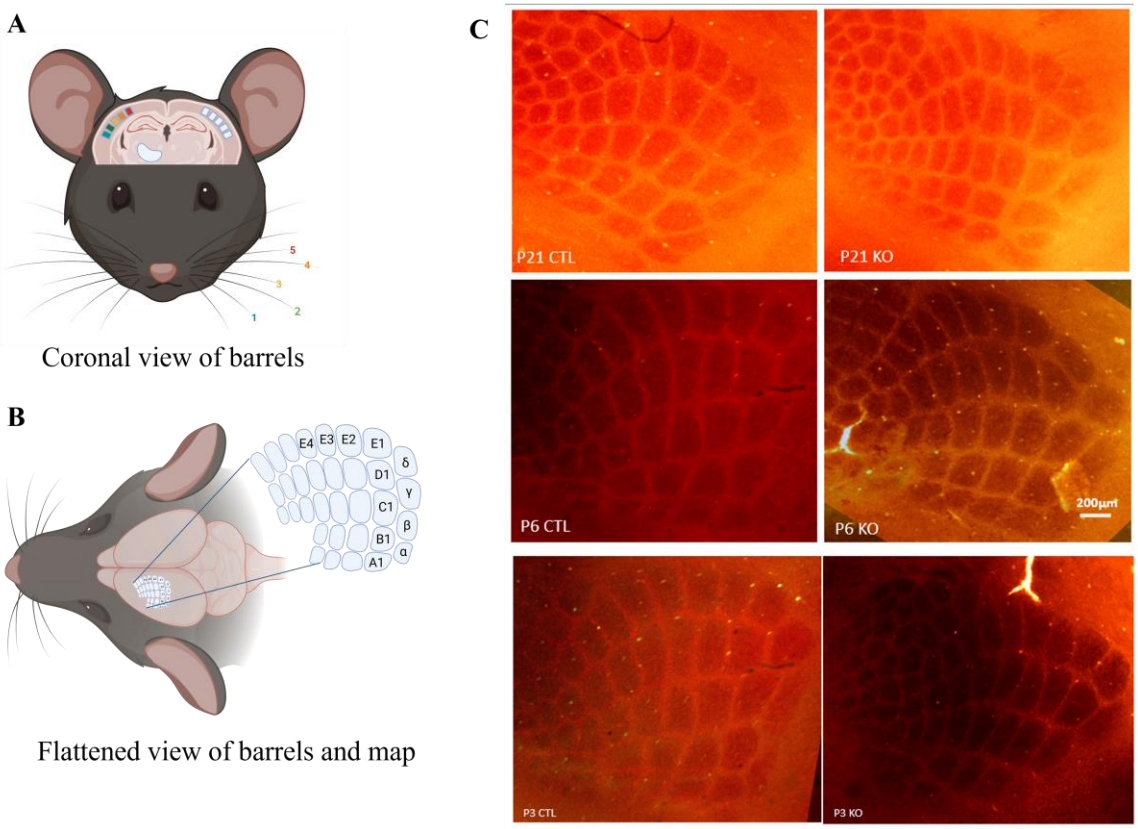

Figure 3.8 *Flattened barrel imaging shows that P3, P6, and P21 KO of Shox2 does not disrupt gross barrel formation*

A) Coronal view of barrels **B)** Flattened view of barrels, map of flattened barrel cortex where Greek letters and alpha-numeric numbering outlines the border of the full barrel cortex. **C)** CO staining was performed on flattened barrel cortices of unilateral, VB, P21, P6, and P3, *Shox2*-KO mice. Sections were imaged and images were aligned to generate a reconstruction of barrel fields from P21 (top row), P6 (middle row), and P3 (bottom row) CTL (left column) and knockdown (right column) mice. Upon comparison to the barrel cortex map, all barrels are present at each KO timepoint, thus no gross differences were observed.

3.4 Discussion Aim 2

Previously, our lab has shown that Shox2 is highly expressed in neurons of the VPM (Yu et al., 2021) and preliminary data in our lab suggest that *Shox2*-expressing, TCN projections densely innervate the barrels of layer IV. In this chapter, I used IHC to reveal that *Shox2*-expressing TCN projections synapse glutamatergically on PV^+ interneurons of the layer IV and layer VI cortex, and the reticular nucleus. Further, I confirmed these to be synapses by optogenetically stimulating these projections and recording layer IV field responses. This elicited a response that had both a glutamatergic and GABAergic component. Together, these findings strongly indicate that Shox2-expressing TCNs synapse on excitatory and/or PV+ inhibitory interneurons layers IV and VI of the cortex, and PV^+ interneurons of the reticular nucleus.

A sticky tape whisker test revealed that VB KO of *Shox2* increases the latency to removal on the KO side of a unilateral KO mouse, this suggests that VB *Shox2* expression is necessary for whisker somatosensation. Thus, Shox2 activity within the VB thalamus is critical for proper sensory perception.

We hypothesized that, due to the significant effect to TCN firing (reduction of action potentials) in our *Shox2* KO model, the fact that TCN firing is critical for cortical barrel formation, and Shox2 has been shown to be important developmentally, a *Shox*2 KO at a critical developmental window for barrels (P6) would impair barrel formation. However, our results reveal that P3 and P6 KO of VB Shox2 does not affect gross cortical target organization (barrels), since all are present, disproving our hypothesis.

These data collectively suggest that thalamic *Shox*2 expression is critical for relay of sensory information to the cortex.

Chapter 4 Aim 3: Thalamus-generated sleep spindle oscillations are thalamic-Shox2 dependent

4.1 Introduction Aim 3: Sleep spindles are generated in the thalamus and dependent on proper TCN firing

Reciprocal connections from the cortex synapse on the reticular nucleus of the thalamus, which sends GABAergic projections back to the VB, completing the oscillatory thalamocortical circuit. Oscillation frequencies of this circuit are determined by field activity in the cortex. This thalamocortical circuit produces spindle oscillations, which can be detected by cortical EEG recordings and are generated by the thalamus (Steriade et al., 1985, 1987). Spindle oscillations are a 7-15Hz frequency oscillation that occur during non-REM (NREM) sleep and are important for sleep maintenance and possibly memory consolidation (Latchoumane et al., 2017; Steriade et al., 1986). Sleep spindle onset coincides with a high-frequency burst firing in TCNs that was shown to be mediated by T-type Ca^{2+} channel activation (Bal et al.1995). While it is widely considered to be the inhibitory thalamic reticular neurons (TRNs) that generate spindle oscillations (Barthó et al., 2014), the TRN reciprocal connections with TCNs, and the resulting TCN bursts delivered to the cortex are critical to spindle maintenance (Halassa et al., 2011). TCN bursting activity for maintenance of sleep, it is also hypothesized to play a role in sleep-wake transitions. Notably, optogenetic stimulation of cholinergic

brainstem projections—that synapse upon TCNs—causes immediate transitions to wakefulness or REM sleep (Han et al., 2014).

Generation of these spindles, along with all oscillatory thalamic behavior, relies upon precisely-timed burst and tonic firing of TCNs (Halassa et al., 2011; Kandel & Buzsáki, 1997; J. Lee et al., 2013). Upon the receipt of sensory input, TCNs either burst or tonic fire (Guido & Weyand, 1995; S. M. Sherman, 2001), and proper cortical receipt of this sensory information relies critically upon the timing and synchrony of this firing, as demonstrated in vitro and in vivo (Borden et al., 2022; Lesica et al., 2006; Lesica & Stanley, 2004; M. S. Sherman, 2001; S. M. Sherman, 2001; Stanley et al., 2012; Swadlow, 2002; Swadlow & Gusev, 2001; Wang et al., 2010; Whitmire et al., 2016). This signal is then returned to TCNs via corticothalamic projections as a modulatory input, where precisely timed burst firing of TCNs generate thalamocortical oscillations that underlie higher order thalamic functions, such as the sleep spindles that underlie memory consolidation (Jones, 2007; Latchoumane et al., 2017; LMJ & A, 2020; S. Murray. Sherman & Guillery, 2013). As such, the TCN membrane properties that regulate TCN firing, are foundational to sensory perception and thalamocortical related cognition. Therefore, we **hypothesize** that since Shox2 transcriptional activity regulates expression of proper firing characteristics of TCNs, loss of Shox2 in the VB will perturb reduce spindle activity. This hypothesis is represented in the highlighted portion of the graphical abstract in **figure 4.1**. I address this aim and hypothesis in two different models, a computational model (**aim 3a**) and a mouse model (**aim 3b**). The methods and results are described in the following text.

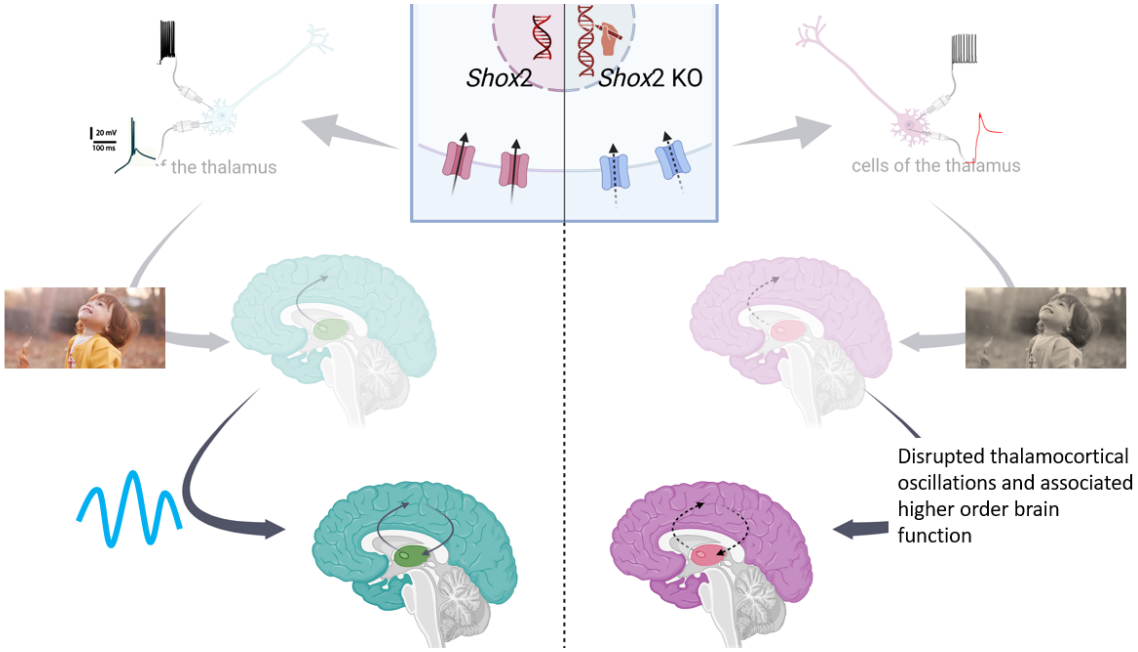

Figure 4.1 *Graphical abstract of Aim 3: Thalamus-generated sleep spindles are thalamic-Shox2 dependent.*

Bottom left: TCN firing activity underlies proper thalamus-derived spindle oscillations. **Bottom right:** I hypothesize that since Shox2 KO disrupts TCN firing activity, thalamus-derived spindle oscillation will be significantly reduced in a *Shox2* KO model.

4.2 Methods Aim 3

4.3 Methods Aim 3a: *Shox2* expression is critical for sleep spindle oscillations in a computational model of the thalamocortical circuit.

The computational model of the thalamocortical circuit oscillates at a baseline frequency of 8Hz, generating a computational representation of sleep spindles. A pathological frequency that can happen during sleep and is associated with absence epilepsy is the Spike and Wave frequency, 3-4Hz. In this model, a 50% reduction of cortical $GABA_A$ currents and simultaneous delayed activation or reduction of reticular T-type Ca^{2+} channel currents induce this pathological 3Hz frequency (Knox et al., 2018a). We hypothesize that mimicking deficits of T-type and HCN, as a result of global Shox2 KO (Yu et al., 2021), will perturb the computational model from the 8 Hz spindle frequency to pathological 3Hz absence epilepsy frequency.

The computational model to be used for this aim is available here: https://senselab.med.yale.edu/modeldb/ShowModel?mo del=234233#tabs-1 and is outlined extensively by Destexhe et al. (1994) and Destexhe et al. (1998). This model has been previously described by Knox et al., but briefly, it consists of 100 TCNs, 100 cortical interneurons, 100 cortical pyramidal (PY) neurons, and 100 thalamoreticular (RE) neurons with local network connections. Cell type–specific current parameters and synaptic conductances were fit to experimental data (Destexhe et al. 1998). Here, we will focus on the two currents found to be altered in Shox2 KO mice, the hyperpolarization-activated cation nonselective (HCN) current I_H and the T-Type Ca^{2+} channel $I_{Ca,T}$. Previously, the network model was used to assess the effects of T-type calcium channel gene variants in RE neurons (Knox et al. 2018), and the TCN model was used to assess

the effect of HCN channel modulation on TCN firing (Wang et al. 2002; Knox et al. 2018). $I_{Ca,T}$ is described by a Hodgkin-Huxley (1952) formalism:

$$I_{Ca,T} = \boldsymbol{g} m^2 h (V - E_{Ca}) \quad (1)$$

where g is the conductance of the channel, m and h are the activation and inactivation gating variables of the channel, respectively, V represents the membrane potential, and ECa is the reversal potential for calcium. The activation of T-type Ca^{2+} channel, m, is described by the

following differential equation:

$$\acute{m} = \frac{m - m_{\infty}(V)}{\tau_m(V)} \quad (2)$$

where τ_m represents the inactivation time and $m\infty$ is the steady state activation:

$$m_{\infty}(V) = \frac{1}{1 + e^{\frac{-(V+shift+57)}{6.2}}} \quad (3)$$

Initially, we will set the parameters of the model to generate nonpathological oscillations (waxing and waning sleep spindles, 8–10 Hz) in response to square pulse stimulation of 5 TCNs, as described in Knox et al. 2018. Then, we will mimic the KO deficiencies of T-type and HCN channels of 70 random TCNs and analyze whether these changes alone perturbed the network into generating pathological oscillations (spike and wave, 3–4 Hz).

Baseline parameter settings for the nonpathological state include setting the $GABA_A$ synaptic conductance for cortical interneurons to 50% of its maximal value

(Knox et al. 2018) for increased cortical excitability as in Destexhe (Destexhe et al. 1998). To mimic the voltage dependence of activation of the T-type Ca^{2+} channel in TCNs, *shift* will be changed, in thalamocortical cells of KO cells only, until a shift in half activation as observed in the experimental KO is achieved. To mimic the decrease in HCN current density in Shox2 KO mice, the conductance of the TCN HCN channels will be reduced to 0.6 μS, which is 30% of the baseline value, 2 μS. Fast Fourier transform (FFT) analysis of the pyramidal neuron spikes times was performed by creating a histogram of spike times and analyzing it with the FFT function in python. Raster plots will be generated in NEURON using the raster command.

4.4 Methods Aim 3b: VB, *Shox2* expression is critical for sleep spindle oscillations in a mouse model

The mouse model used for this aim has been previously described in chapter 2, briefly, we injected $Shox2^{fl/fl}$ mice bilaterally with a GFPCre-AAV2 virus into the VB of the thalamus, littermate controls were injected with a non-specific RFP-AAV2 virus that results in fluorescence of cells, but no Cre recombination. Mice were aged to adulthood, P40, and sleep cycles were observed. Mice were then shipped to Baylor College of medicine and EEG and EMG recordings, and secondary sleep cycle analysis were obtained at P90.

Sleep cycle observation:

8 KO and 8 CTL mice were housed (paired with a like treatment mouse from their original cage) in an isolated room with a timed 12-hour light and 12-hour dark cycle. They were recorded over a 24-hour period and videos were analyzed by blinded observers for frequency and duration of sleep episodes in CTL vs. KO mice. Observation

of mice was conducted in 15 minutes bins. Mice were given a 1 (sleep), 2 (transition), or 3 (exploring) for their behavior, and each mouse was scored by 2 separate blinded observers to control observer bias.

EEG implantation and spindle frequency detection

Animal experiments were conducted in accordance with approved IACUC guidelines at Baylor College of Medicine. To record EEG activity, WT and *Shox2* KO mice (age P90) were implanted with subdural stainless-steel screw and intracranial electrodes (PlasticsOne) using aseptic surgical technique. Two hours prior to surgery, mice were given sustained-release buprenorphine (1mg/kg b.w.). Mice were anesthetized with isoflurane (5% induction, 1-2% maintenance) and fixed to a stereotaxic frame with a heating pad for thermal support. Hair was removed from the surgical site with clippers and depilation cream and then cleaned with three alternating swabs of betadine scrub and alcohol. A local injection of lidocaine/bupivacaine block was given and a 1-2cm midline sagittal cut was made along the scalp. After removal of periosteum from the skull, three small burr holes were drilled at the following coordinates (Medial-Lateral, Anterior-Posterior, Dorsal-Ventral): somatosensory cortex (3mm, -1.5mm, 0.5mm), motor cortex (1.5mm, 1.5mm, 0.5mm), and reference electrode (-1.5mm, 1.5mm, 0.5mm). A smaller hole was drilled for an intracranial straight wire electrode to record from VB thalamus (1.5mm, -1.5mm, 3.5mm). A spring wire electrode was sutured into the paraspinous cervical muscle to record electromyoe vEEG activity was analyzed blind to genotype. To determine spectral power, raw EEG signals were bandpass filtered at 0.5-50Hz in LabChart and converted to the frequency domain using fast Fourier transform with the Hann (cosine-bell) method and 2000 FFT size with 50% window overlap (Martinez et al,

2020; Born et al, 2021). EMG was bandpass filtered at 50-200Hz to optimize classification of vigilance states. Five-minute epochs, free of noise and muscle artifact, were selected for spectral power analysis. Sleep scoring was carried out for a full 24hr light/dark cycle (14hr/10hr) by examining EEG traces and EEG spectral heat maps. Wake/sleep transition states were confirmed by visual inspection of video recordings. Awake states were defined as high amplitude EMG/low amplitude, high frequency EEG activity. Sleep states were segmented into slow-wave sleep (non-REM) and REM sleep. Non-REM was defined by low amplitude EMG/high amplitude, low frequency EEG activity. REM sleep was defined by low amplitude EMG/low amplitude, high frequency EEG activity. Sleep duration and spectral power were quantified in each sleep state during light and dark cycles. Sleep spindles were detected by filtering the EEG signal at the sigma frequency as previously (Copping & Silverman, 2021a; Kim et al., 2015). Briefly, spindles were detected from S1 and VB EEG signals in Labchart by first applying a bandwidth filter in the sigma frequency (9-16Hz), then applying a Butterworth filter, followed by obtaining the root mean square in 750ms square windows. The resulting filtered signal was then cubed to reduce background noise and amplify sigma frequency peaks. Spindles were quantified using the Peak analysis function in Labchart. Due to variability in spindle amplitude, spindle threshold was determined empirically for each mouse, however, mean threshold between genotypes did not differ (WT 97.5mV ± 44.7μV and KO 52.3mV±30.4μV, $p>0.05$) Total spindle frequency was quantified during the light cycle. Spindle frequency was also compared during the one minute immediately before the state transition from non-REM to REM sleep and separately during the transition from non-REM to the wake state.

4.5 Results Aim 3

4.5.1 Results Aim 3a: Computational modeling predicts that Shox2 expression favors normal spindle activity.

The goal of aim 3a was to test the hypothesis that *Shox2* transcriptional activity in the thalamus is important for sleep spindles generated by the thalamocortical circuit in a computational model. The model is a well-established computational model of the thalamocortical circuit, originally constructed by Destexhe et al., and recently reconstructed by Knox et al. (Destexhe 1998; Knox et al. 2018a).

With this model, I demonstrated that the Shox2-mediated alterations in I_T and I_H currents are predicted to affect thalamocortical oscillation frequencies. With the original, default parameters under baseline conditions, which are described in the *Methods*, the thalamocortical model network exhibits transient, waxing and waning, nonpathological spindle oscillations (7–8 Hz, figure 31) in response to a stimulus that simulates a perturbation of the network. The heat maps in figures 4.1 and 4.2 are generated by recording the membrane potential of the 100-neuron populations over time, with neuron index on y-axis and time on the x-axis. Dark colors indicate a membrane potential near resting while light colors indicate depolarizations and spikes. Lines of yellow and orange show a synchronous population spike. The frequency of oscillations in the pyramidal neuron (PY) population can be roughly quantified by counting the number of population spikes per second. To generate a computational *Shox*2 KO, we computationally mimicked the observed deficits in T-type and HCN currents in a randomly selected 70%

of TCNs, as our anatomical data showed that *Shox2* was expressed in approximately 70% of the TCNs.

First, to calibrate the model to experimental KO based on experimental results shown in **figure 4.2.a**, we reduced I_H by 60% of its original value (**figure 4.2.b**). With only this change to I_H, the 8Hz spindle oscillations were not disrupted (**figure 4.2.c**). Next, we matched the shift in half activation of I_T. Boltzmann equations were used to determine half activations of control (−60 mV) and KO (−57 mV) experimental T-type currents (**figure 4.2.d**), revealing a positive shift of 3 mV in the KO. This shift was mimicked in the computational KO I_T (**figure 4.2.e,** gray trace) compared with control (black trace). This half-activation shift also served to reduce the current to 70%, as observed experimentally (Fig 5). This was due to an increased overlap of the steady-state activation curve with the steady-state inactivation curve (**figure 4.2.e,** black, negative slope trace). Again, this disruption to I_T alone did not perturb the model out of baseline spindle oscillation state (data not shown).

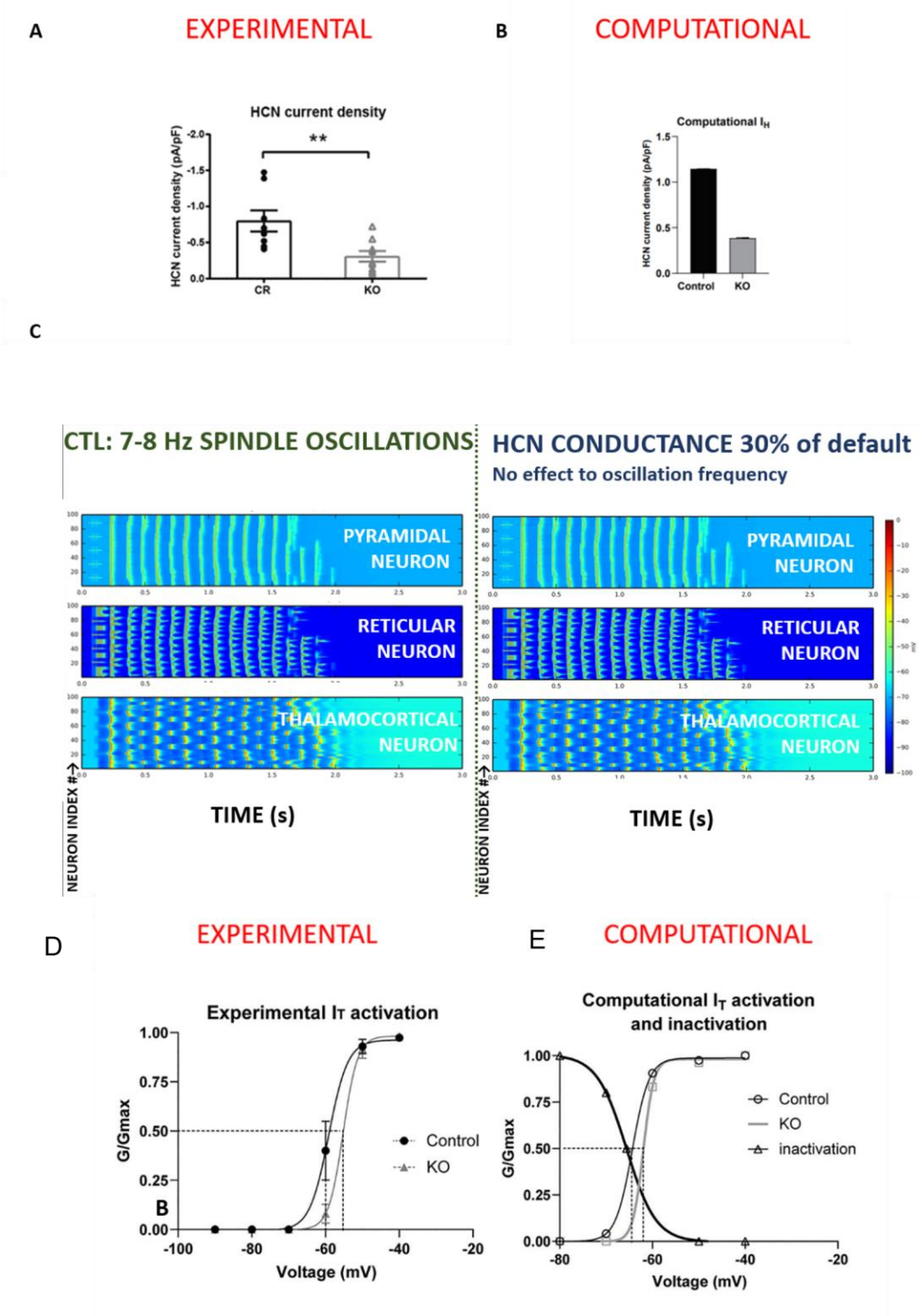

Figure 4.2 *Computationally mimicking Shox2 KO alterations in I_H or I_T alone does not disrupt spindle oscillations*

Figure 4.3 *Computationally mimicking Shox2 KO alterations in I_H or I_T alone does not disrupt spindle oscillations*

A) Global KO experimental data reveals a 60% reduction in HCN current density **B)** Computational I_H conductance was reduced by 60% as in global KO **C)** Baseline conditions of computational model, pyramidal neurons fire at a waxing waning spindle frequency of 8 Hz (left) and reduction of I_H did not perturb spindle oscillations in model (right). **D)** Plot of experimental activation and Boltzmann showing half-activation of I_T for cells recorded in WT (−60 mV) and KO mice (−57 mV). **E)** Plot of activation of computational T-type current was generated, and Boltzmann fit showed a half activation voltage of −65 mV that shifted to −62 mV for the KO.

However, when both the half-activation of the TCN T-type channel is shifted by 3 mV and the current through the HCN channel is reduced by 60% in 70 random TCNs to mimic the *Shox*2 KOs, PY neuron firing activity is disrupted. The population-wide oscillations slow to near 4.5 Hz (**figure 33C**), a frequency comparable to that of pathological spike and wave-frequency oscillations (~4 Hz). Moreover, the oscillatory tendencies are more sustained, indicating the network may be susceptible to absence seizure generation in the simulated knockout network (spike raster plot in the top right of **figure 33D**) compared with control (same plot in figure **33B**). The population frequency was quantified by performing a Fast Fourier transform (FFT) on the peri-stimulus time histogram of the spikes in the PY neuron population (**figure 33B, D, bottom**). We found that it was necessary to mimic both T-type and HCN deficiencies caused by *Shox2* KO in TCNs to result in this near 4 Hz frequency; neither manipulation in isolation was sufficient.

Aim 3a summary and discussion

Patch-clamp electrophysiological analysis revealed that Shox2 regulation of T-type Ca^{2+} and HCN channels and their corresponding currents contributes to the intrinsic firing properties in these neurons. Computational modeling showed that modulation of currents regulated by Shox2 is predicted to shift network oscillation frequency from spindle oscillations to a frequency associated with spike and wave patterns that characterize seizures, suggesting that Shox2 is important to maintain normal function of thalamocortical network activity.

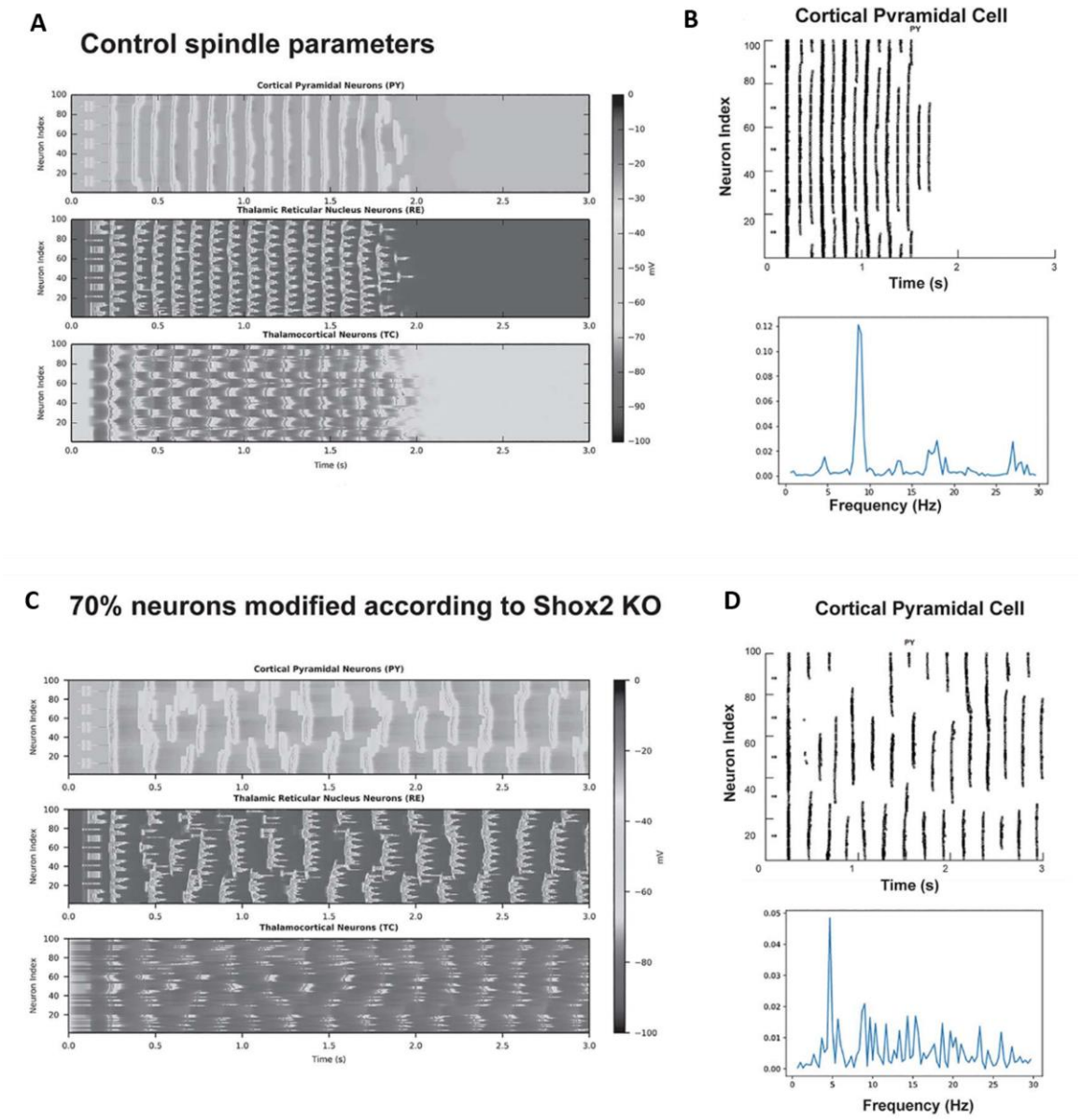

Figure 4.4 *Computational model suggests that Shox2-expression favors thalamocortical spindle oscillations.* **A)** The model is set to baseline parameters that generate spindle oscillations (8 Hz). Each heat map displays the activity of a cell-type population (PY, TCN, or RE) with cell index number on the y-axis and time on the x-axis. Oscillation frequency is determined by the number of PY population events per second. **B&D)** Raster plots of computational pyramidal cell spike times. Frequency was determined by Fast Fourier transform (FFT) analysis of control **(A)** and KO **(C)** raster plots. PY neurons in thalamocortical network reveals a peak at 8 Hz for control and~4.5 Hz for KO paradigms.

4.5.2 Results Aim 3b: Expression of thalamic Shox2 promotes sleep spindle oscillations in a mouse model

The goal of aim 3a was to test the hypothesis that *Shox2* transcriptional activity in the thalamus is important for sleep spindles generated by the thalamocortical circuit in a mouse model. The experimental mouse model used to address this aim was the previously described bilateral, VB, P21, *Shox2* KO and the controls were littermate, *Shox2*$^{fl/fl}$ that received bilateral VB injections at P21 of the non-specific RFP virus that did not induce cre recombination, thus, leaving the genome unaltered.

Preliminary sleep cycle analysis reveals VB Shox2 KO does not alter time spent sleeping

Sleep spindles occur during NREM sleep. Thus, our first step in being able to compare sleep spindles in CTL versus KO mice was to determine whether the mice were sleeping for the same amount of time. Preliminary experiments to observe the sleep cycles in CTL versus KO mice were performed at Tulane University. 8 KO and 8 CTL mice were housed (paired with a like treatment mouse from their original cage) in an isolated room with a timed 12-hour light and 12-hour dark cycle. They were recorded over a 24-hour period and videos were analyzed by blinded observers for frequency and duration of sleep episodes. I found no discernable differences in sleep patterns, except that during the early hours after transition from dark to light, CTL and KO mice were antiphase. KO mice woke up when the vivarium technician entered to check on them at 7 am, whereas the CTL mice entered a sleep phase at the beginning of the light cycle. A plot of control versus KO behavior over the 24-hours reveals their sleep rhythms (**figure 4.5,** top). We quantified the amount of time the mice spent doing each behavior and found no significant differences between scores (**figure 4.5,** bottom).

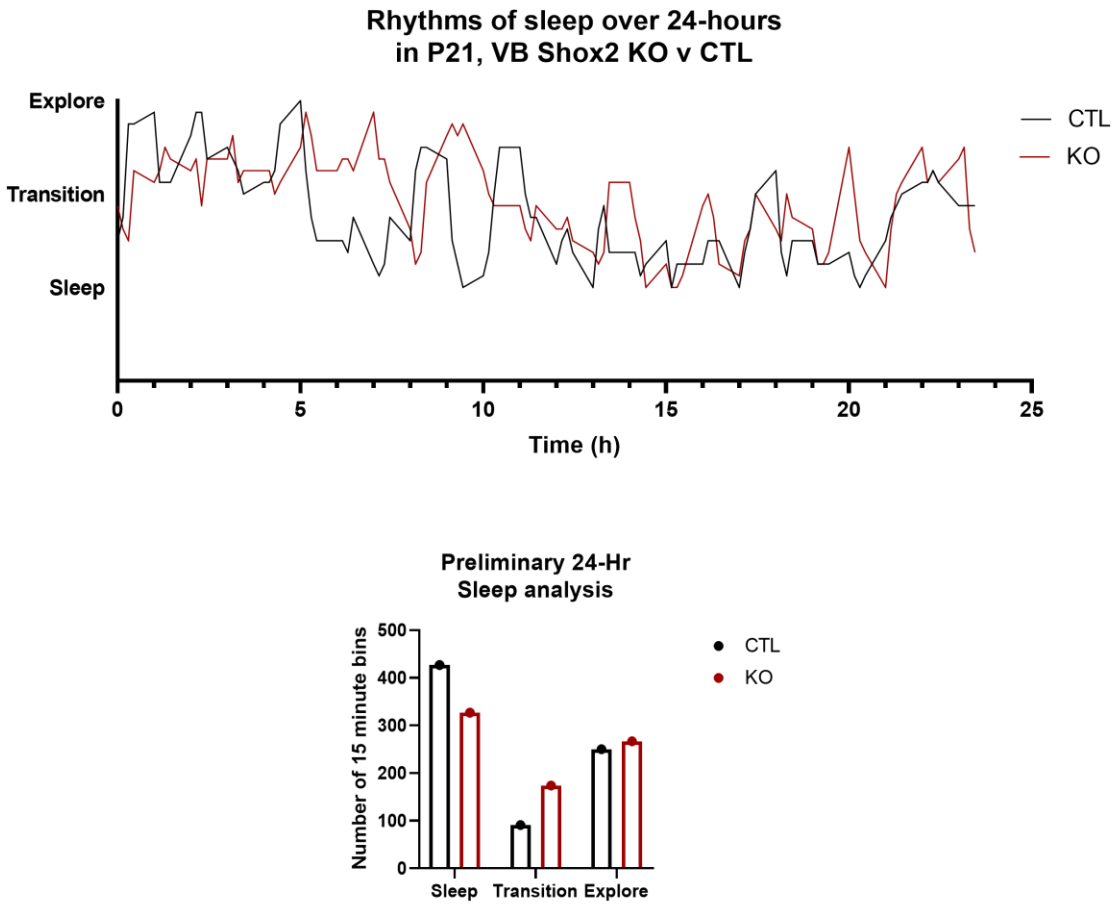

Figure 4.5 *Preliminary sleep analysis reveals no differences in sleep rhythms or activity between CTL and KO mice over 24 hours.*

8 CTL and 8 P21, VB, *Shox2*-KO mice were housed (paired with a like treatment mouse from their original cage) in an isolated room with a timed 12-hour light and 12-hour dark cycle and recorded. Videos were analyzed by blinded observers for frequency and duration of sleep episodes. **Top:** Plot of CTL versus KO mouse activity over 24 hours. Mice were scored in 15-minute bins as either asleep, transitioning from awake to asleep or asleep to awake, or exploring. **Bottom:** Quantification of time spent doing each activity in KO v CTL.

EEG, EMG, and secondary sleep cycle analysis:

To analyze sleep rhythms using muscle activity rather than observation, and to observe in-vivo thalamocortical oscillations activity, the same 8 KO and 8 CTL mice were placed with cortical electrodes in the somatosensory cortex and the ventrobasal nucleus of the thalamus (VB) to record EEG activity, as well as electromyography (EMG) recordings of muscle activity to conclusively determine asleep versus awake states. **Figure 4.6**.a is a diagram of the electrode placement, and example traces of the collected data. The results were analyzed for differences in duration of sleep and cortical EEG power.

In agreement with our previous 24-hour sleep analysis, there were no differences between male or female, control, or KO, in the amount of time spent sleeping, or when the mice slept (**figure 4.6.b**).

We then analyzed whether the KO mice were spending more or less time in slow wave sleep (SWS) or REM sleep. This was an important metric to measure, because spindles occur during SWS, so to compare spindles, it is important to know if KO mice spent more or less time in SWS. We found no difference in the amount of time spent in SWS or REM sleep between CTL and KO mice (**figure 4.6.c**).

Power analysis of cortical EEGs reveals no differences in oscillation frequency power between control or KO mice (**figure 4.6.d**). However, analysis of the frontal EEG trace during slow wave sleep, using a band-pass filter of 9-16Hz, revealed that the density (number of spindles per minute) of sleep spindles recorded in the cortex was significantly reduced in the *Shox2* KO mouse (**figure 4.6.e**).

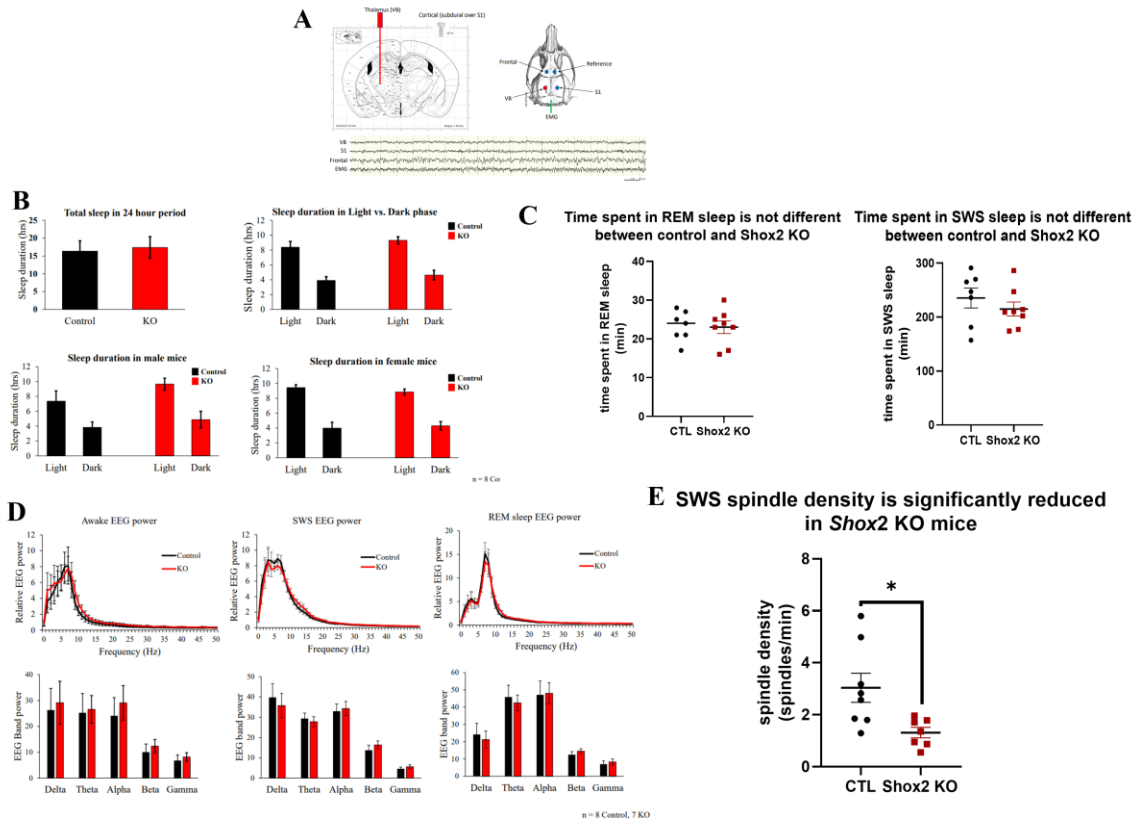

Figure 4.6 *Spindle density during slow-wave sleep (SWS) is significantly reduced in P21, VB, Shox2-KO mice.*

A) Top: Diagram showing coronal location of VB probe placement (left) and dorsal location of frontal, reference, VB, S1, and EMG probes (right). Bottom: Example trace recordings from each probe. **B)** Time spent sleeping in CTL vs. KO during light or dark phases and between male and female is not different. **C)** Time spent in slow wave sleep (SWS) and REM sleep is not different between control and KO mice. **D)** Power analysis of cortical EEGs reveals no differences in oscillation frequency power between control or KO mice. **E)** *SWS spindle density is significantly reduced in Shox2 KO mice.* A bandpass filter of 9-16Hz was used to analyze the frontal EEG of CTL v KO mice during SWS. Analysis reveals that Shox2 KO mice have a significantly reduced density of sleep spindles (spindles/min) as determined by a student's t-test, p=0.0173.

Aim 3b summary and conclusion

Our results indicate that KO of Shox2 in the thalamus does not disrupt sleep activity (neither rhythms nor amount of time in SWS versus REM sleep) but that it does perturb thalamic activity such that either spindle generation or spindle relay to the cortex is significantly reduced.

Sleep spindles are functionally associated with memory consolidation. Previous data from our lab found that global Shox2 KO mice have impaired memory consolidation (tested via a novel object recognition task). These mice also have somatosensory deficits, so to ensure that recognition of novel objects was not sensory impairment dependent, we utilized another Shox2 KO mouse model, $Shox2^{fl/fl}$;GBX;ErtCre. This cre mouse model expresses cre along the midline of the thalamus, which does not include the primary sensory thalamic nuclei. These mice did not exhibit somatosensory impairments (as determined by the sticky tape test) but did maintain memory consolidation deficits (novel object recognition). This provides evidence that the reduced discrimination between novel and non-novel object is a memory consolidation impairment, resulting from a reduced spindle density, not a sensory deficit.

Chapter 5 Discussion and Future

5.1 Summary of Dissertation

Shox2, expressed in both human and mouse thalamus (Nagalski et al., 2016), is involved in the regulation of rhythmic firing properties in the heart, spinal cord, and thalamus (Ha & Dougherty, 2018; Puskaric et al., 2010; Sun et al., 2015; Yu et al., 2021). Here, I validate our previous findings that *Shox2* expression is critical for HCN and T-type currents within a different nucleus of the thalamus, VB rather than PVN, using a VB targeted KO model. In aim 1, we analyzed the effect to TCN burst firing, tonic firing, and membrane properties. In aim 2, we established cortical and reticular connectivity of *Shox2*-expressing TCNs and determined that *Shox2* expression in the VB maintains whisker somatosensory relay, but that it is not critical for development of gross cortical barrel organization. In aim 3, we used a computational and mouse model to show that expression of *Shox2* within the thalamus is necessary for proper cortical spindle activity, which underlies memory consolidation. This bolsters our previous findings that *Shox2*-KO mice have memory consolidation deficits. These experiments provide evidence that the transcriptional activity of Shox2 generates TCN firing characteristics that promote proper thalamic function, specifically: sensory perception and memory consolidation.

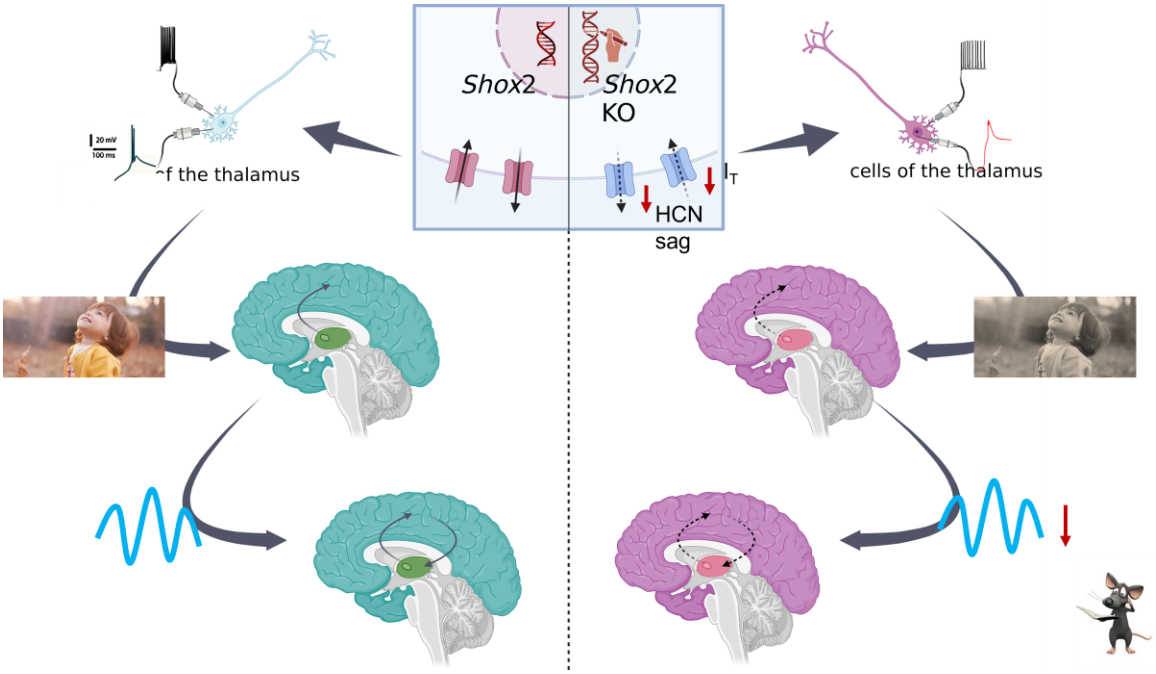

Figure 5.1 *Graphical summary of findings*

Left (starting from top): I hypothesized that activity of the transcription factor, Shox2, within the thalamus of mice, is critical for ion current dynamics that underlie firing characteristics of thalamocortical neurons, relay of sensory information, and proper thalamic oscillatory activity. **Right (starting from top):** Results from a within thalamus, *Shox2* KO, revealed that 1) key ion currents are reduced, action potentials during burst and tonic firing of TCNs are significantly reduced, 2) *Shox2*-expressing TCNs synapse in the cortex and reticular nucleus of the thalamus and expression is necessary for sensory perception, and 3) proper thalamus-derived spindle oscillation activity is thalamic, *Shox2*-expression dependent.

5.2 Discussion

5.2.1 Shox2 expression in thalamocortical neurons

A subset of Shox2-expressing TCNs was difficult to distinguish. There were no readily apparent differences in *Shox2*-expressing versus *Shox2*-negative TCNs. For example, given the previously observed effect to T-type Ca^{2+} and HCN channels, I_T and I_H, we expected that *Shox2*-negative TCNs would either not burst fire at all, or that there was a distinct difference in their burst firing. While we did observe a significantly greater number of action potentials per burst in the *Shox2*-expressing TCNs, both *Shox2*-expressing and *Shox2*-negative TCNs exhibit burst firing with single or multiple action potentials.

Burst firing of thalamocortical neurons can have a different phenotype depending on what nucleus the neuron is located in. In general, burst firing with a single action potential is more associated with higher order nuclei, whereas burst firing with multiple action potential is associated with first order nuclei (Desai & Varela, 2021). Specifically, the VB, being a first order nucleus, is mostly comprised of TCNs that burst fire with multiple action potentials. The first spike of a bust is mediated by sodium and potassium currents, and the following spikes within a burst involve the recruitment of a high-threshold Ca^{2+} spike (Tennigkeit et al., 1998) and an A-type potassium current (Kanyshkova et al., 2011a). The coupling of these currents with the T-type Ca^{2+} facilitate the multiple action potentials observed in first order nuclei TCN bursts.

We did not observe a significant difference in the T-type current density or the HCN attributed sag between the two cell types. Rather, we saw a range of both metrics in both cell types. This indicates that Shox2 may directly regulate a different ion channel

that has downstream effects to HCN and t-type. A-type potassium channels are rapidly activating and slowly inactivating channels that generate an inward current, I_A, that acts to counter the low threshold spike generated by T-type calcium channels, and repolarizes the membrane, contributing to proper termination of the burst. In TCNs that fire a single post-anodal action potential in control conditions, the blocking of I_A causes the cell to fire multiple action potentials during a post-anodal burst (Kanyshkova et al., 2011b). Blockade of A-type potassium with high concentrations of 4-AP results in the failure of the cell to repolarize after a burst and during tonic firing (Tennigkeit et al., 1998). Thus, it is possible that I_A is reduced in *Shox2*-expressing TCNs, resulting in a more 'bursty' TCN. This hypothesis could also explain the reduction in the number of action potentials observed in the *Shox2* negative TCNS and *Shox2* KOs.

5.2.2 A-type potassium channel role in TCN burst firing

A-type potassium current has similar kinetics to T-type Ca^{2+} but opposite effects on the membrane potential of the cell. It is a rapidly activating and slowly inactivating outward current that is activated after a depolarization following hyperpolarization. Thus, while I_T is responsible for the *generation* of the post-anodal low threshold spike (LTS), the temporal alignment and opposing effects of I_{As} makes it responsible for the regulation and *termination* of the calcium generated LTS. I_{AS} also modulates the number of action potentials per burst by facilitating the coupling of the low LTS to activate calcium generated high-threshold spikes (HTS). HTSs are action potentials that happen during a burst but are calcium dependent and blocked by Cd^{2+}(Tennigkeit et al., 1998). These spikes occur after the first sodium generated spike in a burst. So, the presence of I_{AS} allows for multiple action potentials per burst.

Given that a reduced number of action potentials per burst was a significant difference between *Shox2*-exprssing and *Shox2*-negative TCNs, it stands to reason that Shox2 is involved in the regulation of the A-type potassium current, and that the effects that result from a loss of Shox2 involve the dysregulation of I_A, I_T, and I_H. Whether the effects to I_T and I_H are directly attributed to Shox2 regulation of T-type Ca^{2+} and HCN channels is unclear, however, given that there was no significant difference between the HCN and I_T in *Shox2*-expressing versus *Shox2*-negative TCNs, the hypothesis that Shox2 is involved in the regulation of A-type potassium channels and that the effects to HCN and T-type in the KO are compensatory, is more supported.

Shox2 KO TCNs had a significantly reduced action potential frequency and action potential peak amplitude. Also, many *Shox2* KO TCNs displayed a 'plateau' during tonic firing when depolarized sufficiently. The plateau can be described as 1-2 action potentials, followed by an absence of repolarization where the membrane remains at a potential near the peak of the last AP until the current injection ends. This same phenomenon has been observed during the blocking of A-type potassium current. Blockade of I_{AS} with 4-AP resulted in this same 'plateau' effect, where the membrane does not repolarize itself after high frequency tonic firing during large current injections. Other potassium channels involved in the regulation of tonic firing, such as Kv3.4, do not have this same effect (Kasten et al., 2007).

5.2.3 Implications of reduced and ill-timed TCN action potentials

Regardless of mechanism, *Shox2* KO significantly reduced the number of action potentials fired by thalamocortical neurons. These neurons, even from first order relay nuclei, synapse on all layers of the cortex. We specifically defined layer IV input to

excitatory and inhibitory cortical neurons. Lee & Sherman investigated the release properties of these projections. While recording from 13 layer IV cells in the somatosensory cortex and electrically stimulating in the VPM, they found that all cells responded with paired-pulse depression, all-or-none responses, and the absence of a metabotropic component, which they describe as class I, or, first order relay (C. C. Lee & Sherman, 2008). We showed specific connectivity of these first order synapses to PV^{+} interneurons in layer IV barrel cortex. The literature supports that these are indeed the inhibitory postsynaptic components observed in field recordings.

Cortical inhibitory GABAergic neuron populations can be described in a nearly non-overlapping schema if classified by their expression of parvalbumin (PV), somatostatin (SST) and vasoactive intestinal peptide (VIP)(Rudy et al., 2011). Thalamic input from VB is reportedly weak onto somatostatin neurons(Cruikshank et al., 2010). Further, SST+ and VIP+ interneurons favor septal compartments, while PV+ neurons favor the barrel interiors (Almási et al., 2019), which VB projections have been reported to selectively innervate. Conclusively, Sermet et al demonstrated that VB projections to layer IV synapse on PV+ inhibitory interneurons almost exclusively (Sermet et al., 2019). These inhibitory neurons provide synchrony for the cortex and thalamocortical oscillations, this synchrony is critical for sensory perception (Bruno, 2011). Thus, although we did not directly show that the cortex receives fewer and ill-timed action potentials, and that this is the cause for somatosensory disruption and a decrease in spindle density, the observed reduction in action potentials would likely prevent activation of the cortex and reduce the probability of eliciting an action potential in cortical targets (Swadlow & Gusev, 2001). Further, we observed a significant increase in

input resistance in KO TCNs. Thalamic state influences timing precision in the thalamocortical circuit, and differences in input resistance alters TCN membrane response to synaptic inputs (Whitmire et al., 2021). Additionally, it is well accepted that "the modulation and extent of bursting in thalamic neurons are important in the generation of synchronized oscillations during sleep and pathological states" (Huguenard & Prince, 1994; Steriade et al., 1993).

5.2.4 Other thalamic transcription factors

Transcription factors are integral determinants of cell identity. Despite the critical role of the thalamus in cognition, relatively little is known about the transcription factors that regulate thalamic neuron membrane properties. Most investigation into the function of thalamic transcription factors examine embryonic and developmental determinants of thalamic nuclei organization (Bluske et al., 2009; Jones & Rubenstein, 2004; Nakagawa & O'leary, 2001; Nakagawa & O'Leary, 2003; Tou et al., 2007; Yuge et al., 2011). In the adult mouse thalamus, combinatorial expression of Tcf7l2, Lef1, Gbx2, Prox1, Pou4f1, Esrrg, and Six3 define molecular divisions that loosely correlate with established nuclei divisions (Nagalski et al., 2016). Pax6 and Gli2 have been identified as a transcription factors that are critical to the development of thalamocortical projections (Pratt et al. 2000; Callejas-Marin et al. 2022). TCF7L2, expressed throughout the thalamus as well as the habenula, has also been shown to be critical for thalamocortical projections and habenula organization (Lipiec et al., 2019). All studies cite the importance of thalamic function as motivation for their findings, however, none have demonstrated that these

factors are necessary for the generation of bigger picture neuronal function associated with thalamocortical oscillations.

5.2.5 Possibility of translational effects

While the physiology and intrinsic properties of thalamic relay neurons are well characterized, the genetic factors that establish the expression patterns of these channels are unknown. Shox2 represents a possible candidate that may control channel expression in the thalamic relay neurons and ultimately pattern pacemaker activity. Several lines of evidence indicate that these studies of the role of Shox2 in pacemaker function in mice are also applicable to humans. Shox2 is a super-conserved gene with 99% amino acid identity between human SHOX2 and mouse Shox2. A recent study found that two missense mutations within the human SHOX2 gene are associated with early-onset atrial fibrillation, likely caused by a defect in pacemaker activity(Hoffmann et al., 2016; N. Li et al., 2018). In addition, while mice do not express the Shox gene, human SHOX and SHOX2 have 79% similar amino acid identity, and the same DNA-binding domains and putative phosphorylation sites. The functional redundancy in the regulation of heart pacemaker cells' differentiation between human SHOX and mouse Shox2 has been demonstrated in mouse models (Liu et al., 2011). Therefore, investigation of Shox2 function in mouse can extend to evaluate the role of human SHOX and SHOX2 in humans. Turner syndrome (TS) is one of the most common sex chromosome abnormalities (JACOBS et al. 1997) and results from the complete or partial loss of the X chromosome. Most individuals with TS have short stature, which is associated with the loss of the SHOX gene (Blaschke et al., 1998; Joseph et al., 1996; Oliveira & Alves, 2011). These individuals are at increased risk for neurodevelopmental issues, including

learning disabilities, visuo- spatial, social, and executive function impairments (Mauger et al., 2018), and epilepsy (Jhang et al., 2014; Magara et al., 2015; Puusepp et al., 2008; Saad et al., 2014; Zhao & Lian, 2015). Interestingly, the smallest chromosomal deletion associated with the neurocognitive phenotype included SHOX (Knickmeyer & Davenport, 2011), "suggesting that loss of SHOX may play a role in cognitive impairments in humans." Additionally, sleep spindle density is positively correlated with mental acuity (Bódizs et al., 2005), and reduced sleep spindle density has been identified as a biomarker for autism and schizophrenia (Copping & Silverman, 2021b; Manoach et al., 2016). While the mechanisms of the neurodevelopmental issues in these patients is unclear, our current study indicates that altering expression of SHOX- or SHOX2-related genes may contribute to thalamic dysfunctions and some of these neurodevelopmental impairments.

5.3 Future

Further studies are necessary to determine the specific contribution of Shox2-expressing neurons to thalamocortical circuitry, and the role Shox2 may play beyond regulation of firing properties. Future studies will investigate whether Shox2 plays a critical role during thalamic development and differentiation, the contribution of these Shox2-regulated currents to overall TCN function, and the mechanisms by which Shox2 regulates their expression.

List of References

Abbas, S. Y., Ying, S. W., & Goldstein, P. A. (2006). Compartmental distribution of hyperpolarization-activated cyclic-nucleotide-gated channel 2 and hyperpolarization-activated cyclic-nucleotide-gated channel 4 in thalamic reticular and thalamocortical relay neurons. *Neuroscience*, *141*(4), 1811–1825. https://doi.org/10.1016/J.NEUROSCIENCE.2006.05.034

Abramson, B. P., & Chalupa, L. M. (1985). The laminar distribution of cortical connections with the tecto- and cortico-recipient zones in the cat's lateral posterior nucleus. *Neuroscience*, *15*(1), 81–95. https://doi.org/10.1016/0306-4522(85)90125-3

Agmon, A., & Connors, B. W. (1991). THALAMOCORTICAL RESPONSES OF MOUSE SOMATOSENSORY (BARREL) CORTEX IN VITRO. In *Neuroscience* (Vol. 41, Issue 213).

Almási, Z., Dávid, C., Witte, M., & Staiger, J. F. (2019). Distribution Patterns of Three Molecularly Defined Classes of GABAergic Neurons Across Columnar Compartments in Mouse Barrel Cortex. *Frontiers in Neuroanatomy*, *0*, 45. https://doi.org/10.3389/FNANA.2019.00045

Altomare, C., Terragni, B., Brioschi, C., Milanesi, R., Pagliuca, C., Viscomi, C., Moroni, A., Baruscotti, M., & DiFrancesco, D. (2003). Heteromeric HCN1–HCN4 Channels: A Comparison with Native Pacemaker Channels from the Rabbit Sinoatrial Node. *The Journal of Physiology*, *549*(2), 347–359. https://doi.org/10.1113/JPHYSIOL.2002.027698

Amarillo, Y., Tissone, A. I., Mato, G., & Nadal, M. S. (2018). Inward rectifier potassium current I Kir promotes intrinsic pacemaker activity of thalamocortical neurons. *J Neurophysiol*, *119*, 2358–2372. https://doi.org/10.1152/jn.00867.2017.-Slow

Amarillo, Y., Zagha, E., Mato, G., Rudy, B., & Nadal, M. S. (2014). The interplay of seven subthreshold conductances controls the resting membrane potential and the oscillatory behavior of thalamocortical neurons. *J Neurophysiol*, *112*, 393–410. https://doi.org/10.1152/jn.00647.2013.-The

Andersen, P., & Eccles, J. (1962). Inhibitory phasing of neuronal discharge. *Nature*, *196*(4855), 645–647. https://doi.org/10.1038/196645a0

Anderson, M. P., Mochizuki, T., Xie, J., Fischler, W., Manger, J. P., Talley, E. M., Scammell, T. E., & Tonegawa, S. (2005). Thalamic Cav3.1 T-type Ca2+ channel plays a crucial role in stabilizing sleep. *Proceedings of the National Academy of Sciences of the United States of America*, *102*(5), 1743–1748. https://doi.org/10.1073/PNAS.0409644102/SUPPL_FILE/09644FIG6.PDF

Andreasen, N. C. (1997). The Role of the Thalamus in Schizophrenia. *The Canadian Journal of Psychiatry*, *42*(1), 27–33. https://doi.org/10.1177/070674379704200104

Andreasen, N. C., Paradiso, S., & O'Leary, D. S. (1998). "Cognitive dysmetria" as an integrative theory of schizophrenia: a dysfunction in cortical-subcortical-cerebellar circuitry? *Schizophrenia Bulletin*, *24*(2), 203–218. https://doi.org/10.1093/OXFORDJOURNALS.SCHBUL.A033321

Astori, S., Wimmer, R. D., Prosser, H. M., Corti, C., Corsi, M., Liaudet, N., Volterra, A., Franken, P., Adelman, J. P., & Lüthi, A. (2011). The Ca v3.3 calcium channel is the major sleep spindle pacemaker in thalamus. *Proceedings of the National Academy of*

Sciences of the United States of America, *108*(33), 13823–13828. https://doi.org/10.1073/pnas.1105115108

Barthó, P., Slézia, A., Mátyás, F., Faradzs-Zade, L., Ulbert, I., Harris, K., & Acsády, L. (2014). Ongoing network state controls the length of sleep spindles via inhibitory activity. *Neuron*, *82*(6), 1367–1379. https://doi.org/10.1016/J.NEURON.2014.04.046

Beenhakker, M. P., & Huguenard, J. R. (2009). Neurons that Fire Together Also Conspire Together: Is Normal Sleep Circuitry Hijacked to Generate Epilepsy? *Neuron*, *62*(5), 612–632. https://doi.org/10.1016/J.NEURON.2009.05.015

Blaschke, R. J., Monaghan, A. P., Schiller, S., Schechinger, B., Rao, E., Padilla-Nash, H., Ried, T., & Rappold, G. A. (1998). SHOT, a SHOX-related homeobox gene, is implicated in craniofacial, brain, heart, and limb development. *Proceedings of the National Academy of Sciences of the United States of America*, *95*(5), 2406–2411. https://doi.org/10.1073/PNAS.95.5.2406

Bluske, K. K., Kawakami, Y., Koyano-Nakagawa, N., & Nakagawa, Y. (2009). Differential activity of Wnt/β-catenin signaling in the embryonic mouse thalamus. *Developmental Dynamics*, *238*(12), 3297–3309. https://doi.org/10.1002/DVDY.22167

Bódizs, R., Kis, T., Lázár, A. S., Havrán, L., Rigó, P., Clemens, Z., & Halász, P. (2005). Prediction of general mental ability based on neural oscillation measures of sleep. *Journal of Sleep Research*, *14*(3), 285–292. https://doi.org/10.1111/J.1365-2869.2005.00472.X

Borden, P. Y., Wright, N. C., Morrissette, A. E., Jaeger, D., Haider, B., & Stanley, G. B. (2022). Thalamic bursting and the role of timing and synchrony in thalamocortical signaling in the awake mouse. *Neuron*. https://doi.org/10.1016/J.NEURON.2022.06.008

Bordes, S., Werner, C., Mathkour, M., McCormack, E., Iwanaga, J., Loukas, M., Lammle, M., Dumont, A. S., & Tubbs, R. S. (2020). Arterial Supply of the Thalamus: A Comprehensive Review. *World Neurosurgery*, *137*, 310–318. https://doi.org/10.1016/J.WNEU.2020.01.237

Braus, D. F., Weber-Fahr, W., Tost, H., Ruf, M., & Henn, F. A. (2002). Sensory Information Processing in Neuroleptic-Naive First-Episode Schizophrenic Patients: A Functional Magnetic Resonance Imaging Study. *Archives of General Psychiatry*, *59*(8), 696–701. https://doi.org/10.1001/ARCHPSYC.59.8.696

Brown, R. E., Basheer, R., McKenna, J. T., Strecker, R. E., & McCarley, R. W. (2012). Control of Sleep and Wakefulness. *Physiological Reviews*, *92*(3), 1087–1187. https://doi.org/10.1152/physrev.00032.2011

Bruno, R. M. (2011). Synchrony in sensation. *Current Opinion in Neurobiology*, *21*(5), 701–708. https://doi.org/10.1016/j.conb.2011.06.003

Burns, T. F., & Rajan, R. (2021). Sensing and processing whisker deflections in rodents. *PeerJ*, *9*. https://doi.org/10.7717/PEERJ.10730

Buzsáki, G. (2006). Rhythms of the Brain. *Rhythms of the Brain*, 1–464. https://doi.org/10.1093/ACPROF:OSO/9780195301069.001.0001

Callejas-Marin, A., Moreno-Bravo, J. A., Company, V., Madrigal, M. P., Almagro-García, F., Martínez, S., & Puelles, E. (2022). Gli2-Mediated Shh Signaling Is

Required for Thalamocortical Projection Guidance. *Frontiers in Neuroanatomy*, *16*. https://doi.org/10.3389/FNANA.2022.830758

Campbell, X. P. W., Govindaiah, G., Masterson, S. P., Bickford, X. M. E., & Guido, W. (2020). Synaptic properties of the feedback connections from the thalamic reticular nucleus to the dorsal lateral geniculate nucleus. *Journal of Neurophysiology*, *124*(2), 404–417. https://doi.org/10.1152/JN.00757.2019

Carrera, E., & Bogousslavsky, J. (2006). The thalamus and behavior. *Neurology*, *66*(12), 1817–1823. https://doi.org/10.1212/01.WNL.0000219679.95223.4C

Cheong, E., & Shin, H. S. (2013). T-type Ca2+ channels in normal and abnormal brain functions. *Physiological Reviews*, *93*(3), 961–992. https://doi.org/10.1152/PHYSREV.00010.2012

Coetzee, W. A., Amarillo, Y., Chiu, J., Chow, A., Lau, D., McCormack, T., Moreno, H., Nadal, M. S., Ozaita, A., Pountney, D., Saganich, M., Vega-Saenz De Miera, E., & Rudy, B. (1999). Molecular Diversity of K+ Channels. *Annals of the New York Academy of Sciences*, *868*(1), 233–255. https://doi.org/10.1111/J.1749-6632.1999.TB11293.X

Constantinople, C. M., & Bruno, R. M. (2013). Deep Cortical Layers are Activated Directly by Thalamus. *Science (New York, N.Y.)*, *340*(6140), 1591. https://doi.org/10.1126/SCIENCE.1236425

Copping, N. A., & Silverman, J. L. (2021a). Abnormal electrophysiological phenotypes and sleep deficits in a mouse model of Angelman Syndrome. *Molecular Autism*, *12*(1). https://doi.org/10.1186/S13229-021-00416-Y

Copping, N. A., & Silverman, J. L. (2021b). Abnormal electrophysiological phenotypes and sleep deficits in a mouse model of Angelman Syndrome. *Molecular Autism*, *12*(1). https://doi.org/10.1186/S13229-021-00416-Y

Cribbs, L. L. (2010). T-type calcium channel expression and function in the diseased heart. *Channels (Austin, Tex.)*, *4*(6). https://doi.org/10.4161/CHAN.4.6.12870

Cruikshank, S. J., Urabe, H., Nurmikko, A. V., & Connors, B. W. (2010). Pathway-Specific Feedforward Circuits between Thalamus and Neocortex Revealed by Selective Optical Stimulation of Axons. *Neuron*, *65*(2), 230–245. https://doi.org/10.1016/J.NEURON.2009.12.025

Dakin, S., & Frith, U. (2005). Vagaries of visual perception in autism. *Neuron*, *48*(3), 497–507. https://doi.org/10.1016/J.NEURON.2005.10.018

David, N., Rose, M., Schneider, T. R., Vogeley, K., & Engel, A. K. (2010). Brief report: Altered horizontal binding of single dots to coherent motion in autism. *Journal of Autism and Developmental Disorders*, *40*(12), 1549–1551. https://doi.org/10.1007/S10803-010-1008-9/FIGURES/1

De Witte, L., Brouns, R., Kavadias, D., Engelborghs, S., De Deyn, P. P., & Mariën, P. (2011). Cognitive, affective and behavioural disturbances following vascular thalamic lesions: A review. *Cortex*, *47*(3), 273–319. https://doi.org/10.1016/J.CORTEX.2010.09.002

Desai, N. V., & Varela, C. (2021). Distinct burst properties contribute to the functional diversity of thalamic nuclei. *The Journal of Comparative Neurology*, *529*(17), 3726. https://doi.org/10.1002/CNE.25141

Destexhe, A. (1998). Spike-and-wave oscillations based on the properties of GABA(B) receptors. *Journal of Neuroscience*, *18*(21), 9099–9111. https://doi.org/10.1523/JNEUROSCI.18-21-09099.1998

Espinosa, F., Torres-Vega, M. A., Marks, G. A., & Joho, R. H. (2008a). *Ablation of Kv3.1 and Kv3.3 Potassium Channels Disrupts Thalamocortical Oscillations In Vitro and In Vivo*. https://doi.org/10.1523/JNEUROSCI.0747-08.2008

Espinosa, F., Torres-Vega, M. A., Marks, G. A., & Joho, R. H. (2008b). *Ablation of Kv3.1 and Kv3.3 Potassium Channels Disrupts Thalamocortical Oscillations In Vitro and In Vivo*. https://doi.org/10.1523/JNEUROSCI.0747-08.2008

Farmer, C. A., Chilakamarri, P., Thurm, A. E., Swedo, S. E., Holmes, G. L., & Buckley, A. W. (2018). Spindle activity in young children with autism, developmental delay, or typical development. *Neurology*, *91*(2), e112–e122. https://doi.org/10.1212/WNL.0000000000005759

Fernandez, L. M. J., Vantomme, G., Osorio-Forero, A., Cardis, R., Béard, E., & Lüthi, A. (2018). Thalamic reticular control of local sleep in mouse sensory cortex. *ELife*, *7*. https://doi.org/10.7554/eLife.39111

Fogerson, P. M., & Huguenard, J. R. (2016). Tapping the Brakes: Cellular and Synaptic Mechanisms that Regulate Thalamic Oscillations. In *Neuron* (Vol. 92, Issue 4, pp. 687–704). https://doi.org/10.1016/j.neuron.2016.10.024

Groen, W. B., Van Orsouw, L., Huurne, N. Ter, Swinkels, S., Van Der Gaag, R. J., Buitelaar, J. K., & Zwiers, M. P. (2009). Intact spectral but abnormal temporal processing of auditory stimuli in autism. *Journal of Autism and Developmental Disorders*, *39*(5), 742–750. https://doi.org/10.1007/S10803-008-0682-3/FIGURES/2

Gröhn, C., Norgren, E., & Eriksson, L. (2021). A systematic review of the neural correlates of multisensory integration in schizophrenia. *Schizophrenia Research. Cognition*, *27*. https://doi.org/10.1016/J.SCOG.2021.100219

Guido, W., & Weyand, T. (1995). Burst Responses in Thalamic Relay Cells of the Awake Behaving Cat. *Journal of Neurophysiology*, *74*(4), 1782–1786.

Ha, N. T., & Dougherty, K. J. (2018). Spinal Shox2 interneuron interconnectivity related to function and development. *ELife*, *7*. https://doi.org/10.7554/eLife.42519

Halassa, M., Siegle, J., Ritt, J., Ting, J., Feng, G., & Moore, C. (2011). Selective optical drive of thalamic reticular nucleus generates thalamic bursts and cortical spindles. *Nature Neuroscience*, *14*(9), 1118–1120. https://doi.org/10.1038/NN.2880

Han, Y., Shi, Y. F., Xi, W., Zhou, R., Tan, Z. B., Wang, H., Li, X. M., Chen, Z., Feng, G., Luo, M., Huang, Z. L., Duan, S., & Yu, Y. Q. (2014). Selective activation of cholinergic basal forebrain neurons induces immediate sleep-wake transitions. *Current Biology*, *24*(6), 693–698. https://doi.org/10.1016/j.cub.2014.02.011

Hoffmann, S., Clauss, S., Berger, I. M., Weiß, B., Montalbano, A., Röth, R., Bucher, M., Klier, I., Wakili, R., Seitz, H., Schulze-Bahr, E., Katus, H. A., Flachsbart, F., Nebel, A., Guenther, S. P. W., Bagaev, E., Rottbauer, W., Kääb, S., Just, S., & Rappold, G. A. (2016). Coding and non-coding variants in the SHOX2 gene in patients with early-onset atrial fibrillation. *Basic Research in Cardiology*, *111*(3), 1–15. https://doi.org/10.1007/S00395-016-0557-2

Huguenard, J. R., & Prince, D. A. (1994). Intrathalamic rhythmicity studied in vitro: nominal T-current modulation causes robust antioscillatory effects. *Journal of*

Neuroscience, *14*(9), 5485–5502. https://doi.org/10.1523/JNEUROSCI.14-09-05485.1994

Iftinca, M. C. (2011). Neuronal T–type calcium channels: What's new? Iftinca: T–type channel regulation. *Journal of Medicine and Life*, *4*(2), 126.

JACOBS, P., DALTON, P., JAMES, R., MOSSE, K., POWER, M., ROBINSON, D., & SKUSE, D. (1997). Turner syndrome: a cytogenetic and molecular study. *Annals of Human Genetics*, *61*(Pt 6), 471–483. https://doi.org/10.1046/J.1469-1809.1997.6160471.X

Jahnsen, H., & Llinas, R. (1984). ELECTROPHYSIOLOGICAL PROPERTIES OF GUINEA-PIG THALAMIC NEURONES: AN IN VITRO STUDY. In *J. Physiol* (Vol. 349).

Jahnsen, H., & Llinás, R. (1984). Ionic basis for the electro-responsiveness and oscillatory properties of guinea-pig thalamic neurones in vitro. *The Journal of Physiology*, *349*(1), 227–247. https://doi.org/10.1113/jphysiol.1984.sp015154

Jhang, K. M., Chang, T. M., Chen, M., & Liu, C. S. (2014). Generalized epilepsy in a patient with mosaic Turner syndrome: a case report. *Journal of Medical Case Reports*, *8*(1). https://doi.org/10.1186/1752-1947-8-109

Jones, E. G. (2007). *The Thalamus 2 Volume Set*. 1708. http://books.google.de/books?id=IR0fSgAACAAJ

Jones, E. G., & Rubenstein, J. L. R. (2004). Expression of regulatory genes during differentiation of thalamic nuclei in mouse and monkey. *Journal of Comparative Neurology*, *477*(1), 55–80. https://doi.org/10.1002/CNE.20234

Joseph, M., Cantú, E. S., Pai, G. S., Willi, S. M., Papenhausen, P. R., & Weiss, L. (1996). Xp pseudoautosomal gene haploinsufficiency and linear growth deficiency in three girls with chromosome Xp22;Yq11 translocation. *Journal of Medical Genetics*, *33*(11), 906–911. https://doi.org/10.1136/JMG.33.11.906

Kadlaskar, G., Mao, P. H., Iosif, A. M., Amaral, D., Wu Nordahl, C., & Miller, M. (2022). Patterns of sensory processing in young children with autism: Differences in autism characteristics, adaptive skills, and attentional problems. *Https://Doi.Org/10.1177/13623613221115951*. https://doi.org/10.1177/13623613221115951

Kandel, A., & Buzsáki, G. (1997). Cellular-Synaptic Generation of Sleep Spindles, Spike-and-Wave Discharges, and Evoked Thalamocortical Responses in the Neocortex of the Rat. *The Journal of Neuroscience*, *17*(17), 6783–6797.

Kanyshkova, T., Broicher, T., Meuth, S. G., Pape, H.-C., & Budde, T. (2011a). A-type K + currents in intralaminar thalamocortical relay neurons. *European Journal of Physiology*. https://doi.org/10.1007/s00424-011-0953-2

Kanyshkova, T., Broicher, T., Meuth, Sven. G., Pape, H.-C., & Budde, T. (2011b). A-type K+ currents in intralaminar thalamocortical relay neurons. *Pflügers Archiv - European Journal of Physiology*, *461*(5), 545–556. https://doi.org/10.1007/s00424-011-0953-2

Kasten, M. R., Rudy, B., Anderson, M. P., & Anderson, M. P. (2007). Differential regulation of action potential firing in adult murine thalamocortical neurons by Kv3.2, Kv1, and SK potassium and N-type calcium channels. *J Physiol*, *584*, 565–582. https://doi.org/10.1113/jphysiol.2007.141135

Kim, D., Hwang, E., Lee, M., Sung, H., & Choi, J. H. (2015). Characterization of topographically specific sleep spindles in mice. *Sleep*, *38*(1), 85–96. https://doi.org/10.5665/SLEEP.4330

Kim, D., Song, I., Keum, S., Lee, T., Jeong, M.-J., Kim, S.-S., Mcenery, M. W., & Shin, H.-S. (2001). Lack of the Burst Firing of Thalamocortical Relay Neurons and Resistance to Absence Seizures in Mice Lacking 1G T-Type Ca 2 Channels al The hyperpo-larization of membrane potentials induced by the activa-tion of GABA B receptors evokes rebound burst dis-c. In *Neuron* (Vol. 31). Huguenard and Prince.

Knickmeyer, R. C., & Davenport, M. (2011). Turner syndrome and sexual differentiation of the brain: implications for understanding male-biased neurodevelopmental disorders. *Journal of Neurodevelopmental Disorders*, *3*(4), 293–306. https://doi.org/10.1007/S11689-011-9089-0

Knox, A. T., Glauser, T., Tenney, J., Lytton, W. W., & Holland, K. (2018a). Modeling Pathogenesis and Treatment Response in Childhood Absence Epilepsy. *Epilepsia*, *59*(1), 135–145. https://doi.org/10.1111/epi.13962

Knox, A. T., Glauser, T., Tenney, J., Lytton, W. W., & Holland, K. (2018b). Modeling Pathogenesis and Treatment Response in Childhood Absence Epilepsy HHS Public Access. *Epilepsia*, *59*(1), 135–145. https://doi.org/10.1111/epi.13962

Kopelman, M. D. (1995). The Korsakoff syndrome. *British Journal of Psychiatry*, *166*(FEB.), 154–173. https://doi.org/10.1192/BJP.166.2.154

Latchoumane, C., Ngo, H., Born, J., & Shin, H. (2017). Thalamic Spindles Promote Memory Formation during Sleep through Triple Phase-Locking of Cortical,

Thalamic, and Hippocampal Rhythms. *Neuron*, *95*(2), 424-435.e6. https://doi.org/10.1016/J.NEURON.2017.06.025

Lee, C. C., & Sherman, S. M. (2008). Synaptic Properties of Thalamic and Intracortical Inputs to Layer 4 of the First-and Higher-Order Cortical Areas in the Auditory and Somatosensory Systems. *J Neurophysiol*, *100*, 317–326. https://doi.org/10.1152/jn.90391.2008

Lee, J., Song, K., Lee, K., Hong, J., Lee, H., Chae, S., Cheong, E., & Shin, H. S. (2013). Sleep spindles are generated in the absence of T-type calcium channel-mediated low-threshold burst firing of thalamocortical neurons. *Proceedings of the National Academy of Sciences of the United States of America*, *110*(50), 20266–20271. https://doi.org/10.1073/PNAS.1320572110/SUPPL_FILE/PNAS.201320572SI.PDF

Lefort, S., Tomm, C., Floyd Sarria, J. C., & Petersen, C. C. H. (2009). The Excitatory Neuronal Network of the C2 Barrel Column in Mouse Primary Somatosensory Cortex. *Neuron*, *61*(2), 301–316. https://doi.org/10.1016/J.NEURON.2008.12.020

Lesica, N. A., & Stanley, G. B. (2004). Encoding of Natural Scene Movies by Tonic and Burst Spikes in the Lateral Geniculate Nucleus. *The Journal of Neuroscience*, *24*(47), 10731. https://doi.org/10.1523/JNEUROSCI.3059-04.2004

Lesica, N. A., Weng, C., Jin, J., Yeh, C. I., Alonso, J. M., & Stanley, G. B. (2006). Dynamic Encoding of Natural Luminance Sequences by LGN Bursts. *PLOS Biology*, *4*(7), e209. https://doi.org/10.1371/JOURNAL.PBIO.0040209

Li, H., Fertuzinhos, S., Mohns, H., Hnasko, T., Verhage, M., Edwards, R., Sestan, N., & Crair, M. (2013). Laminar and columnar development of barrel cortex relies on

thalamocortical neurotransmission. *Neuron*, *79*(5), 970–986. https://doi.org/10.1016/J.NEURON.2013.06.043

Li, N., Wang, Z. S., Wang, X. H., Xu, Y. J., Qiao, Q., Li, X. M., Di, R. M., Guo, X. J., Li, R. G., Zhang, M., Qiu, X. B., & Yang, Y. Q. (2018). A SHOX2 loss-of-function mutation underlying familial atrial fibrillation. *International Journal of Medical Sciences*, *15*(13), 1564–1572. https://doi.org/10.7150/IJMS.27424

Lipiec, M. A., Kozinski, K., Zajkowski, T., Dabrowski, M., Chakraborty, C., Toval, A., Ferran, J., Nagalski, A., & Wisniewska, M. B. (2019). The transcription factor TCF7L2 functions as a terminal selector in thalamic and habenular regions of the brain. *BioRxiv*, 515874. https://doi.org/10.1101/515874

Liu, H., Chen, C.-H., Espinoza-Lewis, R. A., Jiao, Z., Sheu, I., Hu, X., Lin, M., Zhang, Y., & Chen, Y. (2011). Functional Redundancy between Human SHOX and Mouse Shox2 Genes in the Regulation of Sinoatrial Node Formation and Pacemaking Function. *Journal of Biological Chemistry*, *286*(19), 17029–17038. https://doi.org/10.1074/jbc.M111.234252

Llano, D. A., & Sherman, S. M. (2008). Evidence for nonreciprocal organization of the mouse auditory thalamocortical-corticothalamic projection systems. *Journal of Comparative Neurology*, *507*(2), 1209–1227. https://doi.org/10.1002/CNE.21602

LMJ, F., & A, L. (2020). Sleep Spindles: Mechanisms and Functions. *Physiological Reviews*, *100*(2), 805–868. https://doi.org/10.1152/PHYSREV.00042.2018

Ludwig, A., Budde, T., Stieber, J., Moosmang, S., Wahl, C., Holthoff, K., Langebartels, A., Wotjak, C., Munsch, T., Zong, X., Feil, S., Feil, R., Lancel, M., Chien, K. R., Konnerth, A., Pape, H.-C., Biel, M., & Hofmann, F. (2003). Absence epilepsy and

sinus dysrhythmia in mice lacking the pacemaker channel HCN2. *The EMBO JOurnal*, *22*(2), 216–224.

Lüthi, A., & McCormick, D. A. (1998). H-current: properties of a neuronal and network pacemaker. *Neuron*, *21*(1), 9–12. https://doi.org/10.1016/S0896-6273(00)80509-7

M, D., M, P., JP, R., & M, S. (1984). Electrophysiology of neurons of lateral thalamic nuclei in cat: resting properties and burst discharges. *Journal of Neurophysiology*, *51*(6), 1196–1219. https://doi.org/10.1152/JN.1984.51.6.1196

Magara, S. ichi, Kawashima, H., Kobayashi, Y., Akasaka, N., Yamazaki, S., & Tohyama, J. (2015). Rub epilepsy in an infant with Turner syndrome. *Brain & Development*, *37*(7), 725–728. https://doi.org/10.1016/J.BRAINDEV.2014.11.004

Manoach, D. S., Pan, J. Q., Purcell, S. M., & Stickgold, R. (2016). Reduced sleep spindles in schizophrenia: A treatable endophenotype that links risk genes to impaired cognition? *Biological Psychiatry*, *80*(8), 599. https://doi.org/10.1016/J.BIOPSYCH.2015.10.003

Mashour, G. A., & Alkire, M. T. (2013). Consciousness, Anesthesia, and the Thalamocortical System. *Anesthesiology*, *118*(1), 13–15. https://doi.org/10.1097/ALN.0B013E318277A9C6

Matsumoto-Makidono, Y., Nakayama, H., Yamasaki, M., Miyazaki, T., Kobayashi, K., Watanabe, M., Kano, M., Sakimura, K., & Hashimoto, K. (2016). Ionic Basis for Membrane Potential Resonance in Neurons of the Inferior Olive. *Cell Reports*, *16*(4), 994–1004. https://doi.org/10.1016/J.CELREP.2016.06.053

Mauger, C., Lancelot, C., Roy, A., Coutant, R., Cantisano, N., & Le Gall, D. (2018). Executive Functions in Children and Adolescents with Turner Syndrome: A

Systematic Review and Meta-Analysis. *Neuropsychology Review*, *28*(2), 188–215. https://doi.org/10.1007/S11065-018-9372-X

McCormick, D. A., & Pape, H. C. (1990). Properties of a hyperpolarization-activated cation current and its role in rhythmic oscillation in thalamic relay neurones. *The Journal of Physiology*, *431*(1), 291. https://doi.org/10.1113/JPHYSIOL.1990.SP018331

Milne, E., Swettenham, J., Hansen, P., Campbell, R., Jeffries, H., & Plaisted, K. (2002). High motion coherence thresholds in children with autism. *Journal of Child Psychology and Psychiatry*, *43*(2), 255–263. https://doi.org/10.1111/1469-7610.00018

Minzenberg, M. J., Laird, A. R., Thelen, S., Carter, C. S., & Glahn, D. C. (2009). Meta-analysis of 41 Functional Neuroimaging Studies of Executive Function in Schizophrenia. *Archives of General Psychiatry*, *66*(8), 811–822. https://doi.org/10.1001/ARCHGENPSYCHIATRY.2009.91

Nagalski, A., Puelles, L., Dabrowski, M., Wegierski, T., Kuznicki, J., & Wisniewska, M. B. (2016). Molecular anatomy of the thalamic complex and the underlying transcription factors. *Brain Struct Funct*, *221*, 2493–2510. https://doi.org/10.1007/s00429-015-1052-5

Nair, A., Treiber, J. M., Shukla, D. K., Shih, P., & Mü, R.-A. (2013). Impaired thalamocortical connectivity in autism spectrum disorder: a study of functional and anatomical connectivity. *Brain: A Journal of Neurology*, *136*, 1942–1955. https://doi.org/10.1093/brain/awt079

Nakagawa, Y., & O'leary, D. D. M. (2001). Combinatorial Expression Patterns of LIM-Homeodomain and Other Regulatory Genes Parcellate Developing Thalamus. *Journal of Neuroscience*, *21*(8), 2711–2725.

Nakagawa, Y., & O'Leary, D. D. M. (2003). Dynamic Patterned Expression of Orphan Nuclear Receptor Genes RORα and RORβ in Developing Mouse Forebrain. *Developmental Neuroscience*, *25*(2–4), 234–244. https://doi.org/10.1159/000072271

Notomi, T., & Shigemoto, R. (2004). Immunohistochemical localization of Ih channel subunits, HCN1-4, in the rat brain. *The Journal of Comparative Neurology*, *471*(3), 241–276. https://doi.org/10.1002/CNE.11039

Oberlaender, M., De Kock, C. P. J., Bruno, R. M., Ramirez, A., Meyer, H. S., Dercksen, V. J., Helmstaedter, M., & Sakmann, B. (2012). Cell Type–Specific Three-Dimensional Structure of Thalamocortical Circuits in a Column of Rat Vibrissal Cortex. *Cerebral Cortex*, *22*(10), 2375–2391. https://doi.org/10.1093/CERCOR/BHR317

Oh, S. W., Harris, J. A., Ng, L., Winslow, B., Cain, N., Mihalas, S., Wang, Q., Lau, C., Kuan, L., Henry, A. M., Mortrud, M. T., Ouellette, B., Nguyen, T. N., Sorensen, S. A., Slaughterbeck, C. R., Wakeman, W., Li, Y., Feng, D., Ho, A., … Zeng, H. (2014). A mesoscale connectome of the mouse brain. *Nature 2014 508:7495*, *508*(7495), 207–214. https://doi.org/10.1038/nature13186

Ojima, H., & Murakami, K. (2011). Triadic synaptic interactions of large corticothalamic terminals in non-lemniscal thalamic nuclei of the cat auditory system. *Hearing Research*, *274*(1–2), 40–47. https://doi.org/10.1016/J.HEARES.2010.05.009

Oliveira, C. S., & Alves, C. (2011). The role of the SHOX gene in the pathophysiology of Turner syndrome. *Endocrinologia y Nutricion : Organo de La Sociedad Espanola de Endocrinologia y Nutricion*, *58*(8), 433–442. https://doi.org/10.1016/J.ENDONU.2011.06.005

O'malley, J. J., Seibt, F., Chin, J., & Beierlein, M. (2020). *Cellular/Molecular TRPM4 Conductances in Thalamic Reticular Nucleus Neurons Generate Persistent Firing during Slow Oscillations*. https://doi.org/10.1523/JNEUROSCI.0324-20.2020

O'Riordan, M. A., Plaisted, K. C., Driver, J., & Baron-Cohen, S. (2001). Superior visual search in autism. *Journal of Experimental Psychology: Human Perception and Performance*, *27*(3), 719–730. https://doi.org/10.1037/0096-1523.27.3.719

Paxinos, G. (2004). The Rat Nervous System. *The Rat Nervous System*, 1–1309. https://doi.org/10.1016/B978-0-12-547638-6.X5000-7

Perez-Reyes, E. (2006). Molecular characterization of T-type calcium channels. *Cell Calcium*, *40*(2), 89–96. https://doi.org/10.1016/J.CECA.2006.04.012

Pratt, T., Vitals, T., Warren, N., Edgar, J., Mason, J., & Price, D. (2000). Role of Pax6 in thalamic development. *Development*, *127*, 5167–5178.

Puskaric, S., Schmitteckert, S., Mori, A. D., Glaser, A., Schneider, K. U., Bruneau, B. G., diger Blaschke, R. J., Steinbeisser, H., & Rappold, G. (2010). Shox2 mediates Tbx5 activity by regulating Bmp4 in the pacemaker region of the developing heart. *Human Molecular Genetics*, *19*(23), 4625–4633. https://doi.org/10.1093/hmg/ddq393

Puusepp, H., Zordania, R., Paal, M., Bartsch, O., & Õunap, K. (2008). Girl with partial Turner syndrome and absence epilepsy. *Pediatric Neurology*, *38*(4), 289–292. https://doi.org/10.1016/J.PEDIATRNEUROL.2007.11.008

Rubio-Garrido, P., Perez-de-Manzo, F., Porrero, C., Galazo, M. J., & Clasca, F. (2009). Thalamic Input to Distal Apical Dendrites in Neocortical Layer 1 Is Massive and Highly Convergent. *Cerebral Cortex*, *19*, 2380–2395.

Rudy, B., Chow, A., Lau, D., Amarillo, Y., Ozaita, A., Saganich, M., Moreno, H., Nadal, M. S., Hernandez-Pineda, R., Hernandez-Cruz, A., Erisir, A., Leonard, C., & Vega-Saenz De Miera, E. (1999). Contributions of Kv3 channels to neuronal excitability. *Annals of the New York Academy of Sciences*, *868*, 304–343. https://doi.org/10.1111/J.1749-6632.1999.TB11295.X

Rudy, B., Fishell, G., Lee, S., & Hjerling-Leffler, J. (2011). Three groups of interneurons account for nearly 100% of neocortical GABAergic neurons. *Developmental Neurobiology*, *71*(1), 45–61. https://doi.org/10.1002/DNEU.20853

Rudy, B., & Mcbain, C. J. (2001). Kv3 channels: voltage-gated K + + channels designed for high-frequency repetitive firing. In *TRENDS in Neurosciences* (Vol. 24, Issue 9).

Saad, K., Abdelrahman, A. A., Abdel-Raheem, Y. F., Othman, E. R., Badry, R., Othman, H. A. K., & Sobhy, K. M. (2014). Turner syndrome: review of clinical, neuropsychiatric, and EEG status: an experience of tertiary center. *Acta Neurologica Belgica*, *114*(1), 1–9. https://doi.org/10.1007/S13760-013-0264-9

Sermet, B. S., Truschow, P., Feyerabend, M., Mayrhofer, J. M., Oram, T. B., Yizhar, O., Staiger, J. F., & Petersen, C. C. (2019). Pathway-, layer- and cell-type-specific

thalamic input to mouse barrel cortex. *ELife*, *8*. https://doi.org/10.7554/ELIFE.52665

Shah, A., & Frith, U. (1983). AN ISLET OF ABILITY IN AUTISTIC CHILDREN: A RESEARCH NOTE. *Journal of Child Psychology and Psychiatry*, *24*(4), 613–620. https://doi.org/10.1111/J.1469-7610.1983.TB00137.X

Shenton, M. E., Dickey, C. C., Frumin, M., & McCarley, R. W. (2001). A review of MRI findings in schizophrenia. *Schizophrenia Research*, *49*(1–2), 1–52. https://doi.org/10.1016/S0920-9964(01)00163-3

Sheridan, N., & Tadi, P. (2022). Neuroanatomy, Thalamic Nuclei. *StatPearls*.

Sherman, M. S. (2001). Tonic and burst firing: dual modes of thalamocortical relay. *TRENDS in Neuroscience*, *24*(2), 122.

Sherman, S. M. (2001). A wake-up call from the thalamus. *Nature Neuroscience*, *4*(4), 344–346.

Sherman, S. M. (2017). Functioning of Circuits Connecting Thalamus and Cortex. *Comprehensive Physiology*, *7*(2), 713–739. https://doi.org/10.1002/CPHY.C160032

Sherman, S. Murray., & Guillery, R. W. (2013). *Functional Connections of Cortical Areas : a New View from the Thalamus*. MIT Press.

Simon, D. M., & Wallace, M. T. (2016). Dysfunction of sensory oscillations in Autism Spectrum Disorder. *Neuroscience and Biobehavioral Reviews*, *68*, 848–861. https://doi.org/10.1016/j.neubiorev.2016.07.016

Stanley, G. B., Jin, J., Wang, Y., Desbordes, G., Wang, Q., Black, M. J., & Alonso, J. M. (2012). Visual orientation and directional selectivity through thalamic synchrony.

Journal of Neuroscience, *32*(26), 9073–9088. https://doi.org/10.1523/JNEUROSCI.4968-11.2012

Steriade, M., Deschenes, M., Domich, L., & Mulle, C. (1985). Abolition of spindle oscillations in thalamic neurons disconnected from nucleus reticularis thalami. *Journal of Neurophysiology*, *54*(6), 1473–1497. https://doi.org/10.1152/JN.1985.54.6.1473

Steriade, M., Domich, L., & Oakson, G. (1986). Reticularis thalami neurons revisited: activity changes during shifts in states of vigilance. *The Journal of Neuroscience : The Official Journal of the Society for Neuroscience*, *6*(1), 68–81. https://doi.org/10.1523/JNEUROSCI.06-01-00068.1986

Steriade, M., Domich, L., Oakson, G., & Deschenes, M. (1987). The deafferented reticular thalamic nucleas generates spindle rhythmicity. *Journal of Neurophysiology*, *57*(1), 260–273. https://doi.org/10.1152/JN.1987.57.1.260

Steriade, M., & Llinas, R. R. (1988). The functional states of the thalamus and the associated neuronal interplay. In *Physiological Reviews* (Vol. 68, Issue 3, pp. 649–742). https://doi.org/10.1152/physrev.1988.68.3.649

Steriade, M., McCormick, D. A., & Sejnowski, T. J. (1993). Thalamocortical Oscillations in the Sleeping and Aroused Brain. *Science*, *262*(5134), 679–685.

Sun, C., Yu, D., Ye, W., Liu, C., Gu, S., Sinsheimer, N. R., Song, Z., Li, X., Chen, C., Song, Y., Wang, S., Schrader, L., & Chen, Y. (2015). The short stature homeobox 2 (Shox2)-bone morphogenetic protein (BMP) pathway regulates dorsal mesenchymal protrusion development and its temporary function as a pacemaker during

cardiogenesis. *The Journal of Biological Chemistry*, *290*(4), 2007–2023. https://doi.org/10.1074/jbc.M114.619007

Swadlow, H. A. (2002). Thalamocortical control of feed-forward inhibition in awake somatosensory "barrel" cortex. *Philosophical Transactions of the Royal Society B: Biological Sciences*, *357*(1428), 1717–1727. https://doi.org/10.1098/rstb.2002.1156

Swadlow, H. A., & Gusev, A. G. (2001). The impact of "bursting" thalamic impulses at a neocortical synapse. *Nature Neuroscience*, *4*(4), 402–408. https://doi.org/10.1038/86054

Talley, E. M., Cribbs, L. L., Lee, J. H., Daud, A., Perez-Reyes, E., & Bayliss, D. A. (1999). Differential distribution of three members of a gene family encoding low voltage-activated (T-type) calcium channels. *The Journal of Neuroscience : The Official Journal of the Society for Neuroscience*, *19*(6), 1895–1911. https://doi.org/10.1523/JNEUROSCI.19-06-01895.1999

Tennigkeit, F., Schwarz, D. W. F., & Puil, E. (1998). Modulation of bursts and high-threshold calcium spikes in neurons of rat auditory thalamus. *Neuroscience*, *83*(4), 1063–1073. https://doi.org/10.1016/S0306-4522(97)00458-2

Timofeev, I., & Steriade, M. (1996). Low-frequency rhythms in the thalamus of intact-cortex and decorticated cats. *Journal of Neurophysiology*, *76*(6), 4152–4168. https://doi.org/10.1152/jn.1996.76.6.4152

Tou, Y. V., Aaker, J., Taniguchi, A., Kazemzadeh, C., Skidmore, J. M., Martin, D. M., Martin, J. F., Treier, M., & Nakagawa, Y. (2007). Characterization of progenitor domains in the developing mouse thalamus. *Journal of Comparative Neurology*, *505*(1), 73–91. https://doi.org/10.1002/CNE.21467

Vertes, R. P., Linley, S. B., & Hoover, W. B. (2015). LIMBIC CIRCUITRY OF THE MIDLINE THALAMUS. *Neuroscience and Biobehavioral Reviews*, *54*, 89. https://doi.org/10.1016/J.NEUBIOREV.2015.01.014

von Krosigk, M., Bal, B., & McCormick, D. (1993). Cellular mechanisms of a synchronized oscillation in the thalamus. *Science (New York, N.Y.)*, *261*(5119), 361–364. https://doi.org/10.1126/SCIENCE.8392750

Wang, Q., Webber, R. M., & Stanley, G. B. (2010). Thalamic synchrony and the adaptive gating of information flow to cortex. *Nature Neuroscience 2010 13:12*, *13*(12), 1534–1541. https://doi.org/10.1038/nn.2670

Weiser, M., Bueno, E., Sekirnjak, C., Marione, M. E., Baker, H., Hillman, D., Chen, S., Thornhill, W., Ellisman, M., & Rudy, B. (1995). The potassium channel subunit KV3.1b is localized to somatic and axonal membranes of specific populations of CNS neurons. *Journal of Neuroscience*, *15*(6), 4298–4314. https://doi.org/10.1523/JNEUROSCI.15-06-04298.1995

Weiser, M., Vega-Saenz De Miera, E., Kentros, C., Moreno, H., Franzen, L., Hillman, D., Baker, H., & Rudy, B. (1994). Differential expression of Shaw-related K+ channels in the rat central nervous system. *Journal of Neuroscience*, *14*(3), 949–972. https://doi.org/10.1523/JNEUROSCI.14-03-00949.1994

Whitmire, C. J., Liew, Y. J., & Stanley, G. B. (2021). Thalamic state influences timing precision in the thalamocortical circuit. *Journal of Neurophysiology*, *125*(5), 1833–1850. https://doi.org/10.1152/jn.00261.2020

Whitmire, C. J., Waiblinger, C., Schwarz, C., & Stanley, G. B. (2016). Information Coding through Adaptive Gating of Synchronized Thalamic Bursting. *Cell Reports*, *14*(4), 795–807. https://doi.org/10.1016/J.CELREP.2015.12.068

Wimmer, V. C., Bruno, R. M., de Kock, C. P. J., Kuner, T., & Sakmann, B. (2010). Dimensions of a Projection Column and Architecture of VPM and POm Axons in Rat Vibrissal Cortex. *Cerebral Cortex*, *20*(10), 2265–2276. https://doi.org/10.1093/CERCOR/BHQ068

Woodward, N. D., Karbasforoushan, H., & Heckers, S. (2012). Thalamocortical dysconnectivity in schizophrenia. *Am J Psychiatry*, *169*(10), 1–13. https://doi.org/10.1176/appi.ajp.2012.12010056

Woolsey, T. A., & Van der Loos, H. (1970). The structural organization of layer IV in the somatosensory region (S I) of mouse cerebral cortex: The description of a cortical field composed of discrete cytoarchitectonic units. *Brain Research*, *17*(2), 205–242. https://doi.org/10.1016/0006-8993(70)90079-X

Yu, D., Febbo, I. G., Maroteaux, M. J., Wang, H., Song, Y., Han, X., Sun, C., Meyer, E. E., Rowe, S., Chen, Y., Canavier, C. C., & Schrader, L. A. (2021). The Transcription Factor Shox2 Shapes Neuron Firing Properties and Suppresses Seizures by Regulation of Key Ion Channels in Thalamocortical Neurons. *Cerebral Cortex*, *31*(7), 3194–3212. https://doi.org/10.1093/CERCOR/BHAA414

Yuge, K., Kataoka, A., Yoshida, A. C., Itoh, D., Aggarwal, M., Mori, S., Blackshaw, S., & Shimogori, T. (2011). Region-specific gene expression in early postnatal mouse thalamus. *Journal of Comparative Neurology*, *519*(3), 544–561. https://doi.org/10.1002/CNE.22532

Zhao, H., & Lian, Y. J. (2015). Epilepsy associated with Turner syndrome. *Neurology India*, *63*(4), 631–633. https://doi.org/10.4103/0028-3886.162113

Zhou, Z., & January, C. T. (1998). Both T- and L-type Ca2+ channels can contribute to excitation-contraction coupling in cardiac Purkinje cells. *Biophysical Journal*, *74*(4), 1830–1839. https://doi.org/10.1016/S0006-3495(98)77893-2

Zobeiri, M., Chaudhary, R., Blaich, A., Rottmann, M., Herrmann, S., Meuth, P., Bista, P., Kanyshkova, T., Lüttjohann, A., Narayanan, V., Hundehege, P., Meuth, S. G., Romanelli, M. N., Urbano, F. J., Pape, H. C., Budde, T., & Ludwig, A. (2019). The Hyperpolarization-Activated HCN4 Channel is Important for Proper Maintenance of Oscillatory Activity in the Thalamocortical System. *Cerebral Cortex (New York, NY)*, *29*(5), 2291. https://doi.org/10.1093/CERCOR/BHZ047

Biography

Isabella G Febbo was born the fourth of five children to Mark and Christine Febbo in a yellow house in Groveland, Massachusetts. A few years later, the family of seven and their two dogs moved into a yellow school bus and toured the hot springs and National Parks of the United States. She would turn 11 on the road. After a brief tour in Tennessee, the family settled into a tall, skinny, yellow house in the swamps of old Florida, Punta Gorda to be exact. After graduating high school, she took her own solo tour of the hot springs and National Parks of the U.S. She then obtained her degree in biomedical engineering from Florida International University in Miami, FL, and went on to obtain her PhD in Neuroscience at Tulane University in New Orleans, LA. As she writes this, she has a prospective postdoc position at the University of Oxford, UK, where she will continue to study how the brain generates sensory perception. She loves the great outdoors, math, the thalamus, and dogs.